

**ABSORPTION OF CARBON DIOXIDE IN AQUEOUS  
BLENDS OF DIETHANOLAMINE AND  
METHYLDIETHANOLAMINE**

by

**SHRIKAR CHAKRAVARTI, B.S.**

**THESIS**

Presented to the Faculty of the Graduate School of  
The University of Texas at Austin  
in Partial Fulfillment  
of the Requirements  
for the Degree of  
MASTER OF SCIENCE IN ENGINEERING

THE UNIVERSITY OF TEXAS AT AUSTIN

December, 1992

Copyright  
by  
Shrikar Chakravarti  
1992

To my parents,  
grandparents and brother

## ACKNOWLEDGMENTS

I take this golden opportunity to express my gratitude to Professor Gary Rochelle for his guidance and support over the last couple of years. I learnt a lot from his practical way of approaching problems. It was to my benefit that he was willing and eager to answer even the smallest of my queries.

The company of Harold, Rajesh, Mshewa, Kurt and Chris made life enjoyable in the labs. They are a great bunch to be with. I would like to thank Jeremy for helping me run some simulations and archive the computer code. The assistance of K.D with the carbon analyzer is appreciated. Thanks to Missa for helping out with the formatting of the thesis.

Most importantly, I would like to thank God, my grandparents, my parents and my brother Shreyas for their moral and psychological support. Shreyas helped me prepare a number of the tables in the appendix.

I would like to acknowledge the financial support provided by Texaco Chemical Company, Gas Research Institute (Contract No. 5090-260-2013) and the Separations Research Program. Thanks to Texaco for promptly supplying the MDEA and DEA.

Shrikar Chakravarti

The University of Texas at Austin  
December, 1992

## **ABSTRACT**

### **ABSORPTION OF CARBON DIOXIDE IN AQUEOUS BLENDS OF DIETHANOLAMINE AND METHYLDIETHANOLAMINE**

by

**SHRIKAR CHAKRAVARTI, B.S.**

**SUPERVISING PROFESSOR: GARY T. ROCHELLE**

Absorption of CO<sub>2</sub> in aqueous alkanolamines is a phenomenon of gas-liquid mass transfer with chemical reaction at the interface. An attempt was made at modeling this problem in the framework of ASPEN PLUS. The effect of chemical reaction on mass transfer was accounted for by an enhancement factor. The feasibility of incorporating the enhancement factor approach into RATEFRAC, the rate-based model of ASPEN PLUS in order to model the gas absorption problem was investigated. Outside of RATEFRAC, two models of single stage contactors were developed. One accounted for the effect of changing interfacial composition on activity coefficients while the other used the activity coefficients calculated from equilibrium.

Absorption rates of CO<sub>2</sub> into 50 wt% aqueous alkanolamine solutions were measured at 25°C and 40°C. The amines considered in this work were pure MDEA, pure DEA, 10% DEA - 90%MDEA and 50% DEA - 50% MDEA. Equilibrium data extracted from these rate measurements were compared to the predictions of the VLE model (Austgen, 1989). Normalized fluxes and pseudo first order rate constants were estimated from the rate data. The pseudo first order rate constants were regressed to yield rate parameters. The predictions from the model with these parameters were compared with the experimental measurements to validate the obtained data.

## TABLE OF CONTENTS

ACKNOWLEDGMENTS .....	v
ABSTRACT .....	vi
LIST OF TABLES .....	xi
LIST OF FIGURES .....	xiii
CHAPTER ONE: INTRODUCTION .....	1
1.1 Process Flowsheet of an Acid Gas Treating Unit .....	1
1.2 Alkanolamines and their applications .....	3
1.3 Objectives and scope of this work .....	6
CHAPTER TWO: MODELING .....	8
2.1 Features of Aspen Plus .....	12
2.1.1 Creating and running an ASPEN input file .....	12
2.1.2 Apparent and True Components .....	14
2.1.3 Equilibrium .....	15
2.1.4 Physical Properties and Models .....	16
2.2 Reactions .....	24
2.2.1 Rate-limited reactions .....	24
2.3.2 Bicarbonate reaction rate .....	26
2.3.3 Carbamate reaction rate .....	28
2.3.4 Effect of ionic strength .....	30
2.3.5 Conversion of rate constants from concentration based activities to mole fraction based activities .....	32
2.3.6 Equilibrium activity of CO <sub>2</sub> in blended amines .....	34
2.3 Flash .....	36
2.3.1 Speciation .....	36
2.3.2 NOHPO Compiler .....	36

2.3.3	Minor species correction .....	37
2.4	Enhancement Factor Approach .....	38
2.4.1	Algorithm .....	39
2.4.2	Iterative method .....	42
2.5	Equilibrium Estimation .....	43
2.5.1	Flash2 .....	43
2.5.2	Reactor with large residence time .....	43
2.5.3	Sensitivity Analysis .....	44
2.6	Ratefrac-based Model .....	45
2.6.1	Kinetics Routine .....	46
2.6.2	Carey's Proposal (1990) .....	47
2.6.3	Difficulties .....	47
2.6.4	Modified Approach .....	48
2.6.5	Observations .....	48
2.7	Single Stage Contactor .....	49
2.7.1	Equilibrium or Bulk Activity Coefficients .....	50
2.7.2	Interface Activity Coefficients .....	52
2.7.3	Results .....	54
<b>CHAPTER THREE: EXPERIMENTAL WORK .....</b>		<b>67</b>
3.1	Experimental Apparatus and Methods .....	67
3.1.1	Wetted Wall Column .....	67
3.1.2	Overall Setup .....	70
3.1.3	Calibration of Mass Flow Controllers .....	72
3.1.4	Carbon dioxide analyzers .....	74
3.1.5	Carbon analyzer .....	76
3.2	Physical calibration .....	77
3.2.1	Theory .....	77
3.2.2	Procedure .....	79
3.2.3	Dimensionless Mass Transfer Correlation .....	79
3.3	Reactive absorption .....	84
3.3.1	General Methodology .....	84



3.3.2 Equilibrium measurements .....	88
3.3.3 Rate Measurements .....	98
<b>CHAPTER FOUR: CONCLUSIONS .....</b>	<b>127</b>
4.1 Summary .....	127
4.2 Results and Conclusions from the Modeling work .....	128
4.3 Results and Conclusions from the Experimental work .....	130
4.4 Recommendations .....	132
<b>APPENDIX A: EXPERIMENTAL DATA .....</b>	<b>134</b>
<b>APPENDIX B: PHYSICAL PROPERTY CORRELATIONS .....</b>	<b>149</b>
B.1 Viscosity of the Unloaded Solution .....	149
B.2 Viscosity of the Loaded Solution .....	150
B.3 Density of the Solution .....	150
B.4 Diffusion Coefficients .....	151
B.4.1 Diffusion Coefficient of CO <sub>2</sub> .....	151
B.4.2 Diffusion Coefficient of the Amines .....	152
B.5 Solubility of CO <sub>2</sub> in Amines .....	153
<b>APPENDIX C: DETAILED SIMULATION RESULTS .....</b>	<b>156</b>
<b>APPENDIX D: DEPLETION CALCULATIONS .....</b>	<b>161</b>
<b>APPENDIX E: DETAILED SIMULATION RESULTS .....</b>	<b>165</b>
E.1 Introduction .....	165
E.2 Gas Phase Error Analysis .....	166
E.3 CO <sub>2</sub> Partial Pressure Error Analysis .....	170
E.4 Error in Concentration Measurements .....	171
<b>APPENDIX F: SPECIATION .....</b>	<b>173</b>
<b>APPENDIX G: SRP REPORT</b>	
<b>ABSORPTION OF CARBON DIOXIDE IN AQUEOUS</b>	
<b>BLENDS OF DIETHANOLAMINE AND</b>	
<b>METHYLDIETHANOLAMINE .....</b>	<b>177</b>
<b>NOMENCLATURE .....</b>	<b>194</b>
<b>BIBLIOGRAPHY .....</b>	<b>196</b>
<b>VITA .....</b>	<b>204</b>

## LIST OF TABLES

Table 2.1	Summary of Numerical Studies of Absorption with Chemical Reaction for the Unsteady-State Theories (Glasscock, 1990) .....	9
Table 2.2	Summary of Numerical Studies of Absorption with Chemical Reaction Using Film Theory (Glasscock, 1990) .....	10
Table 2.3	Mole Fraction- Based Equilibrium Constants Used in the Model (Austgen, 1989) .....	17
Table 2.4	Henry's Constant Expressions for H <sub>2</sub> S and CO <sub>2</sub> (Austgen, 1989) .....	18
Table 2.5	Rackett Binary Interaction Parameters (Austgen, 1989) .....	18
Table 2.6	Pure Component Molecular Weight and Critical Properties for DEA, MDEA, and DGA .....	19
Table 2.7	Pure Component Vapor Pressures of H <sub>2</sub> O, MEA, DEA, MDEA and DGA (Austgen, 1989) .....	20
Table 2.8	Dielectric constants for pure MEA, DEA, MDEA, and DGA (Austgen, 1989) .....	21
Table 2.9	NRTL Molecular Interaction Parameters Used in the Model (Austgen, 1989) .....	22
Table 2.10	NRTL Molecule - Ion Pair Interaction Parameters Used in the Model .....	23
Table 2.11	Equilibrium Regression Results (Glasscock, 1990) .....	25
Table 2.12	Rate Parameters Used (Glasscock, 1990) .....	33
Table 2.13	Comparison of activity coefficients for a 25% DEA solution at 0.5 loading and T = 25°C .....	64
Table 2.14	Comparison of enhancement factors predicted by approximate methods developed in ASPEN PLUS .....	65

Table 3.1 Conditions for absorption of CO <sub>2</sub> into 50 wt% alkanolamine solutions.....	84
Table 3.3 Ranges of flow controllers .....	87
Table 3.3 Flow controllers for different amines and partial pressures of CO <sub>2</sub> .....	87
Table 3.4 Experimental measurement of CO <sub>2</sub> solubility in solutions of DEA and MDEA at 25°C and 40°C .....	94
Table 3.5 Summary of rate data at 25°C .....	108
Table 3.6 Summary of rate data at 40°C .....	109
Table 3.7 Estimate of depletion of free DEA at the interface .....	110
Table 3.8 Indirect estimate of depletion of hydroxide at the interface .....	111
Table 3.9 Comparison of parameter values from regression on different basis .....	113
Table 3.10 Parameters used in predictions to compare with experimental data.....	116
Table 3.11 Comparison of Results with Literature Data .....	122
Table G.1 Comparison of Results with Literature Data.....	192
Table G.2 Comparison of enhancement factors predicted by approximate methods developed in ASPEN PLUS.....	193

## LIST OF FIGURES

Figure 1.1 Typical Absorber/Stripper System for Acid Gas Removal .....	2
Figure 2.1 Apparent and true components in the nomenclature of ASPEN PLUS .....	15
Figure 2.2 Comparison of approximate to rigorous flux as a function of the rigorous enhancement factor for loading = 0.01 mol CO <sub>2</sub> /mol amine, $k_L = 10^{-4}$ m/s, T = 40°C.....	55
Figure 2.3 Comparison of approximate to rigorous flux as a function of the rigorous enhancement factor for loading = 0.1 mol CO <sub>2</sub> /mol amine, $k_L = 10^{-4}$ m/s, T = 40°C.....	56
Figure 2.4 Comparison of approximate to rigorous flux as a function of the rigorous enhancement factor for loading = 0.01 mol CO <sub>2</sub> /mol amine, $k_L = 10^{-5}$ m/s, T = 40°C. ....	57
Figure 2.5 Comparison of approximate to rigorous flux as a function of rigorous enhancement factor for loading = 0.1 mol CO <sub>2</sub> /mol amine, $k_L = 10^{-5}$ m/s, T = 40°C.....	58
Figure 2.6 Comparison of approximate to rigorous flux as a function of CO <sub>2</sub> partial pressure for loading = 0.01 mol CO <sub>2</sub> /mol amine, $k_L = 10^{-4}$ m/s, T = 40°C.....	59
Figure 2.7 Comparison of approximate to rigorous flux as a function of CO <sub>2</sub> partial pressure for loading = 0.1 mol CO <sub>2</sub> /mol amine, $k_L = 10^{-4}$ m/s, T = 40°C.....	60

Figure 2.8 Comparison of approximate to rigorous flux as a function of CO <sub>2</sub> partial pressure for loading = 0.01 mol CO <sub>2</sub> /mol amine, $k_L = 10^{-5}$ m/s, T = 40°C.....	61
Figure 2.9 Comparison of approximate to rigorous flux as a function of CO <sub>2</sub> partial pressure for loading = 0.1 mol CO <sub>2</sub> /mol amine, $k_L = 10^{-5}$ m/s, T = 40°C.....	62
Figure 3.1 Detailed diagram of the wetted wall column .....	68
Figure 3.2 Schematic of overall setup .....	71
Figure 3.3 Dimensionless mass transfer correlation for the desorption of CO <sub>2</sub> from aqueous ethylene glycol solutions of varying strengths in a wetted wall column.....	82
Figure 3.4 Comparison of different dimensionless mass transfer correlations for a wetted wall column .....	83
Figure 3.5 Extraction of CO <sub>2</sub> solubility based on the outlet partial pressure for 50 wt% aqueous solution of MDEA at a loading of 0.044.....	89
Figure 3.6 Extraction of CO <sub>2</sub> solubility based on the log mean partial pressure and normalized flux for 50 wt% aqueous solution of MDEA at a loading of 0.044.....	90
Figure 3.7 Extraction of CO <sub>2</sub> solubility based on the log mean partial pressure and normalized flux for 50 wt% aqueous solution of DEA at a loading of 0.613 .....	91
Figure 3.8 Normalized CO <sub>2</sub> solubility from interpolation of log mean P <sub>CO2</sub> in a 50 wt% aqueous solution of DEA..	

Curves refer to the VLE model (Austgen, 1989) predictions. Points are the experimental data.....	92
Figure 3.9 Normalized CO <sub>2</sub> solubility from interpolation of log mean P <sub>CO2</sub> in a 50 wt% aqueous solution of MDEA.. Curves refer to the VLE model (Austgen, 1989) predictions. Points are the experimental data.....	95
Figure 3.10 Normalized CO <sub>2</sub> solubility from interpolation of log mean P <sub>CO2</sub> in a 50 wt% aqueous amine solution with 10 mol% DEA and 90 mol% MDEA.....	96
Figure 3.11 Normalized CO <sub>2</sub> solubility from interpolation of log mean P <sub>CO2</sub> in a 50 wt% aqueous amine solution with 50 mol% DEA and 50 mol% MDEA.....	97
Figure 3.12 Comparison of experimental data on CO <sub>2</sub> solubility from interpolation of log mean P <sub>CO2</sub> at 25° C to VLE model.....	99
Figure 3.13 Comparison of experimental data on CO <sub>2</sub> solubility from interpolation of log mean P <sub>CO2</sub> at 40° C to VLE model.....	100
Figure 3.14 VLE model (Austgen, 1989) prediction versus experimental data for CO <sub>2</sub> solubility in 50 wt% blended amines with 10%DEA-90%MDEA and 50%DEA- 50%MDEA (mole basis) at 25°C .....	101
Figure 3.15 VLE model (Austgen, 1989) prediction versus experimental data for CO <sub>2</sub> solubility in 50 wt% blended amines with 10%DEA-90%MDEA and 50%DEA- 50%MDEA (mole basis) at 40°C .....	102

Figure 3.16 Normalized flux of CO <sub>2</sub> as a function of loading at 25°C for 50 wt% amines.....	105
Figure 3.17 Normalized flux of CO <sub>2</sub> as a function of loading at 40°C for 50 wt% amines.....	106
Figure 3.18 Predicted and experimental pseudo first order rate constants at 25°C as a function of loading.....	118
Figure 3.19 Predicted and experimental pseudo first order rate constants at 40°C as a function of loading.....	119
Figure 3.20 Comparison of predicted to experimental values of the rate constants as a function of loading .....	120
Figure 3.21 Comparison of predicted to experimental values of rate constants as a function of mole fraction of free DEA.....	121
Figure 3.22 Contribution of different mechanisms to the pseudo first order rate constant for 10% DEA - 90% MDEA as a function of loading at 40°C.....	124
Figure 3.23 Contribution of different mechanisms to the pseudo first order rate constant for 50% DEA - 50% MDEA as a function of loading at 40°C.....	125
Figure G.1 Comparison of experimental data on CO <sub>2</sub> solubility at 25° C to VLE model (Austgen, 1989) prediction .....	183
Figure G.2 Comparison of experimental data on CO <sub>2</sub> solubility at 40° C to VLE model (Austgen, 1989) prediction .....	184
Figure G.3 VLE model (Austgen, 1989) prediction versus experimental data for CO <sub>2</sub> solubility in 50 wt% blended	

amines with 10%DEA-90%MDEA and 50%DEA-50%MDEA (mole basis) at 40°C .....	185
Figure G.4 Extraction of CO <sub>2</sub> solubility based on the log mean partial pressure and normalized flux for 50 wt% aqueous solution of MDEA at a loading of 0.044.....	186
Figure G.5 Normalized flux of CO <sub>2</sub> as a function of loading at 40°C for 50 wt% amines.....	187
Figure G.6 Predicted and experimental pseudo first order rate constants at 25°C as a function of bulk loading.....	188
Figure G.7 Comparison of predicted to experimental values of rate constants as a function of mole fraction of free DEA.....	189
Figure G.8 Contribution of different mechanisms to the pseudo first order rate constant for 10% DEA - 90% MDEA as a function of loading at 40°C.....	190
Figure G.9 Comparison of approximate to rigorous flux as a function of CO <sub>2</sub> partial pressure for loading = 0.01 mol CO <sub>2</sub> /mol amine, $k_L = 10^{-4}$ m/s, T = 40°C.....	191



## **CHAPTER ONE**

### **INTRODUCTION**

Acid gas removal, gas sweetening or gas treating are analogous terms and they refer to the removal of acid gases like  $\text{H}_2\text{S}$  and  $\text{CO}_2$  from gas streams. This process is a major component of natural gas refining. Other applications of this process are in oil refining, ammonia manufacture and sulfur recovery. Kohl and Riesenfeld (1985) provide a comprehensive review of acid gas treating technologies. Acid gas absorption is typically accomplished by absorbing into an aqueous alkanolamine solution (Astarita et al., 1983). This technique dates over 60 years when Bottoms (1930) patented a process to remove  $\text{CO}_2$  using alkanolamines.

#### **1.1 Process Flowsheet of an Acid Gas Treating Unit**

Figure 1.1 is a schematic of a typical absorber/stripper system for the removal of acid gas. The sour gas with a high content of  $\text{CO}_2$  and  $\text{H}_2\text{S}$  enters the bottom of the absorber where it is contacted countercurrently with the

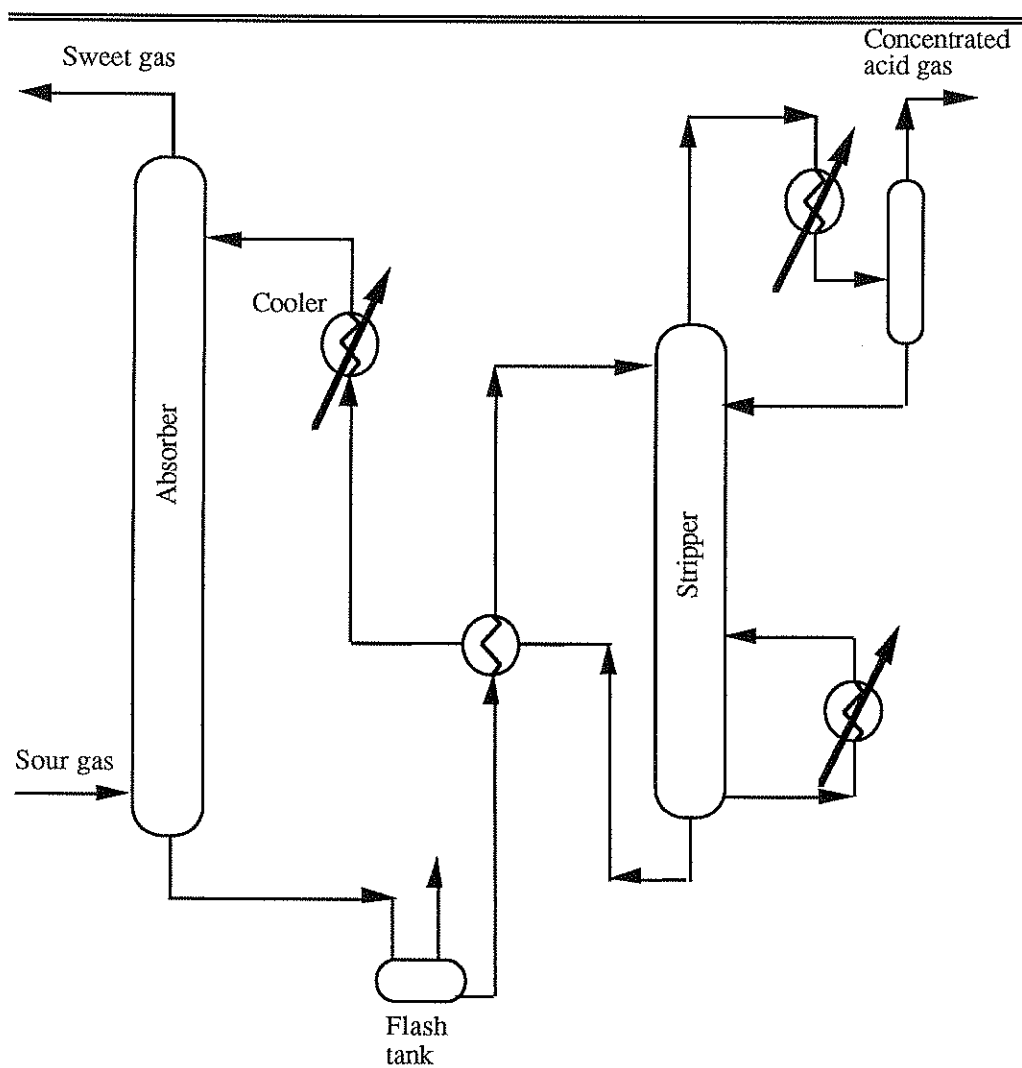


*Figure 1.1 Typical Absorber/Stripper System for Acid Gas Removal*

alkanolamine solution. The absorption of acid gases into an alkanolamine solution is an exothermic process. The operating temperature is around 40°C. The sweet gas emerges from the top while the loaded solution goes to the flash tank for removal of hydrocarbons from the bottom of the absorption tower. The solution is then heated to about 120°C and fed to the top of the countercurrent stripping column. The stripping is accomplished by means of reboiled steam. Steam reduces the vapor phase partial pressure of CO<sub>2</sub> and thus provides a driving force for desorption. The energy of the steam also serves to reverse the reactions of CO<sub>2</sub> and H<sub>2</sub>S with the alkanolamines. Blauwhoff et al. (1985) found that the reboiler heat duty is the most significant operating cost. The lean solution emerging from the bottom of the stripping column is cooled to 40°C and sent to the absorber. The outlet gas from the top of the stripper when rich in H<sub>2</sub>S is sent to a Claus unit for recovery of elemental sulfur. The absorption and stripping columns are either packed columns or tray towers.

## **1.2 Alkanolamines and their applications**

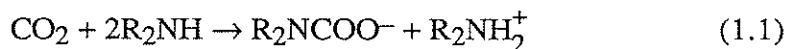
Alkanolamines contain both hydroxyl and amino groups. The hydroxyl groups serve to reduce the vapor pressure as well as enhance solubility in water. The amino group provides the basicity necessary to absorb the acid gases.

Reaction of H<sub>2</sub>S with aqueous alkanolamines proceeds through an essentially instantaneous mechanism of proton transfer. Carbon dioxide reacts

at a finite rate with alkanolamines making liquid phase mass transfer the controlling step. Most often, the gas phase resistance can be neglected for CO<sub>2</sub>. The reaction rates vary for different alkanolamines and govern the choice of solvents for a given application - bulk removal of acid gases or selective removal of H<sub>2</sub>S.

Commercially used alkanolamines primarily include monoethanolamine (MEA), diethanolamine (DEA), and methyldiethanolamine (MDEA). Other amines that have found industrial use are diglycolamine (DGA) and diisopropanolamine (DIPA). A category of alkanolamines referred to as hindered amines is also gaining industrial popularity. Rochelle et al. (1992) review the performance of some proprietary hindered amines most of which have been manufactured by Exxon..

MEA (a primary amine) and DEA (a secondary amine) have fast rates of reaction with CO<sub>2</sub>. For this reason, they have been used for bulk removal of acid gases. The heats of reaction are 20 kcal/mole and 16 kcal/mole respectively (Kohl and Riesenfeld, 1985). The reaction proceeds through the formation of a stable carbamate which restricts the capacity to absorb CO<sub>2</sub>.



The stoichiometry of reaction 1.1 indicates that to absorb 1 mole of CO<sub>2</sub>, two moles of amine are required.

MDEA (a tertiary amine) reacts at a much slower rate with CO<sub>2</sub> with a heat of reaction of 11.6 kcal/mole (Kohl and Riesenfeld, 1985). MDEA finds an automatic application in the selective removal of H<sub>2</sub>S. The reaction with CO<sub>2</sub> proceeds through the formation of bicarbonate.



To remove one mole of CO<sub>2</sub>, one mole of MDEA is necessary indicating that MDEA has a higher capacity to absorb CO<sub>2</sub> as compared to DEA and MEA. Also the lower heat of reaction with MDEA reduces the energy requirements in the regeneration process. Due to corrosion problems MEA is used in 10-20 wt% solutions and DEA in 20-35 wt% solutions. MDEA is much less corrosive and can be used in 50 wt% solutions which could compensate to a certain extent for the slow rate of reaction and hence favor the use of MDEA for bulk removal of acid gases too.

A novel technique to accelerate this reaction is to add small amounts of MEA or DEA to promote the rate of reaction. This has been found to significantly enhance the absorption rate of CO<sub>2</sub> into the MDEA based solvent while retaining the low energy requirement (Polasek et al., 1990, Campbell and Weiland, 1989; Critchfield, 1988; Katti and Wolcott, 1987).

### **1.3 Objectives and scope of this work**

This effort has focused on two areas:

1. Modeling the absorption of CO<sub>2</sub> into blends of DEA and MDEA using ASPEN PLUS, a commercial simulator.
2. Measuring the absorption rates of CO<sub>2</sub> into concentrated aqueous blends (50 wt%) of MDEA and DEA.

Absorption of CO<sub>2</sub> into an aqueous alkanolamine solution occurs by gas liquid mass transfer with chemical reaction at the interface. Often approximate techniques are used to solve this problem since a rigorous approach would involve solution of a system of differential and algebraic equations. The approximations help reduce it to a set of algebraic equations.

The modeling effort is to a large extent based on the work of Glasscock (1990), Glasscock and Rochelle (1990) and Carey (1990). Glasscock and Rochelle (1990) took into account all possible reactions in a CO<sub>2</sub>-DEA-MDEA system but developed approximations for the prediction of absorption rates. The predictions of absorption fluxes from this technique compared well with the results from the rigorous calculations of Glasscock (1990). Carey initiated the work with ASPEN PLUS in his attempts to build a system model of the acid gas treating unit.

The main goal of this work was to develop the approximate approach in the framework of ASPEN PLUS. This involved modeling of a single stage contactor to handle bench scale experimental data. An attempt was also made to use RATEFRAC, a rate-based model to handle this problem so that the approximate approach could be scaled up to do system modeling.

Glasscock (1990) and Critchfield (1988) have measured absorption rates of CO<sub>2</sub> into blends of MDEA and DEA up to amine concentrations of 30 wt%. There is no experimental data in the literature that describes the kinetics of CO<sub>2</sub> absorption into blends of 50 wt%.

The objective of the experimental work was to obtain the absorption rate of CO<sub>2</sub> into 50 wt% solutions of pure MDEA and DEA, and blends of 10 mol% DEA-90 mol% MDEA and 50 mol% DEA-50 mol% MDEA over a range of partial pressures from 0.001 - 1.0 atm at temperatures of 25°C and 40°C. Loading was varied from 0 to 0.6. The contactor used was a wetted wall column.

## **CHAPTER TWO**

### **MODELING**

Absorption of CO<sub>2</sub> into an alkanolamine solution occurs by gas liquid mass transfer with chemical reaction at the interface. Different theories have been proposed to explain this phenomenon. Prominent among them are the film theory (Lewis and Whitman, 1924), penetration theory (Higbie, 1935) and the surface renewal theory (Danckwerts, 1951). Researchers have used these theories and approached the gas absorption problem using analytical and numerical techniques. The applicability of analytical techniques is more limited. Tables 2.1 and 2.2 summarize numerical methods that have been used (Glasscock, 1990).

The rigorous solution to the problem of CO<sub>2</sub> absorption into an alkanolamine solution involves solving a set of differential and algebraic equations. Glasscock and Rochelle (1989) adopted this approach. Orthogonal collocation on finite elements was used in the spatial dimension. This resulted in a set of differential and algebraic equations for an unsteady-state theory which was integrated through time using DASSL (Petzold, 1983). A set of



**Table 2.1 Summary of Numerical Studies of Absorption with Chemical Reaction for the Unsteady-State Theories (Glasscock, 1990)**

<u>Author</u>	<u>Type of Reaction</u>	<u>Numerical Method Used</u>	
		<u>Space</u>	<u>Time</u>
Perry and Pigford (1953)	2nd-order, reversible, irreversible	finite differences	explicit Euler
Brian et al. (1961)	2nd-order, irreversible unequal diffusion coeff.	finite differences	Crank-Nicolson
Pearson (1963)	2nd-order, irreversible unequal diffusion coeff.	finite differences	Crank-Nicolson
Brian (1964)	general, irreversible $r=k[A]^n[B]^m$ , unequal diffusion coefficients	finite differences	Crank-Nicolson
Brian et al. (1961)	2 step second-order $A+B \Rightarrow C$ , $A+C \Rightarrow D$ A is absorbing species	finite differences time dependent transformation	Crank-Nicolson
Secor et al. (1967)	general, reversible $A + B \rightleftharpoons C + D$ unequal diffusion coeff.	finite differences w/ transformation	implicit Euler
Matheron et al. (1978)	2nd order, irreversible reaction, surface renewal theory	finite differences	Crank-Nicolson
Huang et al. (1980)	$A+B \Rightarrow C$ , $A+C \Rightarrow D$	collocation	method of lines
Cornelisse et al. (1980)	simultaneous absorption	finite differences	implicit 3-point backward formula
Carta and Pigford (1983)	NO in Nitric Acid	finite-difference	implicit finite difference
Ozturk and Shah (1986)	2nd order, irreversible, volatile liquid-phase reactant	collocation on finite elements time dep. trans.	method of lines
Versteeg (1986)	general, reversible	finite differences time dep. trans.	implicit, 3-point backward

**Table 2.2 Summary of Numerical Studies of Absorption with Chemical Reaction Using Film Theory (Glasscock, 1990)**

Author	Type of Reaction	Numerical Method Used
Brian and Beaverstock (1965)	2 step second-order $A+B \Rightarrow C$ , $A+C \Rightarrow D$ A is absorbing species	finite difference
Onda et al. (1970a),(1970b)	$A+B \rightleftharpoons C+D$	finite difference
Huang et al. (1980)	$A+B \Rightarrow C$ , $A+C \Rightarrow D$	collocation
Carta and Pigford (1983)	NO in Nitric Acid	finite-difference
Ozturk and Shah (1986)	2nd order, irreversible, volatile liquid-phase reactant	collocation on finite elements

coupled, nonlinear algebraic equations result for a steady-state theory which was solved using DASSL. This approach was applied to the film, penetration and surface renewal theories.

In addition to the aforementioned theories, Glasscock and Rochelle (1989) used two steady-state theories - approximate film theory (Chang and Rochelle, 1982) and a simplified steady-state form of the eddy diffusivity theory (Prasher and Fricke, 1974). The eddy diffusivity theory was first conceived by King (1966) to account for turbulent flow. All other theories assume laminar flow in the boundary layer.

Use of a rigorous method would imply large computation times, a high degree of complexity and significant numerical difficulties. This necessitates

use of simplifying approximations. The simplest example would be the pseudo-first order approximation (Danckwerts, 1970). This however neglects the mass transfer effects in the liquid phase.

Glasscock and Rochelle (1990) developed an approximation for prediction of the absorption rate while accounting for reactions by means of a rigorous mechanism. The kinetics and mass transfer effects are accounted for by means of an enhancement factor. This method involved iteratively solving a set of algebraic equations. The predictions from this approximate method compared favorably with the exact solutions (Glasscock and Rochelle, 1990).

The present work seeks to develop the aforementioned approximate technique (with a few modifications) within the framework of ASPEN PLUS, a commercial simulator with excellent flowsheeting capabilities. The primary reasons for using ASPEN PLUS are :

1. The rigorous thermodynamic package for the CO<sub>2</sub>-H<sub>2</sub>S-MDEA-DEA electrolyte system (Austgen, 1989).
2. An easy input-output format.
3. The facility to supply user FORTRAN routines to model the kinetics and mass and heat transfer.
4. The rate-based modeling block, RATEFRAC.

5. Scaling from bench scale experiment modeling to system modeling would be simplified.

The two tasks addressed in this modeling effort were:

1. Modeling of single stage contactors by accounting for the effects of both mass transfer and chemical reaction. Two approaches were developed. One approach used constant activity coefficients based on equilibrium while the other accounted for the effect of changing composition at the interface on activity coefficients.
2. Investigating the feasibility of using RATEFRAC.

Carey (1990) developed the initial version for the FORTRAN kinetic routine and proposed an algorithm for estimation of enhancement factor for use with RATEFRAC as part of his system modeling effort. These have undergone changes which will be discussed in detail.

## **2.1 Features of Aspen Plus**

### **2.1.1 Creating and running an ASPEN input file**

In order to do a simulation using ASPEN PLUS it is necessary to write an input file in the ASPEN language. The key steps (ASPEN PLUS User Guide, 1988) include defining the process flowsheet, specifying units, components, physical property models to be used, splitting the flowsheet into a

series of unit operation blocks, describing the connectivity, defining the feed streams and setting design specifications and sensitivity analyses. Rate or equilibrium governed reactions are defined in the REACTIONS paragraph. It should be noted that only non-ionic or molecular species can be specified here. Ionic equilibria (as in an electrolyte system) are defined in the CHEMISTRY paragraph (ASPEN PLUS Electrolytes Manual, 1988). Components not present in the databanks of ASPEN PLUS can be simulated by specifying the requisite physical properties and parameters. This has been done for MDEA.

ASPEN PLUS has a preprocessor simulation system. Running an ASPEN input file involves four steps:

1. input translation ( internal generation of an equivalent program in FORTRAN).
2. compilation of the FORTRAN code.
3. module creation
4. simulation program execution

An in-depth explanation is provided in Chapter 8 of the ASPEN PLUS System Maintenance Guide, VAX/VMS Version (1988).

### 2.1.2 Apparent and True Components

When handling electrolyte systems in ASPEN PLUS, there exist two choices - apparent and true component approaches. The apparent component approach considers only molecular (non-ionic) species. The true component approach considers ions as well, implying that it distinguishes between the physically dissolved and chemically combined forms of the electrolyte. Figure 2.1 illustrates the difference for a  $\text{CO}_2\text{-H}_2\text{S-DEA-MDEA}$  system.

It is necessary to define two new apparent components carbonic acid and carbamic acid in order to formulate the reactions since the REACTIONS paragraph in ASPEN PLUS can handle only non-ionic species. Typically, the apparent component approach is adopted in this work.

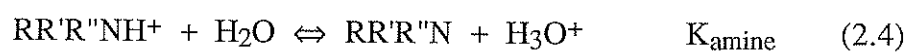
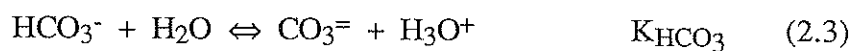
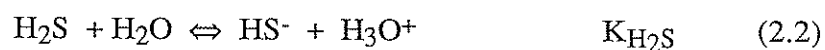
The apparent components can be speciated into true species within any FORTRAN subroutine by using the FLASH routine in ASPEN PLUS (ASPEN PLUS Notes on Interfaces and User Models, 1988). This speciation requires equilibrium information to be specified in the CHEMISTRY paragraph.

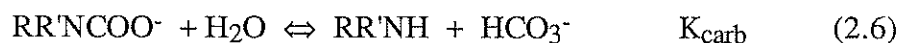
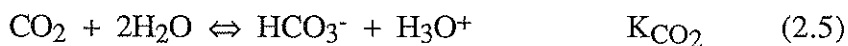
Apparent components	True components
H <sub>2</sub> O	H <sub>2</sub> O, H <sub>3</sub> O <sup>+</sup> , OH <sup>-</sup>
MDEA	MDEA, MDEAH <sup>+</sup>
DEA	DEA, DEAH <sup>+</sup>
CO <sub>2</sub>	CO <sub>2</sub>
H <sub>2</sub> CO <sub>3</sub>	HCO <sub>3</sub> <sup>-</sup> , CO <sub>3</sub> <sup>=</sup>
Carbamic acid (CARB)	DEACOO <sup>-</sup>

*Figure 2.1 Apparent and true components in the nomenclature of ASPEN PLUS*

### 2.1.3 Equilibrium

The distribution of an electrolyte in the liquid phase between its free molecular and chemically combined or ionic forms depends on the ionic equilibria. CO<sub>2</sub> and H<sub>2</sub>S react through an acid-base buffer mechanism in an aqueous alkanolamine solution (Austgen, 1989). The various equilibria considered in this work are :





The mole fraction based equilibrium constants for reactions 2.1 to 2.6 are displayed in Table 2.3. In addition to these there are two equilibria relating to carbonic acid and carbamic acid which are discussed in Section 2.2.1.

#### 2.1.4 Physical Properties and Models

The property set that would be most suitable for the  $\text{CO}_2$ - $\text{H}_2\text{S}$ -DEA-MDEA system is SYSOP15M which has the capability to handle electrolyte systems. In this model, the Redlich-Kwong-Soave equation of state is used to estimate fugacity coefficients in the vapor phase while the NRTL (Non Random Two Liquid) equation calculates activity coefficients in the liquid phase. For more details, one could refer to the ASPEN PLUS Electrolytes Manual (1988).

It is necessary to supply properties for the alkanolamines DGA, DEA, MDEA and their corresponding ionic species i.e. protonated amine and carbamate. For  $\text{CO}_2$  and  $\text{H}_2\text{S}$ , some additional properties like Henry's constants (Table 2.4), NRTL interaction parameters and Rackett parameters need to be specified. The property data are supplied to the input files through a user insert library (ASPEN PLUS System Maintenance Manual, 1988).

The insert library used in this work is essentially the thermodynamic package developed by Austgen (1989). The binary parameters for the Rackett



equation are tabulated in Table 2.5. These are used in the estimation of densities of mixtures. Tables 2.6, 2.7 and 2.8 contain information about critical properties, vapor pressures and dielectric constants for the amines.

**Table 2.3 Mole Fraction- Based Equilibrium Constants Used in the Model (Austgen, 1989)**

$\ln K_i = C_1 + C_2/T + C_3 \ln T + C_4 T$						
Rxn #	Comp	C <sub>1</sub>	C <sub>2</sub>	C <sub>3</sub>	C <sub>4</sub>	Source
2.1	H <sub>2</sub> O	132.899	-13445.9	-22.4773	0.0	a
2.2	H <sub>2</sub> S	214.582	-12995.4	-33.5471	0.0	a
2.5	CO <sub>2</sub>	231.465	-12092.1	-367816	0.0	a
2.3	HCO <sub>3</sub> <sup>-</sup>	216.049	-12431.7	-354819	0.0	a
2.4	MEA	2.1211	-8189.38	0.0	-0.007484	b
2.4	DEA	-6.7936	-5927.65	0.0	0.0	c
2.4	MDEA	-9.4165	-4234.98	0.0	0.0	d
2.4	DGA	1.6957	-8431.65	0.0	-0.005037	e
2.6	MEA	2.8898	-3635.09	0.0	0.0	f
2.6	DEA	4.5146	-3417.34	0.0	0.0	f
2.6	DGA	8.8334	-5274.4	0.0	0.0	f

*a - Edwards et al. (1978); b - Bates and Pinching (1951); c - Bower et al. (1962); d - Schwabe et al. (1959); e - Dingman et al. (1983); f - Austgen (1990)*

**Table 2.4 Henry's Constant Expressions for H<sub>2</sub>S and CO<sub>2</sub>**  
**(Austgen, 1989)**

$\ln H_i \text{ (Pa)} = C_1 + C_2/T + C_3 \ln T + C_4 T$						
	C <sub>1</sub>	C <sub>2</sub>	C <sub>3</sub>	C <sub>4</sub>	Temperature (°C)	Source
H <sub>2</sub> S	358.138	-13236.8	-55.0551	0.059565	0 - 150	a
CO <sub>2</sub>	170.7126	-8477.711	-21.9574	0.005781	0 - 100	b

*a - Edwards et al. (1978); b - Chen et al. (1979).*

**Table 2.5 Rackett Binary Interaction Parameters (Austgen, 1989)**

$k_{ij} = 1.0 - \left[ \frac{2 \sqrt{V_{ci}^{1/3} V_{cj}^{1/3}}}{V_{ci}^{1/3} + V_{cj}^{1/3}} \right]^3$							
Comp.	H <sub>2</sub> O	MDEA	DEA	MEA	DGA	CO <sub>2</sub>	H <sub>2</sub> S
H <sub>2</sub> O	0.0	0.1442	0.1286	0.07696	0.1203	0.01115	0.01331
MDEA	0.1442	0.0	5.87E-4	0.01286	1.41E-3	0.08107	0.07593
DEA	0.1286	5.87E-4	0.0	7.99E-3	1.77E-4	0.06873	0.06395
MEA	0.077	0.01286	7.99E-3	0.0	5.80E-3	0.03118	0.02788
DGA	0.1203	1.41E-3	1.77E-4	5.80E-3	0.0	0.06234	0.05776
CO <sub>2</sub>	0.0112	0.08107	0.06873	0.03118	0.06234	0.0	9.77E-5
H <sub>2</sub> S	0.0133	0.07593	0.06395	0.02788	0.05776	9.77E-5	0.0

**Table 2.6 Pure Component Molecular Weight and Critical Properties for DEA, MDEA, and DGA (Austgen, 1989)**

Comp.	MW	T <sub>c</sub> (°K)	P <sub>c</sub> (kPa)	V <sub>c</sub> $\frac{\text{m}^3}{\text{kmol}}$	Z <sub>c</sub>	$\omega$	Source
DEA	105.14	715.0	3270.0	0.3490	0.192	1.046	a
MDEA	119.16	677.8	3876.1	0.3932	0.192	1.242	b
DGA	105.14	674.6	4354.9	0.327	0.254	1.046	c

*a - Daubert and Danner, DIPPR Data Tables (1985); b - Peng (1988) ;  
c - Texaco Chemical Company.*

Though the properties of MEA and DGA have been displayed, DEA and MDEA are the only alkanolamines of interest in this work. The aqueous databank (ASPEN PLUS Electrolytes Manual, 1988) contains the requisite data for bicarbonate, carbonate and carbamate ions. Carbonic acid and carbamic acid are ascribed the properties of the bicarbonate and carbamate ions respectively. Care is taken to specify a zero ionic charge.

Though ASPEN PLUS calculates density, viscosity and diffusivity, in this work, empirical correlations are used to estimate these properties (Appendix B). This is because the ASPEN estimates are likely to be in error for electrolyte systems.

Table 2.7 Pure Component Vapor Pressures of H<sub>2</sub>O, MEA, DEA, MDEA, and DGA (Austgen, 1989)

Amine	$\ln P^0 \text{ (Pa)} = D_1 + \frac{D_2}{T + D_3} + D_4 T + D_5 \ln T + D_6 T^D_7$							Temp (°C)	Source
	D <sub>1</sub>	D <sub>2</sub>	D <sub>3</sub>	D <sub>4</sub>	D <sub>5</sub>	D <sub>6</sub>	D <sub>7</sub>		
H <sub>2</sub> O	72.55	-7206.7	0.0	0.0	-7.1385	4.046E-6	2	0-374	a
MEA	172.78	-13492.0	0.0	0.0	-21.914	1.3779E-5	2	10-365	
DEA	286.01	-20360.0	0.0	0.032378	-40.422	3.2378E-2	1	28-269	a
MDEA	26.137	-7588.5	0.0	0.0	0.0	0.0	0.0	120-240	b
DGA	20.86	-3314.6	-140.83	0.0	0.0	0.0	0.0	not reported	c

a - Daubert and Danner, DIPPR Data Tables (1985); b - Dow Chemical Co. (1987); c - Sheu (1989).

**Table 2.8 Dielectric constants for pure MEA, DEA, MDEA, and DGA (Austgen, 1989)**

$d_i = A + B \left[ \frac{1}{T} - \frac{1}{273} \right]$			
Amine	A	B	Source
MEA	36.76	14836.0	a
DEA	28.01	9277.0	a
MDEA	24.74	8989.3	b
DGA	28.01	9277.0	*

*a - Ikada et al. (1968); b - Austgen (1989); \* - value arbitrarily set equal to DEA.*

The interaction parameters between all molecules and electrolytes (ion pairs) need to be supplied to the NRTL model. These parameters for the CO<sub>2</sub>-H<sub>2</sub>S-H<sub>2</sub>O-alkanolamine system were obtained by extensive regression of experimental VLE data (Austgen, 1989). These were performed using the data regression system in ASPEN PLUS (ASPEN PLUS Data Regression Manual, 1988). The only molecule-molecule interactions that Austgen (1989) fit with statistical significance were pairs that contained water. All other values were set to zero. The details are in Table 2.9. The only molecule-ion pair and ion pair-molecule parameters that could be estimated with statistical significance were pairs that contained water as the molecule and ion pairs of protonated amine combined with bicarbonate, bisulphide or carbamate ions. All other water-ion

pair and ion pair-water values were set to 8 and -4 respectively. All other molecule-ion pair and ion pair-molecule values were set to 15 and -4 respectively. Table 2.10 contains the values of these parameters.

**Table 2.9 NRTL Molecular Interaction Parameters Used in the Model (Austgen, 1989)**

Accentric Factor=0.2 $\tau = a + b/T$		
Molecule Pair	a	b
H <sub>2</sub> O - MEA	1.674	0.00
MEA - H <sub>2</sub> O	0.000	-649.75
H <sub>2</sub> O - DEA	-0.965	1317.63
DEA - H <sub>2</sub> O	-0.661	-718.08
H <sub>2</sub> O - MDEA *	0.000	0.00
MDEA - H <sub>2</sub> O *	0.000	0.00
H <sub>2</sub> O - DGA	1.992	0.00
DGA - H <sub>2</sub> O	0.000	-770.41
H <sub>2</sub> O - H <sub>2</sub> S	-3.674	1155.9
H <sub>2</sub> S - H <sub>2</sub> O	-3.674	1155.9
H <sub>2</sub> O - CO <sub>2</sub>	10.064	-3268.14
CO <sub>2</sub> - H <sub>2</sub> O	10.064	-3268.14

\* These values were fit by Austgen (1989) but then later set to zero when fitting the molecule-ion pair parameters.

**Table 2.10 NRTL Molecule - Ion Pair Interaction Parameters**  
**Used in the Model (Austgen, 1989)**

Accentric Factor =0.2 $t = a + b/T$		
Molecule - Ion Pair	a	b
<b><u>MEA = RNH<sub>2</sub></u></b>		
H <sub>2</sub> O - (MEA <sup>+</sup> , HS <sup>-</sup> )	6.844	501.83
(MEA <sup>+</sup> , HS <sup>-</sup> ) - H <sub>2</sub> O	-3.560	-197.12
H <sub>2</sub> O - (MEA <sup>+</sup> , HCO <sub>3</sub> <sup>-</sup> )	4.550	1218.19
(MEA <sup>+</sup> , HCO <sub>3</sub> <sup>-</sup> ) - H <sub>2</sub> O	-4.088	0.0
H <sub>2</sub> O - (MEA <sup>+</sup> , MEACOO <sup>-</sup> )	10.268	0.0
(MEA <sup>+</sup> , MEACOO <sup>-</sup> ) - H <sub>2</sub> O	-5.098	0.0
<b><u>DGA = RNH<sub>2</sub></u></b>		
H <sub>2</sub> O - (DGA <sup>+</sup> , HS <sup>-</sup> )	7.744	375.72
(DGA <sup>+</sup> , HS <sup>-</sup> ) - H <sub>2</sub> O	-4.337	0.0
H <sub>2</sub> O - (DGA <sup>+</sup> , HCO <sub>3</sub> <sup>-</sup> )	0.0	2960.94
(DGA <sup>+</sup> , HCO <sub>3</sub> <sup>-</sup> ) - H <sub>2</sub> O	-4.251	0.0
H <sub>2</sub> O - (DGA <sup>+</sup> , DGACOO <sup>-</sup> )	11.424	0.0
(DGA <sup>+</sup> , DGACOO <sup>-</sup> ) - H <sub>2</sub> O	-5.328	0.0
<b><u>DEA = R<sub>2</sub>NH</u></b>		
H <sub>2</sub> O - (DEA <sup>+</sup> , HS <sup>-</sup> )	5.199	1519.60
(DEA <sup>+</sup> , HS <sup>-</sup> ) - H <sub>2</sub> O	-2.836	-636.95
H <sub>2</sub> O - (DEA <sup>+</sup> , HCO <sub>3</sub> <sup>-</sup> )	4.204	1588.19
(DEA <sup>+</sup> , HCO <sub>3</sub> <sup>-</sup> ) - H <sub>2</sub> O	-4.434	0.0
H <sub>2</sub> O - (DEA <sup>+</sup> , DEACOO <sup>-</sup> )	11.549	102.66
(DEA <sup>+</sup> , DEACOO <sup>-</sup> ) - H <sub>2</sub> O	-5.580	0.0
<b><u>MDEA = R<sub>3</sub>N</u></b>		
H <sub>2</sub> O - (MDEA <sup>+</sup> , HS <sup>-</sup> )	3.735	1036.04
(MDEA <sup>+</sup> , HS <sup>-</sup> ) - H <sub>2</sub> O	-3.225	01.1.0
H <sub>2</sub> O - (MDEA <sup>+</sup> , HCO <sub>3</sub> <sup>-</sup> )	5.864	1147.90
(MDEA <sup>+</sup> , HCO <sub>3</sub> <sup>-</sup> ) - H <sub>2</sub> O	-4.511	0.0
H <sub>2</sub> O - (MDEA <sup>+</sup> , RHNCOO <sup>-</sup> )	9.903	0.0
(MDEA <sup>+</sup> , RHNCOO <sup>-</sup> ) - H <sub>2</sub> O	-4.776	0.0
H <sub>2</sub> O - (MDEA <sup>+</sup> , DEACOO <sup>-</sup> )	10.387	0.0
(MDEA <sup>+</sup> , DEACOO <sup>-</sup> ) - H <sub>2</sub> O	-4.965	0.0

Glasscock (1990) used the Electrolyte-NRTL model for rate data simulation and developed a stand-alone equilibrium model to do data regression. The approach was based on the ASPEN model used by Austgen (1989). Using equilibrium constants from Austgen (1989), Glasscock regressed new binary interaction parameters. These regressed parameters do not cover a wide range of temperatures and hence do not show temperature dependence. Table 2.11 compares the parameters regressed by Glasscock (1990) to those by Austgen at 298K. The work in this chapter uses the parameters obtained by Glasscock (1990).

## **2.2 Reactions**

The reaction of CO<sub>2</sub> with primary and secondary alkanolamines proceeds through the formation of carbamate and with tertiary alkanolamines through the formation of bicarbonate. Consequently, for a blend of DEA and MDEA reactions occur through both pathways.

### **2.2.1 Rate-limited reactions**

Keeping in mind the limitation that the REACTIONS paragraph in ASPEN PLUS can handle only non-ionic species (ASPEN PLUS, User Guide, 1988), the reactions are posed as follows:

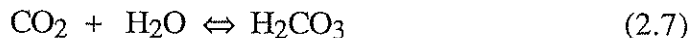




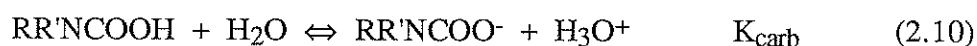
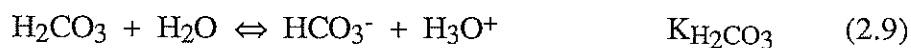
**Table 2.11 Equilibrium Regression Results (Glasscock, 1990)**

Interaction Parameter	Parameter Estimates	Austgen at 25°C
<b><u>MDEA system</u></b>		
H <sub>2</sub> O/MDEAH <sup>+</sup> ,HCO <sub>3</sub> <sup>-</sup>	8.61 ± 1.8%	9.71
MDEAH <sup>+</sup> /HCO <sub>3</sub> <sup>-</sup> ,H <sub>2</sub> O	-3.92 ± 1.7%	-4.25
<b><u>DEA system</u></b>		
H <sub>2</sub> O /DEAH <sup>+</sup> ,DEACOO <sup>-</sup>	12.4 ± 6.0%	11.89
DEAH <sup>+</sup> ,DEACOO <sup>-</sup> /H <sub>2</sub> O	-5.82 ± 7.4%	-5.58
H <sub>2</sub> O/DEAH <sup>+</sup> ,HCO <sub>3</sub> <sup>-</sup>	7.61 ± 4.0%	9.53
<b><u>MEA system</u></b>		
H <sub>2</sub> O/MEAH <sup>+</sup> ,MEACOO <sup>-</sup>	7.55 ± 8.7%	10.27
MEACOO <sup>-</sup> ,MEAH <sup>+</sup> /H <sub>2</sub> O	-3.78 <sup>c</sup>	-4.0 <sup>c</sup>
H <sub>2</sub> O/MEAH <sup>+</sup> ,HCO <sub>3</sub> <sup>-</sup>	4.24 ± 29%	8.64
HCO <sub>3</sub> <sup>-</sup> ,MEAH <sup>+</sup> /H <sub>2</sub> O	-2.12 <sup>c</sup>	-4.0 <sup>c</sup>
<b><u>DEA/MDEA system</u></b>		
H <sub>2</sub> O/MDEAH <sup>+</sup> ,DEACOO <sup>-</sup>	10.6 ± 10%	10.39
MDEAH <sup>+</sup> ,DEACOO <sup>-</sup> /H <sub>2</sub> O	-4.75 ± 11%	-4.97
<b><u>MEA/MDEA system</u></b>		
H <sub>2</sub> O/MDEAH <sup>+</sup> ,MEACOO <sup>-</sup>	11.0 ± 23%	9.90
MDEAH <sup>+</sup> ,MEACOO <sup>-</sup> /H <sub>2</sub> O	-5.5	-4.78

<sup>a</sup> Parameter estimates are expressed as  $\theta \pm \alpha$ , where  $\theta$  is the parameter estimate and  $\alpha$  is the relative standard deviation, i.e.  $\alpha = \sigma/\theta$ .

<sup>c</sup> These parameters could not be estimated with significance.

Reactions 2.5 and 2.6 are posed as kinetically controlled reactions in order to do rate-based modeling (Carey, 1990). The two new species, carbonic and carbamic acids, are related to the bicarbonate and carbamate ions through the following equilibria.



The equilibrium constants are set to a value of unity to ensure that carbonic acid completely dissociates to bicarbonate ion and carbamic acid completely dissociates to carbamate ion. One could also use the dissociation statement DISS to achieve this complete dissociation. But it was observed that this did run into problems occasionally. Hence the former was chosen.

The reaction rates for reactions 2.7 and 2.8 are rigorously expressed as a function of the activities of the various ionic species in this electrolyte system. The rates of formation of carbonic and carbamic acids are essentially the rates of formation of the bicarbonate and carbamate species respectively by virtue of large equilibrium constants for 2.9 and 2.10.

### 2.3.2 Bicarbonate reaction rate

The different paths by which bicarbonate is assumed to be formed are as follows (Glasscock and Rochelle, 1990):





The activity based rate expression for the net rate of formation of the bicarbonate species is expressed as:

$$R_{\text{HCO}_3} = [\mathbf{a}_{\text{CO}_2} - \mathbf{a}_{\text{CO}_2, \text{HCO}_3, \text{e}}] \left[ k'_{\text{tam w}} \mathbf{a}_{\text{tam}} \mathbf{a}_{\text{w}} + k'_{\text{tam OH}} \mathbf{a}_{\text{tam}} \mathbf{a}_{\text{OH}} + \frac{k'_{\text{OH}} \mathbf{a}_{\text{OH}}}{\rho} \right] \rho^3 \quad (2.14)$$

where  $\rho$  is the density of the solution.

$$k_{\text{HCO}_3} = \left[ k'_{\text{tam w}} \mathbf{a}_{\text{tam}} \mathbf{a}_{\text{w}} + k'_{\text{tam OH}} \mathbf{a}_{\text{tam}} \mathbf{a}_{\text{OH}} + \frac{k'_{\text{OH}} \mathbf{a}_{\text{OH}}}{\rho} \right] \rho^3 \quad (2.15)$$

$k_{\text{HCO}_3}$  could be interpreted as the pseudo first order constant for reaction through the bicarbonate mechanism. The activity based rate constants  $k'_{\text{tam w}}$  and  $k'_{\text{tam OH}}$  for 2.11 and 2.12 were obtained by regression of rate data (Glasscock et al., 1991). The rate constant  $k_{\text{OH}}$  for reaction 2.13 was obtained from literature (Astarita et al., 1983). Though it is a concentration based rate constant it was treated as an activity based rate constant by Glasscock et al. (1991). Though a thermodynamic inconsistency, to the extent that the contribution of reaction 2.13 is negligible, it is a valid assumption. Sections 2.3.4 and 2.3.5 will discuss necessary modifications to the rate constants and give the values used.

Reaction 2.11 could also be applicable for a primary or secondary amine like MEA or DEA (Carey, 1990). However Glasscock (1990) did not regress for this parameter. Hence in this work, the possibility suggested by Carey (1990) will not be considered.

Equation 2.14 accounts for the reversibility through  $a_{\text{CO}_2, \text{HCO}_3, e}$  which is the activity of  $\text{CO}_2$  in equilibrium with the bicarbonate ion.

$$a_{\text{CO}_2, \text{HCO}_3, e} = \frac{a_{\text{HCO}_3}}{K_{\text{CO}_2, \text{HCO}_3} a_{\text{OH}}} \quad (2.16)$$

$$K_{\text{CO}_2, \text{HCO}_3} = \frac{K_{\text{CO}_2}}{K_w} \quad (2.17)$$

$K_{\text{CO}_2}$  and  $K_w$  are equilibrium constants for reactions 2.1 and 2.5.

### 2.3.3 Carbamate reaction rate

Primary or secondary amines react with  $\text{CO}_2$  to form carbamate. For MEA the rate of carbamate formation is given as (Glasscock and Rochelle, 1990)

$$R_{\text{MEACOO}} = k'_{\text{pam}} [\text{CO}_2] [\text{MEA}] \quad (2.18)$$

The same rate expression and rate constant apply to DGA by substituting DGA for MEA in (2.18). This rate was found not to be affected in the mixed amine system (Glasscock and Rochelle, 1990).

The DEA system is more complicated. Carbamate can be formed by the following reactions:



Reaction 2.21 is exclusively for a blended amine system of DEA and MDEA. The net rate of carbamate formation in the general case of a mixed amine system is given as:

$$R_{\text{carb}} = a_{\text{am}} [a_{\text{CO}_2} - a_{\text{CO}_2, \text{carb}, e}] [k'_{\text{pam}} a_{\text{pam}} + k'_{\text{w}} a_{\text{w}} + k'_{\text{am}} a_{\text{am}} + k'_{\text{tam}} a_{\text{tam}}] \rho^3 \quad (2.22)$$

where  $k'_{\text{pam}}$  represents the rate constant for the reaction of MEA or DGA to form carbamate,  $k'_{\text{w}}$  represents reaction (2.19),  $k'_{\text{am}}$  represents (2.20), and  $k'_{\text{tam}}$  represents (2.21). These rate constants are also activity based and a detailed discussion follows in sections 2.3.4 and 2.3.5. For the MEA or DGA system,  $k'_{\text{am}}$ ,  $k'_{\text{tam}}$  and  $k'_{\text{w}}$  are set to zero while for the DEA system  $k'_{\text{pam}}$  is set to zero. The term  $a_{\text{CO}_2, \text{carb}, e}$  represents the activity for  $\text{CO}_2$  in equilibrium with the carbamate in solution and is dependent on the type of amine present. The pseudo first order constant for the carbamate mechanism could be expressed as

$$k_{\text{carb}} = [k'_{\text{pam}} + k'_{\text{am}} a_{\text{am}} + k'_{\text{tam}} a_{\text{tam}} + k'_{\text{w}} a_{\text{w}}] \rho^3 \quad (2.23)$$

For DEA, the activity of  $\text{CO}_2$  in equilibrium with the carbamate ion is given as:

$$a_{\text{CO}_2, \text{carb}, e} = \frac{a_{\text{w}} a_{\text{DEACOO}}}{K_{\text{CO}_2, \text{carb}} a_{\text{OH}} a_{\text{DEA}}} \quad (2.24)$$

$$K_{\text{CO}_2, \text{carb}} = \frac{K_{\text{CO}_2}}{K_{\text{DEACOO}} K_w} \quad (2.25)$$

$K_{\text{CO}_2}$ ,  $K_{\text{DEACOO}}$  and  $K_w$  are equilibrium constants of reactions 2.5, 2.6 and 2.1 respectively.

#### 2.3.4 Effect of ionic strength

In non-ideal systems, it would be necessary to have activity based rate expressions as in equations 2.14 and 2.22. Though this accounts for non-idealities it does not compensate for the effects of changing non-idealities as a function of ionic strength. This is done by multiplying the rate constant by a factor beta

$$k' = k \beta \quad (2.26)$$

where  $\beta$  could take different functional forms (Glasscock, 1990). One limiting form is

$$\beta = \prod_{i=1}^{N_r} \gamma_i^{v_{ij}} \quad (2.27)$$

where  $N_r$  is the number of reactants,  $\gamma$  is the activity coefficient and  $v$  is the stoichiometric coefficient. Applying equation 2.27 to 2.26 adjusts only the reverse rate constant as a function of changing non-idealities.

The other limiting form is

$$\beta = \prod_{i=1}^{N_p} \gamma_i^{-\nu_{ij}} \quad (2.28)$$

where  $N_p$  is the number of products.

Applying equation 2.28 to equation 2.26 adjusts only the forward rate constant as a function of changing ionic strength. Since this form provided a better fit to the experimental data over a wide range of ionic strengths it was chosen by Glasscock et al. (1991). In this work, the same form is chosen. The reaction rate expressions 2.14 and 2.22 use the modified rate constants.

For example, the modified rate constant for reaction 2.11 would be

$$k'_{\text{tam w}} = \frac{k_{\text{tam w}}}{\gamma_{\text{HCO}_3^-} \gamma_{\text{MDEAH}^+}} \quad (2.29)$$

It is important to realize that the correction factor  $\beta$  has to be applied to each of the mechanisms by which the reaction can proceed which in this case are 2.11, 2.12 and 2.13 for bicarbonate formation and 2.19, 2.20 and 2.21 for carbamate formation. It is different for each one of them.

### 2.3.5 Conversion of rate constants from concentration based activities to mole fraction based activities

As mentioned before, Glasscock (1990) obtained the rate constants by regressing experimental rate data. The rate constants were fit to the form:

$$k_i = k_{298} \exp\left(-\frac{E_a}{R} \left(\frac{1}{T} - \frac{1}{298}\right)\right) \quad (2.30)$$

The activation energy and pre-exponential factor were obtained by regression. Their values are shown in Table 2.12. The rate constant values are for concentration based activities. In order to use the rate constants in expressions (2.14) and (2.22), a conversion is necessary to account for mole fraction based activities. Carey (1990) proposed that to convert from the concentration scale to the mole fraction basis, the values of  $k_{298}$  be multiplied by the cube of the density of water at 298°C. It has been found that while this factor maintains consistency of units it yields inconsistent results. A more appropriate conversion factor would be the cube of the density of the solution. Equation 2.14 could then be modified to the form

$$R_{HCO_3} = \gamma_{CO_2} [C_{CO_2} - C_{CO_2, HCO_3, e}] \left[ k'_{tam, w} \gamma_{tam} C_{tam} \gamma_w C_w + k'_{tam, OH} \gamma_{tam} C_{tam} \gamma_{OH} C_{OH} k'_{OH} \gamma_{OH} C_{OH} \right] \quad (2.31)$$

Equation 2.31 directly corresponds to the form used by Glasscock and Rochelle (1990).

The density of the solution is calculated on the basis of the physical property correlation in Appendix B.3. This calculation is performed at each



loading for each solution. Rate constants (for mole fraction based activities) for a typical value of density of  $33.5 \frac{\text{kmol}}{\text{m}^3}$  are also shown in Table 2.12.

**Table 2.12 Rate Parameters Used (Glasscock, 1990)**

Rate Expression	Parameter Estimates		
	$k_{298}^a$ ( $\text{m}^6/\text{kmol}^2\text{-s}$ )	$E_a$ ( $\text{kcal}/\text{kmol}\text{-K}$ )	$k_{298}^c$ ( $\text{kmol}/\text{m}^3\text{-s}$ )
<b>DEA parameters</b>			
$k_1(\text{DEA})(\text{H}_2\text{O})(\text{CO}_2)$	30.0	11000	$1.13 \times 10^6$
$k_2(\text{DEA})(\text{DEA})(\text{CO}_2)$	18500	9314	$6.96 \times 10^8$
<b>DEA/MDEA parameters</b>			
$k_3(\text{MDEA})(\text{DEA})(\text{CO}_2)$	3310	-105 <sup>b</sup>	$1.24 \times 10^8$
<b>MDEA parameters</b>			
$k_4(\text{MDEA})(\text{H}_2\text{O})(\text{CO}_2)$	0.0157	3710	590
$k_5(\text{MDEA})(\text{OH}^-)(\text{CO}_2)$	$1.54 \times 10^5$	8107	$5.79 \times 10^9$
hydroxide (Astarita et al., 1983)			
$\log_{10} k_{\text{OH}} = 13.635 - \frac{2895}{T} + 0.08 I_c$			
where $I_c = \sum_{i=1}^N z_i C_i^2$			

<sup>a</sup> The rate constants estimated in the referenced work are based on concentration based activities. In order to convert to mole fraction based activities (Section 2.3.5) it is necessary to multiply by the cube of the density of the solution.

<sup>b</sup> In the referenced work, the activation energy was not regressed with significance based upon the data available.

<sup>c</sup> These rate constants are close to the ones used in the present work. These have been calculated by assuming a density of  $33.5 \text{ kmol}/\text{m}^3$  which is close to the densities of 50 wt% aqueous alkanolamine solutions of DEA and MDEA.

It should be noted that the conversion factor suggested by Carey (1990) would not affect model predictions for solutions that have 10 wt% amine as the density of the solution is close to the density of water. The effect is significant when considering concentrated amine solutions (50 wt%).

### 2.3.6 Equilibrium activity of CO<sub>2</sub> in blended amines

For a solution of MDEA, the equilibrium activity of CO<sub>2</sub> is given by expression 2.16. Similarly for a solution of pure DEA, the corresponding expression is 2.24. However for a blend of MDEA and DEA, the equilibrium activity of CO<sub>2</sub> depends on the distribution of CO<sub>2</sub> between carbamate and bicarbonate. Glasscock and Rochelle (1990) employed the activity of CO<sub>2</sub> in equilibrium with the bicarbonate species for this purpose. Carey (1990) estimated the net activity by the Modified Combined Flux approximation (Glasscock and Rochelle, 1990) which states that the CO<sub>2</sub> is distributed between the bicarbonate and carbamate species according to the net rates of reactions.

$$a_{\text{CO}_2, \text{e}} = f_{\text{carb}} a_{\text{CO}_2, \text{carb}, \text{e}} + (1 - f_{\text{carb}}) a_{\text{CO}_2, \text{HCO}_3, \text{e}} \quad (2.32)$$

$$f_{\text{carb}} = \frac{R_{\text{carb}}}{R_{\text{carb}} + R_{\text{HCO}_3}} \quad (2.33)$$

where  $f_{\text{carb}}$  is the fraction of CO<sub>2</sub> in equilibrium with the carbamate species.

A different approach was adopted in this work. The net rate of reaction of  $\text{CO}_2$  is obtained by combining equations 2.14 and 2.22. Using equations 2.15 and 2.23 also, yields

$$R_{\text{CO}_2} = k_{1\text{HCO}_3}[\mathbf{a}_{\text{CO}_2} - \mathbf{a}_{\text{CO}_2, \text{HCO}_3, \text{e}}] + k_{1\text{carb}}[\mathbf{a}_{\text{CO}_2} - \mathbf{a}_{\text{CO}_2, \text{carb}, \text{e}}] \quad (2.34)$$

where the net rate of reaction of  $\text{CO}_2$  could also be expressed as

$$R_{\text{CO}_2} = k_1 [\mathbf{a}_{\text{CO}_2} - \mathbf{a}_{\text{CO}_2, \text{e}}] \quad (2.35)$$

Equations 2.34 and 2.35 could each be thought of as a combination of two equations, one for the forward rate and another for the reverse rate. Equating the forward rates yields

$$k_1 = k_{1\text{carb}} + k_{1\text{HCO}_3} \quad (2.36)$$

By comparing the reverse rates in conjunction with equation 2.36 it is possible to derive equation 2.32 where

$$f_{\text{carb}} = \frac{k_{1\text{carb}}}{k_{1\text{carb}} + k_{1\text{HCO}_3}} \quad (2.37)$$

Use of equation 2.33 did lead to situations where the net rate of reaction of  $\text{CO}_2$  could be negative during absorption or positive during desorption. Equation 2.37 removes these anomalies.

## **2.3 Flash**

### **2.3.1 Speciation**

The REACTIONS paragraph in ASPEN PLUS can handle only non-ionic species. Hence the reactions in the CO<sub>2</sub>-DEA-MDEA system are formulated as in equations 2.7 and 2.8. However the reaction rate expressions are based on the activities of the ionic species. To estimate the activities of the ionic species it is necessary to use the FLASH routine.

Typically FLASH is used to do bubble point or dew point calculations. However in this case, it is used to speciate from apparent to true components. The relevant equilibrium information is supplied by means of Equations 2.1 to 2.6, 2.9, 2.10 and Table 2.3 in the CHEMISTRY paragraph.

### **2.3.2 NOHPO Compiler**

FLASH uses arrays to store the component flow rates, temperature and pressure (ASPEN PLUS Interfaces and User Models, 1988). It was found that when the FORTRAN routine was compiled using the command FORTRAN filename.FOR, though there were no compilation errors, when the ASPEN input file was run, the FLASH often read the component flow rates, temperature and pressure into the wrong locations. In order to overcome this problem the command FORTRAN/NOHPO filename.FOR was used. This command turned off the vectorising capabilities of the compiler. Consequently, the FLASH worked to allocate quantities to appropriate locations.

### 2.3.3 Minor species correction

When the speciation from FLASH was checked it was found that some equilibria were not satisfied because concentrations of the minor species (hydroxide and hydronium ion) were not estimated correctly. However equilibria that did not involve these two species were being satisfied. An example would be the equilibrium between bicarbonate and protonated amine, a combination of reactions 2.3 and 2.4. This indicated that FLASH did estimate correct concentrations for species like free amine, protonated amine and bicarbonate.

Hence the hydronium ion concentration was back calculated from known concentrations of free MDEA, protonated MDEA and  $pK_b$  of MDEA. Refer reaction 2.4.

$$a_{H_3O^+} = \frac{K_{MDEA} a_{MDEAH^+} a_{H_2O}}{a_{MDEA}} \quad (2.38)$$

This along with  $K_w$  was used to determine the hydroxide concentration..

$$a_{OH^-} = \frac{K_w a_{H_2O}^2}{a_{H_3O^+}} \quad (2.39)$$

After correcting for the minor species (hydroxide and hydronium) concentrations, the specified equilibria (2.1 - 2.4, 2.9, 2.10) were satisfied.

## **2.4 Enhancement Factor Approach**

Absorption of  $\text{CO}_2$  and  $\text{H}_2\text{S}$  into an aqueous alkanolamine solution takes place with reaction at the interface. A rigorous solution to this problem would involve solving a set of differential and algebraic equations. In this work, an approximate technique is used as this reduces the problem to a set of coupled nonlinear algebraic equations. This method involves estimation of an enhancement factor which is applicable even to second order, reversible reactions. The assumptions made in this approach are:

1. Bulk liquid phase is in equilibrium. (Methods to validate this assumption are discussed in Section 2.5).
2. All the reaction takes place at the interface.
3. Gas phase resistance to transfer of  $\text{CO}_2$  is negligible. (The same is not true for  $\text{H}_2\text{S}$  whose reaction at the interface is governed only by equilibrium. Here, gas film resistance plays a significant role.)
4. The kinetic preference of  $\text{CO}_2$  towards one of the dissolved states is determined by means of the Modified Combined Flux approximation (Glasscock and Rochelle, 1990)

5. The effect of solution loading and amine strength on the solubility of  $\text{CO}_2$  in the amine is neglected. This has been done to emulate the approach of Glasscock and Rochelle (1990) where equation 31b indicates that an activity coefficient of unity was used for  $\text{CO}_2$ . However Glasscock(1990) generally used Austgen's equilibrium approach in other work and Austgen (1989) did use an activity coefficient of  $\text{CO}_2$ . ASPEN PLUS can estimate the activity coefficient of  $\text{CO}_2$  which is unsymmetrically normalized and carried by the COMMON block GAMUS.

The enhancement factor at the interface is estimated from the reaction rates at the interface. This calculation consequently yields the absorption or desorption flux. The iterative procedure involved is outlined next.

#### **2.4.1 Algorithm**

The parameters that need to be specified are the mass transfer coefficient, solution loading, the partial pressures of  $\text{CO}_2$  and  $\text{H}_2\text{S}$ , amine concentration and temperature.

Since the apparent component approach is used, the FLASH routine is used to perform speciation. The reaction rates are consequently estimated from the activities.

The bulk liquid phase is in equilibrium and the composition is known. The unknowns in this system are the interfacial concentrations of carbonic acid, carbamic acid and  $H_2S$ . By iteratively solving for these quantities, one can estimate the enhancement factor and then the absorption flux.

It is necessary to guess the interfacial concentrations of carbonic acid, carbamic acid and  $H_2S$ . The first guess typically used is the bulk concentrations of those species. Where two guesses are required (secant or regula falsi technique), the bulk concentration could serve as the lower or upper bound for absorption and desorption respectively. The interfacial concentrations of the other species are determined by means of the following relations.

$$C_{MDEA,i} = C_{MDEA,b} \quad (2.40)$$

$$C_{CO_2,i} = \frac{P_{CO_2}}{H_{CO_2}} \quad (2.41)$$

$$C_{DEA,i} = C_{DEA,b} - \frac{k_{L,carb}^{\circ}}{k_{L,DEA}^{\circ}} (C_{DEA,interface} - C_{DEA,bulk}) \quad (2.42)$$

Equation 2.40 stems from the assumption that  $CO_2$  absorption is liquid film controlled. The ensuing step is to speciate the interfacial composition by means of equilibria described by reactions 2.1 to 2.4, 2.9 and 2.10.

The pseudo first order rate constant for a mixed amine system of DEA and MDEA is calculated using equations 2.15, 2.23 and 2.36. The enhancement factor is then estimated using the relation (Carey, 1990)



$$E_{CO_2} = 1 + (E_i - 1) [1 - \Theta] \quad (2.43)$$

where

$$E_i = \sqrt{1 + M} \quad (2.44)$$

$$M = \frac{k_1 \gamma_{CO_2} D_{CO_2}}{k_L \sigma^2} \quad (2.45)$$

$$\Theta = \frac{a_{CO_2,i,e} - a_{CO_2,b}}{a_{CO_2,i} - a_{CO_2,b}} \quad (2.46)$$

Although, the dimensionless driving force  $\Theta$  has been expressed in terms of activities, it is equivalent to expressing  $\Theta$  as a function of concentrations.  $M$  is the square of the Hatta number. The factor  $\gamma_{CO_2}$  accounts for the conversion from the activity basis to concentration basis (related to equation 2.31).

Having estimated the enhancement factor, it is now necessary to check if the guessed interfacial concentrations are correct. For this three conditions are necessary. The first condition merely states that the gas phase flux of  $H_2S$  should be the same as the flux of  $H_2S$  in the liquid film.

$$k_g [P_{H_2S} - C_{H_2S,i,e} H_{H_2S}] = k_{L^*,H_2S} \Delta C_{H_2S} \quad (2.47)$$

$C_{H_2S,i,e}$  is estimated from the speciation at the interface.

The flux of total  $CO_2$  i.e. free  $CO_2$ , carbonic acid and carbamic acid can be calculated in two different ways.

$$N_{CO_2} = k_{L^*,CO_2} E_{CO_2} [C_{CO_2,i} - C_{CO_2,b}] \quad (2.48)$$

$$N_{CO_2} = k_{L^{\circ},CO_2} \Delta C_{CO_2} + k_{L^{\circ},carb} \Delta C_{carb} + k_{L^{\circ},H_2CO_3} \Delta C_{H_2CO_3} \quad (2.49)$$

Equating 2.47 and 2.48 yields a second criterion for convergence. The third condition is based on the Modified Combined Flux approximation (Glasscock and Rochelle, 1990). Instead of assuming an equilibrium between the carbamate and bicarbonate ions (Critchfield, 1988), this approximation takes into account the kinetic preference of  $CO_2$  towards its dissolved states. The approximation states that the ratio of carbamic acid and carbonic acid fluxes is the ratio of the reaction rates through the respective mechanisms.

$$\frac{k_{L^{\circ},carb} \Delta C_{carb}}{k_{L^{\circ},H_2CO_3} \Delta C_{H_2CO_3}} = \frac{R_{carb}}{R_{H_2CO_3}} \quad (2.50)$$

The guesses are refined until all three criteria are satisfied.

#### 2.4.2 Iterative method

In this work, the three variables are converged successively. The innermost loop converges the interfacial concentration of  $H_2S$ , the middle loop converges the concentration of carbonic acid and the outermost loop converges carbamic acid. For the case of pure MDEA, there would be no carbamic acid. In this case, the outer loop converges on carbonic acid.

The regula falsi technique (Conte and De Boor, 1972) is employed to converge the outer loop while direct substitution of the interfacial concentration of  $H_2S$  and carbonic acid is used for the inner loops. In this work, since only

CO<sub>2</sub>-DEA-MDEA systems were considered, not more than two loops were encountered. However it can be easily extended to H<sub>2</sub>S-CO<sub>2</sub>-DEA-MDEA systems.

## **2.5 Equilibrium Estimation**

This section discusses methods to equilibrate the bulk liquid phase.

### **2.5.1 Flash2**

This was developed by Austgen (1989). Using the unit operation block FLASH2 in ASPEN PLUS, the equilibrium speciation is computed by supplying reactions 2.1 to 2.6 in the CHEMISTRY paragraph. This speciation essentially yields the equilibrium solubility of CO<sub>2</sub> and H<sub>2</sub>S in the amine solution. Carey (1990) and Austgen (1989) have compared predictions from this model to the experimentally measured solubilities of CO<sub>2</sub> in MDEA, DEA, DGA and MEA for different temperatures and concentrations of the amines. Typically, the comparisons were favorable.

### **2.5.2 Reactor with large residence time**

In this work, it was necessary to develop an approach to estimate equilibrium using equilibrium reactions 2.1 - 2.4, 2.9 and 2.10 in conjunction with the kinetically controlled reactions 2.7 and 2.8. This was done with the help of the unit operation block RPLUG. Instead of using the default power law expression for kinetics, a FORTRAN routine was provided.

Since the apparent component approach is used, within the FORTRAN routine a speciation is performed using the ASPEN routine FLASH. The activity coefficients are carried by the ASPEN common block GAMMA.

Since  $\text{CO}_2$  and  $\text{H}_2\text{S}$  are specified as Henry's components in the input file, the values to be used correspond to the unsymmetrically normalized activity coefficients. These are carried by the ASPEN common block GAMUS.

The activities of all species (ionic and non ionic) are calculated. The reaction rates are calculated using expressions 2.14 and 2.22. These rates are returned to ASPEN.

A large residence time ensures that the reaction rates are close to zero for the stream coming out of the reactor. This large time can be achieved by specifying a length of 100 m and diameter of 1m.

### **2.5.3 Sensitivity Analysis**

This feature of ASPEN PLUS allows one to determine function values for a range of values of the variables. In this work, the functions are the bicarbonate and carbamate reaction rates. The variables are two of  $\text{CO}_2$ , carbonic acid and carbamic acid since only two of these can be varied independently for a fixed total  $\text{CO}_2$ .

The technique is to supply a range of values for carbonic and carbamic acid concentrations and find the values for which the carbamate and bicarbonate reaction rates simultaneously go to zero which implies equilibrium.

This is not an efficient way of determining equilibrium. A better purpose of this block is to test the behavior of the rate expressions as a function of different parameters like species concentrations.

## **2.6 Ratefrac-based Model**

RATEFRAC is a rate-based nonequilibrium separation process model that can simulate tray and packed columns (ASPEN PLUS, RATEFRAC Manual, 1991). It has the capability to handle rate-limited reactions. The unique feature about RATEFRAC is that the fundamental heat and mass transfer rate processes are explicitly incorporated in the model, thus obviating the need for efficiencies for tray columns or HETPs for packed columns. An attempt has been made to use RATEFRAC for modeling the acid gas absorption problem which follows the approach recommended by Carey (1990). RATEFRAC handles problems of gas-liquid mass transfer with reaction at the interface in a rigorous manner by integrating the differential equations across the boundary layer.

The default power law model can be used to represent the kinetics.

$$\text{Rate} = k A^n B^m \quad (2.51)$$

The heat and mass transfer coefficients can be calculated from the correlations provided by RATEFRAC. Alternatively, one could supply external FORTRAN routines to calculate the reaction rates, heat and mass transfer coefficients.

### 2.6.1 Kinetics Routine

In the CO<sub>2</sub>-DEA-MDEA system the reactions considered are 2.7 and 2.8. The complex reaction rate expressions (2.14 and 2.22) necessitate use of an external FORTRAN routine. The key steps in this FORTRAN routine are:

1. Estimate the density, viscosity and diffusivities using the empirical correlations (Refer Appendix B) and not the routines in ASPEN PLUS.
2. Speciate the composition using the FLASH routine. This has to be done since RATEFRAC can handle only apparent components.
3. Using GAMMA, GAMUS (COMMON blocks in ASPEN which carry activity coefficients) and the speciation, calculate activities of all components. Calculate the rate parameters using the liquid phase temperature and density. Three temperatures T, TLIQ, TVAP are passed as arguments to the kinetic routine. TLIQ should be used.

4. Calculate the reaction rates for the apparent components.

The liquid holdup parameter (HLDLIQ) should be used to achieve consistent units.

### **2.6.2 Carey's Proposal (1990)**

Carey observed that the rigorous approach adopted by RATEFRAC to account for reaction in the boundary layer could consume a significant amount of computation time. Hence he recommended use of the enhancement factor approach (Section 2.4) to account for reaction at the interface.

The enhancement factor would be calculated in the mass transfer coefficient routine so that the mass transfer coefficients returned to ASPEN would be modified for the effect of chemical reaction at the interface. It would be necessary to call the kinetics routine from the mass transfer coefficient routine for this purpose. Alternatively, the mass transfer routine should be set up to estimate reaction rates.

### **2.6.3 Difficulties**

This recommendation could not be implemented due to the fact that the argument list for the mass transfer coefficient routine contains physical properties and not the vapor and liquid composition. This prevents estimation of reaction rates which precludes calculation of enhancement factor.

A possible workaround could be use of a COMMON block that passes the vapor and liquid compositions from the kinetics routine to the mass transfer routine. But its validity is arguable.

#### **2.6.4 Modified Approach**

Since the approximate technique could not be incorporated into this model, the approach adopted was to let RATEFRAC do the rigorous interfacial calculations. One of the correlations provided by RATEFRAC was used to calculate the physical mass transfer coefficient. The same kinetic routine was used.

In this work, an attempt has been made to model a column with only one non-equilibrium segment so that it could be used to analyze data from a single stage contactor like a stirred cell or a wetted wall column.

#### **2.6.5 Observations**

It should be noted that when RATEFRAC performs its calculations, it begins with a set of equilibrium calculations to provide an initial estimate. When these are converged successfully, it then proceeds to do the actual rate-based calculations. It is very essential that in the specifications for the RATEFRAC block, estimates are supplied for the liquid and vapor product compositions as well as liquid and vapor product flow rates. If these are not supplied, RATEFRAC seems to do some calculations by flashing the feed



stream, runs into FORTRAN errors bringing the simulation to a halt without even commencing the initial or equilibrium calculations of RATEFRAC.

The results from the RATEFRAC based modeling effort have not been encouraging. This model was applied only to CO<sub>2</sub>-MDEA systems. However complete convergence was attained only when CO<sub>2</sub> was in stoichiometric excess and the liquid flow rate was less than the gas flow rate.

The convergence behavior was very closely linked to the temperature estimates. It was necessary to put a lower bound on the temperature to prevent guesses that hindered convergence. Bounds on component content in both phases also helped. For example, an upper bound of 1E-16 for carbonic and carbamic acids in the vapor streams had a positive effect.

Difficulties were faced in other situations i.e. either the initial calculations were completed successfully but the rate-based calculations did not converge or the initial calculations failed to converge. This was purely an empirical observation.

If these difficulties are resolved, modeling of an absorber-stripper system should be an achievable task.

## 2.7 Single Stage Contactor

Since the effort to use RATEFRAC to model CO<sub>2</sub> absorption into alkanolamines was not successful, a stand-alone model was developed that

could model single-stage contactors. This effort primarily involved accounting for the kinetics (as in the RATEFRAC based model) as well as the mass transfer through the enhancement factor approach (Refer Section 2.4). These are supplied as a FORTRAN routine to the USER block which allows users to develop specific unit operation models.

The two methodologies adopted have been described. The underlying principle in both approaches is the same. The specifications required are amine concentration, temperature, partial pressure of CO<sub>2</sub>, solution loading and mass transfer coefficient. The first step involves equilibrating the bulk liquid. This is followed by applying the enhancement factor approach to perform the interfacial calculations. This yields the enhancement factor and absorption rate.

The primary difference is that in one approach the activity coefficients used in the interfacial calculations are the same as those in the bulk equilibrated liquid phase whilst in the other activity coefficients are estimated as a function of composition at every step in the interfacial calculations.

### **2.7.1 Equilibrium or Bulk Activity Coefficients**

Glasscock et al. (1991) used the assumption of bulk liquid phase activity coefficients for the interface in his rigorous approach because allowing the activity coefficients to vary in the boundary layer would necessitate the flux to be expressed as a function of chemical potential gradient and not

concentration gradient. This assumption was also used in testing the approximate technique (Glasscock and Rochelle, 1990).

This model essentially seeks to develop this approximate method in the framework of ASPEN PLUS. Hence it is necessary to make this assumption. Another reason is the rate parameters used in this work are those regressed by Glasscock (1990). This would make possible a check of the performance of this ASPEN model as it can be directly compared to the predictions of Glasscock and Rochelle (1990).

The key steps in this method are outlined as follows

1. Establish equilibrium in the liquid phase using the FLASH2 routine (Section 2.5.1). This step yields both the equilibrium composition as well as the corresponding activity coefficients.
2. The composition is manually fed to the ASPEN input file which does the kinetic and mass transfer calculations.
3. The activity coefficients are supplied externally to the FORTRAN routine.
4. Within the FORTRAN routine, the first step is speciation using the supplied activity coefficients. The FLASH routine uses activity coefficients from the COMMON

block GAMMA which would be evaluated for each composition. To avoid this, a routine was written that essentially performed the job of speciation using the equilibrium constants and the equilibrium activity coefficients. Carey(1990) had written a similar routine. The only difference is the convergence technique employed. Carey (1990) used the secant method while the regula falsi technique is employed in this work.

5. The activities and rate parameters are used to compute the reaction rates.
6. The iterative technique is employed to estimate the enhancement factor and hence the CO<sub>2</sub> flux. (Section 2.4).

### **2.7.2 Interface Activity Coefficients**

A more "rigorous approximate" approach would be to evaluate activity coefficients at every step in the interfacial calculations as a function of composition.

This technique has been coded and is functional and does predict enhancement factors and fluxes. However, it should be noted that the rate parameters used have been regressed by Glasscock (1990) who made the simplifying assumption of using the activity coefficients from the bulk. Hence

there is no platform for comparison with Glasscock's results. However the results from this approach which lets activity coefficients vary as a function of composition could be compared to the predictions of the method outlined in Section 2.7.1 as both have been developed in the same environment. Direct regression of experimental rate data using this approximate approach (that lets activity coefficients vary at the interface) would facilitate its use.

The key steps in this methodology are:

1. Establish equilibrium in the bulk liquid phase by use of the reactor (RPLUG) block as described in Section 2.5.2. The speciation in the kinetics routine of the reactor is performed using the FLASH routine. The activity coefficients are supplied by the COMMON block GAMMA.
2. The equilibrated liquid phase is automatically fed to the next block (USER) where the interfacial calculations are performed. Steps 1 and 2 could be replaced with steps 1 and 2 of the procedure outlined in Section 2.7.1.
3. In the routine for the USER block, the activities of the species in the bulk liquid phase are computed using the FLASH routine.

4. The algorithm outline in Section 2.4 is employed to calculate the enhancement factor and consequently the flux or absorption rate.

### 2.7.3 Results

Both models of the single stage contactor are functional. They need specification of amine weight fraction, loading, physical mass transfer coefficient of CO<sub>2</sub>, temperature and partial pressure of carbon dioxide. Validation of these models would necessitate comparison to the results obtained by Glasscock (1990) since the rate parameters used in this work are identical to those used by Glasscock (1990). Since Glasscock used the activity coefficients from the bulk/equilibrium in the interfacial calculations, only the results from the method outlined in Section 2.7.1 are compared. Figures 2.2 to 2.9 provide the platform for comparison. A more elaborate representation is provided in Appendix C. In each case, the ordinate is the ratio of the approximate to rigorous fluxes as a function of either the rigorous enhancement factor or the CO<sub>2</sub> partial pressure.

Figures 2.2, 2.3, 2.6 and 2.7 show that the approximate method predicts to within 20% of the predictions of the rigorous method for a loading of 0.01 mol CO<sub>2</sub>/mol amine for mass transfer coefficients of 10<sup>-4</sup> m/s and 10<sup>-5</sup> m/s. However for a loading of 0.1 mol CO<sub>2</sub>/mol amine the predictions deteriorate considerably for the blended amines ( 5% DEA - 45% MDEA and 30% DEA - 20% MDEA). (Refer to figures 2.4, 2.5, 2.8 and 2.9). The values

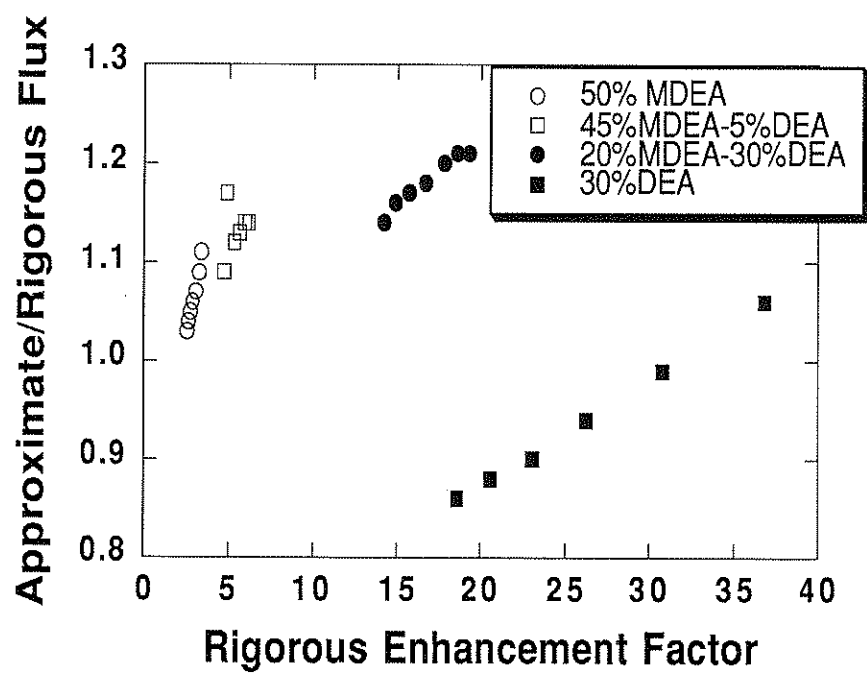


Figure 2.2 Comparison of approximate to rigorous flux as a function of the rigorous enhancement factor for loading = 0.01 mol CO<sub>2</sub>/mol amine,  $k_L = 10^{-4}$  m/s,  $T = 40^\circ\text{C}$ .

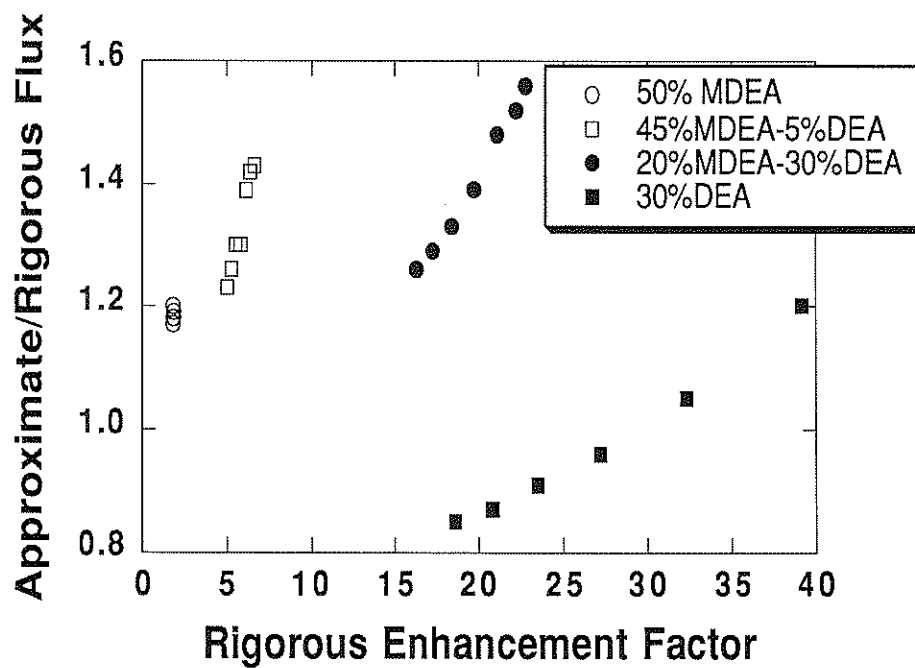


Figure 2.3 Comparison of approximate to rigorous flux as a function of the rigorous enhancement factor for loading = 0.1 mol CO<sub>2</sub>/mol amine,  $k_L = 10^{-4}$  m/s,  $T = 40^\circ\text{C}$ .



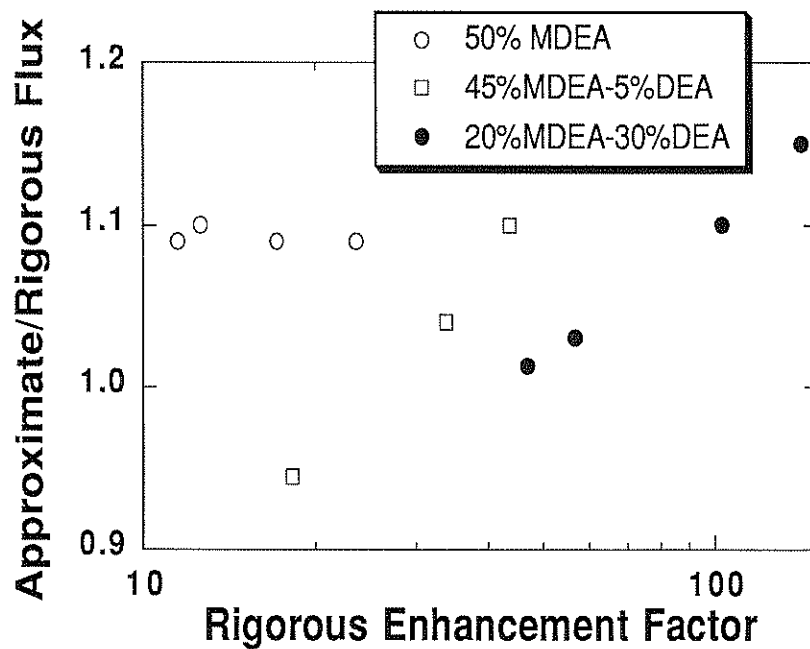


Figure 2.4 Comparison of approximate to rigorous flux as a function of the rigorous enhancement factor for loading = 0.01 mol CO<sub>2</sub>/mol amine,  $k_L = 10^{-5}$  m/s,  $T = 40^\circ\text{C}$ .

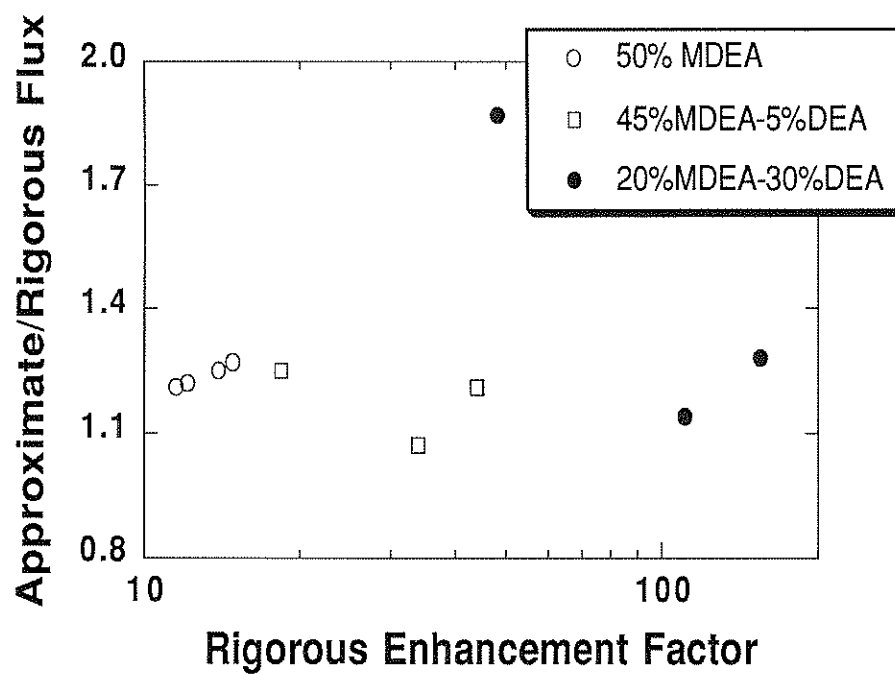


Figure 2.5 Comparison of approximate to rigorous flux as a function of rigorous enhancement factor for loading =  $0.1 \text{ mol CO}_2/\text{mol amine}$ ,  $k_L = 10^{-5} \text{ m/s}$ ,  $T = 40^\circ\text{C}$ .

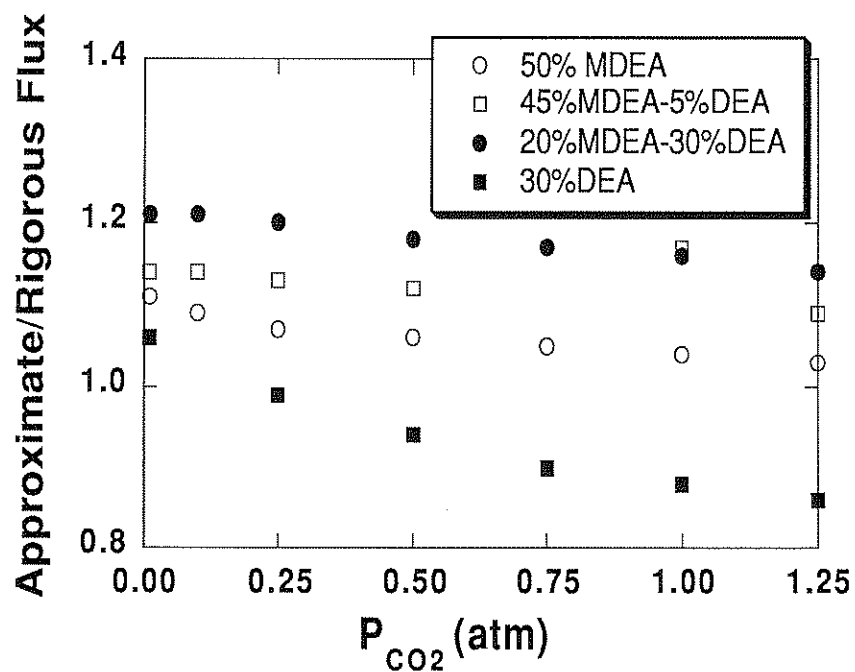


Figure 2.6 Comparison of approximate to rigorous flux as a function of CO<sub>2</sub> partial pressure for loading = 0.01 mol CO<sub>2</sub>/mol amine,  $k_L = 10^{-4}$  m/s,  $T = 40^\circ\text{C}$ .

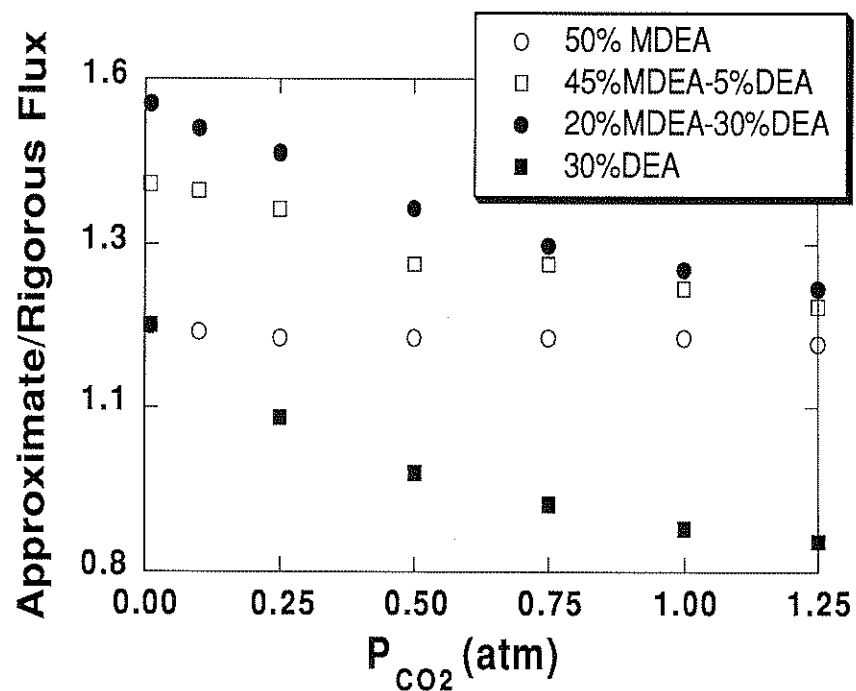


Figure 2.7 Comparison of approximate to rigorous flux as a function of CO<sub>2</sub> partial pressure for loading = 0.1 mol CO<sub>2</sub>/mol amine,  $k_L = 10^{-4}$  m/s,  $T = 40^\circ\text{C}$ .

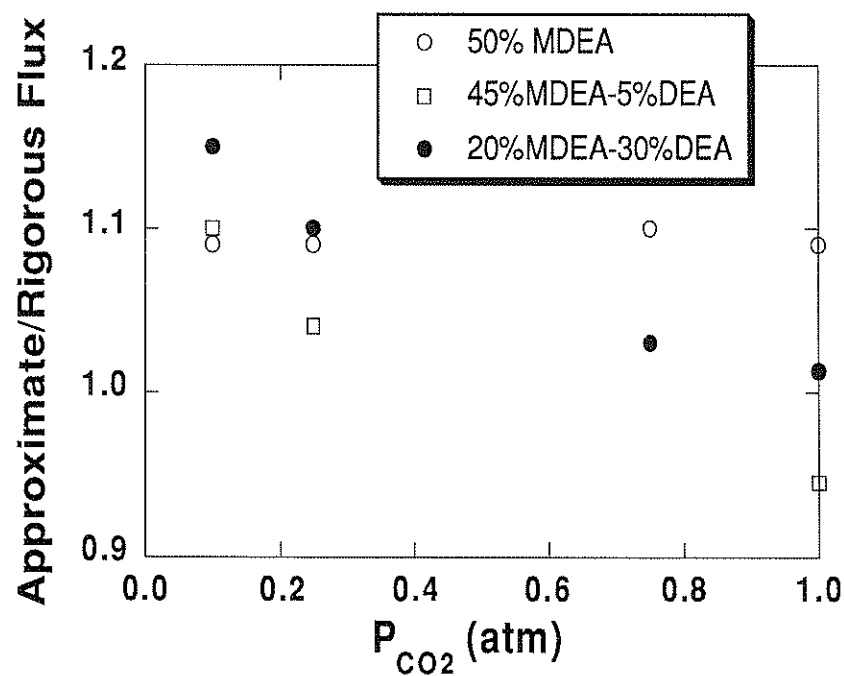


Figure 2.8 Comparison of approximate to rigorous flux as a function of CO<sub>2</sub> partial pressure for loading = 0.01 mol CO<sub>2</sub>/mol amine,  $k_L = 10^{-5}$  m/s,  $T = 40^\circ\text{C}$ .

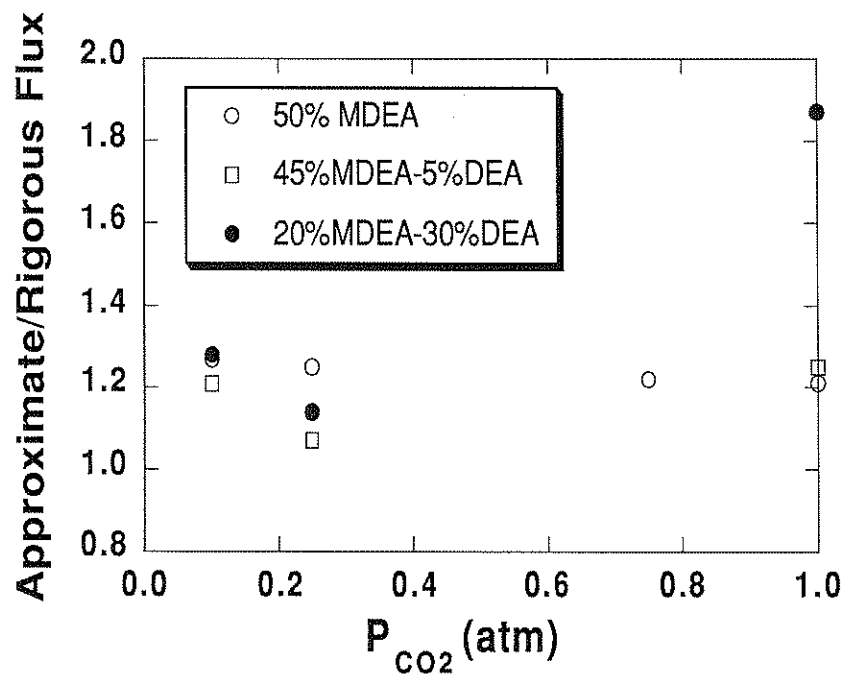


Figure 2.9 Comparison of approximate to rigorous flux as a function of CO<sub>2</sub> partial pressure for loading = 0.1 mol CO<sub>2</sub>/mol amine,  $k_L = 10^{-5}$  m/s,  $T = 40$  °C.

of enhancement factors calculated by the rigorous technique (Glasscock and Rochelle, 1990) were taken from the spreadsheets that were used to make the plots.

It is important to note that in all cases, even at low  $P_{CO_2}$  where the kinetics dominate, there exist significant differences in the predictions of the rigorous approach and the approximate technique used in this work. Though the exact source of this discrepancy is not known as yet, a probable reason could be the difference in the prediction of activity coefficients. The method adopted by Glasscock (1990) and the methodology used in this work which uses ASPEN PLUS estimate the activity coefficients from the Electrolyte-NRTL equation. However there still probably exists differences in their values which could be a source of error. The activity coefficients for 25% DEA at a loading of 0.5 mol  $CO_2$ /mol amine at 25°C obtained by both methods are tabulated in Table 2.13. Notice that there is a considerable difference in the activity coefficients of  $CO_2$ ,  $OH^-$ ,  $H_3O^+$ ,  $HCO_3^-$ ,  $CO_3^{--}$  and carbamate species.

As mentioned before, the predictions of the rigorous approximate approach (Section 2.7.2) cannot be compared to the results of Glasscock and Rochelle (1990). However predictions of the approach outlined in Section 2.7.1 could be a suitable base for comparison as both methods have been developed in ASPEN PLUS.

**Table 2.13 Comparison of activity coefficients for a 25% DEA solution at 0.5 loading and  $T = 25^{\circ}\text{C}$**

Species	Activity coefficient	
	Glasscock (1990)	Present work
$\text{H}_2\text{O}$	1.0	1.0
DEA	0.14	0.14
$\text{CO}_2$	2.0	1.2
$\text{H}_3\text{O}^+$	0.59	0.42
$\text{DEAH}^+$	0.49	0.49
$\text{OH}^-$	0.56	0.40
$\text{DEACOO}^-$	0.55	0.82
$\text{HCO}_3^-$	0.62	0.55
$\text{CO}_3^{=}$	0.14	0.08

Table 2.14 compares the enhancement factors obtained by the approximate approaches outlined in Sections 2.7.1 and 2.7.2. When performing the simulations with the approximate technique outlined in Section 2.7.1, the first two steps were replaced by the first two steps described in Section 2.7.1.

A surprising prediction from the approximate approach that calculates activity coefficients at the interface is that for 30 wt% DEA - 20 wt% MDEA and 30 wt% DEA solutions, at loadings of 0.01 and 0.1 mol  $\text{CO}_2$ /mol amine and mass transfer coefficients of  $10^{-4}$  and  $10^{-5}$  m/s, the enhancement factor increases as partial pressure of  $\text{CO}_2$  increases from 0.01 to 1 atm. Also for 5 wt% DEA - 45 wt% MDEA and 50 wt% MDEA, the enhancement factor



**Table 2.14 Comparison of enhancement factors predicted by approximate methods developed in ASPEN PLUS**

Wt % MDEA	Wt% DEA	$k_L^o$ $\frac{m}{s}$	$P_{CO_2}$ atm	loading $\frac{mol\ CO_2}{mol\ amine}$	$E_{int}^a$	$E_{bulk}^b$
50	0	1.00E-04	0.1	0.01	3.65	3.58
50	0	1.00E-04	1	0.01	3.03	2.76
50	0	1.00E-05	0.1	0.01	27.58	23.62
50	0	1.00E-05	1	0.01	19.15	12.49
50	0	1.00E-04	0.1	0.1	2.34	2.26
50	0	1.00E-04	1	0.1	2.17	2.195
50	0	1.00E-05	0.1	0.1	21.40	18.73
50	0	1.00E-05	1	0.1	16.62	13.91
5	45	1.00E-04	0.1	0.01	7.12	6.8
5	45	1.00E-04	1	0.01	7.03	5.74
5	45	1.00E-05	0.1	0.01	69.15	48.1
5	45	1.00E-05	1	0.01	60.42	17.2
5	45	1.00E-04	0.1	0.1	9.37	9.1
5	45	1.00E-04	1	0.1	9.15	6.68
5	45	1.00E-05	1	0.1	86.74	53.3
5	45	1.00E-05	0.1	0.1	51.20	23.1
20	30	1.00E-04	0.1	0.01	21.58	22.5
20	30	1.00E-04	1	0.01	23.10	17.2
20	30	1.00E-05	0.1	0.01	232.4	162
20	30	1.00E-05	1	0.01	264.7	47.5
20	30	1.00E-04	0.1	0.1	35.90	33.7
20	30	1.00E-04	1	0.1	38.84	22.3
20	30	1.00E-05	0.1	0.1	383.5	199
20	30	1.00E-05	1	0.1	225.4	89.7
0	30	1.00E-04	0.01	0.01	38.80	39
0	30	1.00E-04	1	0.01	42.00	18.1
0	30	1.00E-04	0.01	0.1	48.00	47.2
0	30	1.00E-04	1	0.1	50.31	18.1

<sup>a</sup>  $E_{int}$  refers to the enhancement factor calculated from the approximate method that lets activity coefficients vary at the interface as a function of composition (Section 2.7.1).

<sup>b</sup>  $E_{bulk}$  refers to the enhancement factor calculated from the approximate method that lets activity coefficients vary at the interface as a function of composition (Section 2.7.2).

decreases by a much smaller factor when  $P_{CO_2}$  increases from 0.1 to 1 atm as compared to the approximate approach that uses bulk activity coefficients.

The next step is probably to use any of these techniques to directly regress the experimental data. It might be preferable to adopt the strategy outlined in section 2.7.2 as it accounts for the effect of composition on activity coefficients. In some sense, it is a more 'rigorous approximate' method. ASPEN PLUS has the capability to regress VLE data (ASPEN PLUS, Data Regression Manual, 1988). However it still does not possess a feature where rate data could be regressed. A possible workaround is to pose this regression as an optimization problem where the difference between the predicted flux and experimental flux has to be minimized. However this would be a very time consuming procedure.

## **CHAPTER THREE**

### **EXPERIMENTAL WORK**

The primary goal of the experiments was to measure the absorption rate of CO<sub>2</sub> into 50 wt% solutions of MDEA and DEA as well as blends of MDEA and DEA using a wetted wall column.

#### **3.1 Experimental Apparatus and Methods**

##### **3.1.1 Wetted Wall Column**

The wetted wall column used in this work is shown in Figure 3.1. The liquid flows up through the inside of the inner tube and flows down the outside. The gas enters at the top, contacts with the liquid and leaves through the bottom. This is a co-current contactor. The wetted wall column is made of ordinary glass and has been used for experiments up to 45°C. Some of the previous researchers who have used a wetted wall column include Toman and Rochelle (1989) and Vivian and Peaceman (1956).

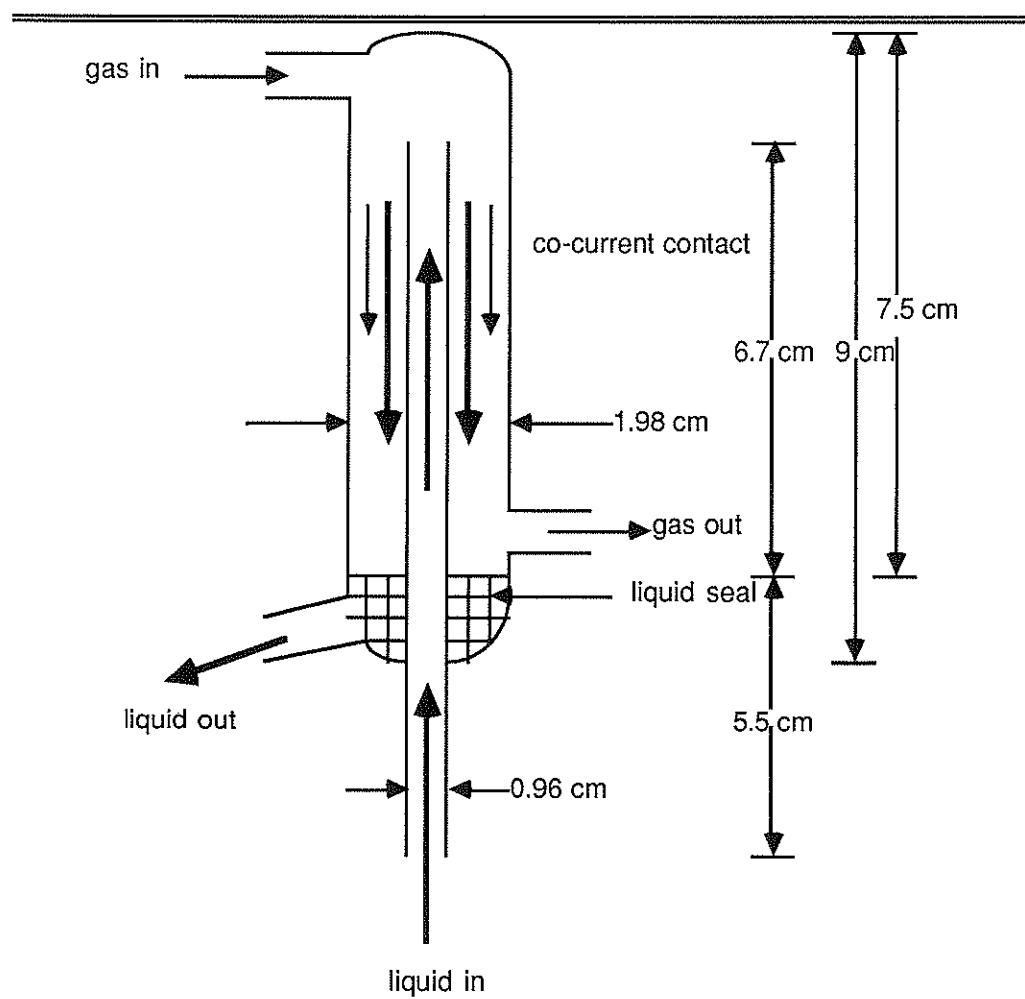


*Figure 3.1 Detailed diagram of the wetted wall column*

The wetted wall column was designed so that the following criteria were satisfied.

1. The vapor holdup was maintained low enough (13.26 mL) so as to facilitate plug flow in the gas phase and also to reduce the response time of the analyzer to changes in gas concentration.
2. The length was short enough to prevent any thickening effects of the liquid film towards the bottom and long enough to prevent the end effects from dominating (Vivian and Peaceman, 1956).

The liquid seal in the wetted wall column prevented any gas leak into the liquid line and had a surface area of  $1.77 \text{ cm}^2$ . The effective contact length was 6.7 cm and the interfacial area along the length was  $20.21 \text{ cm}^2$ . The interfacial area at the top of the inner tube which was estimated to be about  $0.75 \text{ cm}^2$  and contributed to less than 5% of the total area was neglected. The outer diameter of the wetted wall column was 1.98 cm. The corresponding value for the inner tube was 0.96 cm. The thickness of the glass used was about 0.1 cm. The inner tube is so designed that the inner diameter decreases from 0.76 cm at the bottom to about 0.4 cm at the top. This was done to reduce the end effects at the top and also to reduce the likelihood of a gas leak through the inner tube.

### **3.1.2 Overall Setup**

The typical arrangement is shown in Figure 3.2. Two flow controllers regulated the flow of CO<sub>2</sub> and N<sub>2</sub> to attain the desired partial pressures. These were mixed in a tube filled with glass beads. The flow of the mixed gas was then reduced to the required flow rate (about 40 cc/min) by means of another flow controller. A purge provided the outlet for excess gas.

The mixture of CO<sub>2</sub> and N<sub>2</sub> was then either sent through the wetted wall column or through the bypass. The practice in this work was to first send the gas through the bypass to the CO<sub>2</sub> analyzer to perform a calibration. Before the gas reached the analyzer it was diluted to the required level using N<sub>2</sub> (whose flowrate was regulated by a flow controller). The typical flow rate of dilution N<sub>2</sub> varied from 0.5 to 1.5 Lpm. The gas was then sent through the wetted wall column where it contacted the flowing liquid. The gas that left the column was also diluted with nitrogen, then sent through an ice bath, which consisted of an Erlenmeyer flask placed in a beaker filled with ice, to condense water in the gas phase. Placing the condenser after the 4-way valve rather than before it helped to reduce the response time of the analyzer. It also acted as a mixing chamber for the dilution gas and the gas coming out of the wetted wall column. Significant amounts of water in the gas phase could affect the working of the infrared CO<sub>2</sub> analyzer. Deflections on the analyzer were monitored by means of a strip chart recorder which has a precision of  $\pm 1\%$  of full scale.

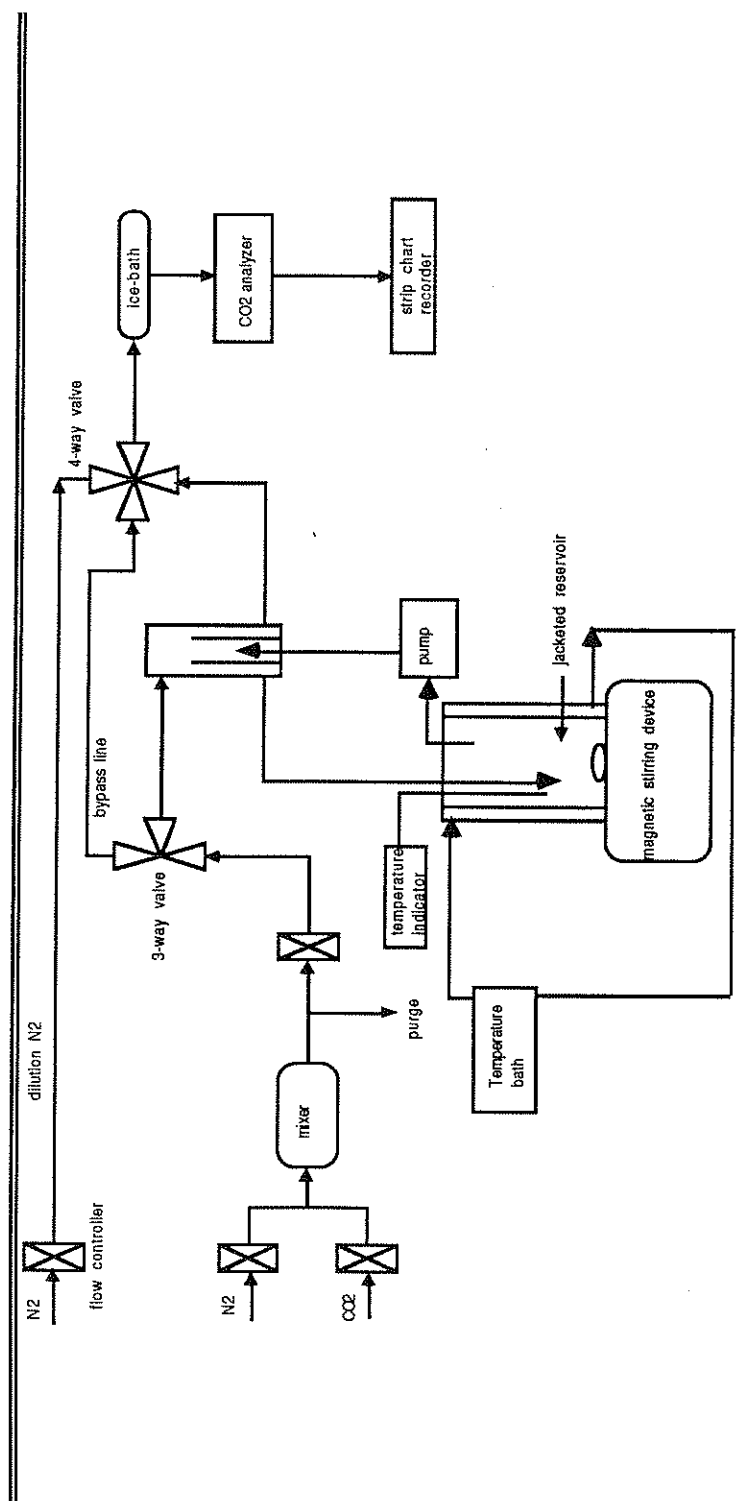


Figure 3.2 Schematic of the experimental setup for absorption of CO<sub>2</sub> ( $PCO_2 < 1 \text{ atm}$ ) into amine solutions.

The liquid was circulated by means of a positive displacement Cole-Parmer micro pump (adapter - L-07002-15, head - L-07002-26). The micro pump was used to pump aqueous solutions of ethylene glycol, MDEA and DEA up to 45°C . A liquid reservoir with a capacity of 600 mL was provided. It was sealed at the top by means of a rubber stopper. Typically there was a gas space of about 30 mL. The solution in the reservoir was constantly stirred by means of a magnetic stirrer to maintain a uniform concentration. The reservoir was jacketed so that the temperature could be controlled by means of a temperature bath. It is this temperature which is referred to in the ensuing discussion. The wetted wall column is assumed to be at the same temperature in spite of the fact that it was not jacketed.

The tubing for the gas lines was made of either teflon or polypropylene. Tygon tubing was used in the liquid line.

### **3.1.3 Calibration of Mass Flow Controllers**

Model 5850E mass flow controllers manufactured by Brooks were used to regulate the flow rates of N<sub>2</sub> and CO<sub>2</sub>.

The gas flowing through the controller is heated. Temperature sensors exist at both ends. The temperature difference between the upstream and downstream sensors helps determine the flow rate. This temperature difference is a function of the flow rate and the specific heat of the gas. The accuracy is reported to be 1% of full scale and repeatability is 0.25% of the rate.



The flow controllers were calibrated for N<sub>2</sub> by means of a soap film meter. The flowrates for CO<sub>2</sub> were obtained by either using a conversion factor (supplied by Brooks) of 0.78 with the N<sub>2</sub> calibration or by directly calibrating for CO<sub>2</sub> with the soap film meter. Both methods yielded consistent results. However the latter is questionable as soap absorbs CO<sub>2</sub>.

While performing these calibrations there were no restrictions between the gas source and the flow controller. So the calibrations were applied with confidence to the flow controllers in the experimental set up which were similarly placed. However, the flow controller which has a mixture of CO<sub>2</sub> and N<sub>2</sub> passing through (Figure 3.2) is down line to two flow controllers. This flow controllers was calibrated in this position itself as well as without the restrictions. The calibrations in both cases were almost identical. In this work, the former was used. These calibrations were performed with only N<sub>2</sub> as well as both N<sub>2</sub> and CO<sub>2</sub>.

For a mixture of gases, one could estimate the flow rate by using the calibration with nitrogen in conjunction with the conversion factor. For a mixture the conversion factor is estimated as follows:

$$\text{Factor} = \frac{100}{\frac{P_1}{C_1} + \frac{P_2}{C_2}} \quad (3.1)$$

where P<sub>1</sub> and P<sub>2</sub> are percentage (by volume) of gases 1 and 2. C<sub>1</sub> and C<sub>2</sub> are the respective conversion factors. For example, the conversion factor for a gas mixture of 30% CO<sub>2</sub> and 70% N<sub>2</sub> would be

$$\text{Factor} = \frac{100}{\frac{30}{0.776} + \frac{70}{1.0}} = 0.92$$

For a few settings this method was checked with the direct calibration of the flow controller with CO<sub>2</sub> and N<sub>2</sub>. Since they compared well (within about 10%), the conversion factor method was subsequently used throughout this work.

The pressure drop across one flow controller is about 30 psi. Since the set up can have two flow controllers in series a pressure of 80 psi is used upstream to the first flow controller.

#### **3.1.4 Carbon dioxide analyzers**

HORIBA PIR-2000 Infrared gas phase analyzers were used to determine the flux of CO<sub>2</sub> from the gas to the flowing liquid in the wetted wall column. These analyzers use infrared absorption spectroscopy to estimate the CO<sub>2</sub> concentration in the gas phase. The reading on the analyzer was monitored by means of a strip chart recorder which has an accuracy of  $\pm 1\%$  of full scale. This accuracy was further enhanced by use of an instrument with a smaller least count within that range of 1% deviation.

It is important to note that measurements close to equilibrium where the difference in the deflections between the inlet and outlet is small ( for example 5) are likely to be much more in error as compared to measurements away from equilibrium where the difference could be as much as 50 out of 100.

The CO<sub>2</sub> flux into the liquid phase from the gas phase was determined by the difference of the CO<sub>2</sub> concentrations in the gas stream in to and out of the wetted wall column. To estimate the former the bypass was used (Figure 3.2). This also served as calibration of the analyzer. Every time an experiment was run, a simultaneous calibration was performed.

Dilution N<sub>2</sub> was used so that the total flow of gas into the analyzer was between 500 and 1500 sccpm. This was prescribed by the manufacturers. It was observed that an increased flow through the analyzer improved its speed of response (expectedly). An ice-bath was used to trap the moisture in the gas entering the analyzer.

The analyzers used in this work had ranges of 0-25% and 0-0.25% (volume basis). The former was used for partial pressures of CO<sub>2</sub> above 0.1 atm and the latter was used when the partial pressure of CO<sub>2</sub> was less than 0.1 atm. It was observed that while the high range analyzer behaved in a linear manner, the low range analyzer had a nonlinear response. So while a straight line was used to fit the calibration of the analyzer with range 0-25%, the calibration of the 0-0.25% range analyzer was fit with a quadratic curve. This nonlinear response was tested by using different flow controllers. It was also observed by Critchfield (1988). Each time an experiment was run, both the linear and quadratic calibration curves were generated.

### **3.1.5 Carbon analyzer**

The liquid phase CO<sub>2</sub> concentration or the amine loading was determined by use of an Oceanography International Model 525 Carbon Analyzer. It uses nitrogen as the carrier gas. A small amount of liquid sample (30 µL) is injected into a solution of 30 wt% phosphoric acid which instantly frees the CO<sub>2</sub> chemically combined with the amine. The total CO<sub>2</sub> is carried by the nitrogen stream to the Horiba analyzer with a range of 0-0.25 vol. %. The total signal is integrated and this value is a direct measure of the carbon dioxide concentration in the liquid phase. To facilitate this interpretation, calibration with a liquid of known CO<sub>2</sub> content becomes necessary. 7mM Na<sub>2</sub>CO<sub>3</sub> solution (prepared by mixing the requisite amounts of solid Na<sub>2</sub>CO<sub>3</sub> with distilled water) was used for this purpose. A calibration was performed every time the carbon analyzer was used. This is essential as the calibration has a tendency to drift.

Depending on the loading, it was necessary to dilute the liquid samples (30 µL) with 0 to 3.5 mL of water so as to reduce the CO<sub>2</sub> concentration to levels used for calibration. A syringe with a capacity of 100 µL was used to take the liquid samples while one with a capacity of 2 mL was used for distilled water. The water was first injected into a vial of 5mL capacity. The liquid sample was then injected into the vial which was then sealed till was analyzed for carbon content.

## 3.2 Physical calibration

### 3.2.1 Theory

The flux of CO<sub>2</sub> (that is being absorbed or desorbed) is given by the following equation:

$$N = E k_L^O \Delta C \quad (3.2)$$

where  $\Delta C$  is the driving force,  $E$  is the enhancement factor and  $k_L^O$  is the physical mass transfer coefficient in the liquid phase. It is difficult to estimate  $k_L^O$  while absorbing CO<sub>2</sub> into a solution of alkanolamine since the mass transfer is accompanied by chemical reaction. Hence it is necessary to run experiments involving purely physical absorption or desorption of CO<sub>2</sub>. For this purpose aqueous solutions of ethylene glycol (which do not react chemically with CO<sub>2</sub>) are used. The enhancement factor  $E$  is unity for this case.

The liquid phase material balance for an absorption experiment is

$$V_L \frac{\partial c}{\partial t} = k_L^O a (c^* - c) = N a \quad (3.3)$$

where  $V_L$  is the liquid inventory,  $c$  is the concentration of CO<sub>2</sub> in the liquid phase,  $c^*$  the equilibrium concentration and  $a$  the interfacial area. Integration yields

$$\ln \frac{(c^* - c)}{(c^* - c)_0} = - \frac{k_L^O a}{V_L} t \quad (3.4)$$

where the subscript o represents the initial condition. The slope of a plot of ( $c^* - c$ ) versus time yields the mass transfer coefficient. However, knowledge of Henry's constant is essential. Toman (1990) noted that if an accurate value of Henry's constant is not used, a straight line will not be obtained. The procedure described uses liquid phase analysis and hence the carbon analyzer.

On the other hand, the mass transfer coefficient can be estimated from desorption data without the Henry's constant. The governing material balance equation for desorption is

$$V_L \frac{\partial c}{\partial t} = -k_L^o a (c^* - c) = Gc_g = Gk X \quad (3.5)$$

where  $G$  is the gas flow rate through the  $\text{CO}_2$  analyzer,  $c_g$  is the concentration of  $\text{CO}_2$  in the gas stream,  $X$  is the reading on the analyzer and  $k$  is the conversion factor  $c_g$  to  $X$ . Substituting for  $c^*$  in terms of  $c_g$  using Henry's law, solving for  $c$  from the second and third terms of equation 3.5 and then integrating the equation that involves the first two terms of equation 3.5 yields

$$\ln \frac{c_g}{c_{go}} = \frac{\frac{k_L^o a}{V_L}}{1 + \frac{k_L^o a}{mG}} t \quad (3.6)$$

where  $m$  is the solubility of  $\text{CO}_2$ . The denominator of the term on the right hand side of equation 3.6 was typically found to be very close to unity and hence assumed to be unity (Toman, 1990). The same assumption is made in this work. Equation 3.6 is reducible to the form

$$\ln X = -\frac{k_L^o a}{V_L} t + \ln \left( -\frac{k_L^o a}{G k_{c g o}} \right) \quad (3.7)$$

The slope of a plot of  $\ln X$  versus time yields the mass transfer coefficient.

### 3.2.2 Procedure

A number of experiments were conducted to measure the mass transfer coefficient of  $\text{CO}_2$  in aqueous solutions with varying weight fractions of ethylene glycol (0 to 1) at ambient temperature. The desorption technique was employed. The set up is similar to the one shown in Figure 3.2. The only difference is that since pure  $\text{CO}_2$  is used there is no necessity to have a mixing chamber. This also implies that only two flow controllers are employed, one for  $\text{CO}_2$  and one for dilution  $\text{N}_2$ . The procedure involved the following steps:

1. Sparging the solution externally for about 2 hours.
2. Filling the liquid reservoir with the solution rich in  $\text{CO}_2$ .
3. Stripping the  $\text{CO}_2$  from the liquid in the wetted wall column using  $\text{CO}_2$ -free  $\text{N}_2$  whose flow rate was 60 cc/min. Before it went to the analyzer it was diluted with  $\text{N}_2$  at 500 cc/min.

### 3.2.3 Dimensionless Mass Transfer Correlation

The detailed data obtained from the desorption experiments are presented in Appendix A. These data could be cast into the form of a

dimensionless correlation which essentially expressed the mass transfer coefficient as a function of different parameters. For a falling film as in a wetted wall column, the following dimensionless correlation was derived from basic hydrodynamics and film theory (Mshewa, 1991)

$$Sh = 0.724 Re^{1/3} Sc^{1/2} Ga^{1/6} \quad (3.8)$$

where Sh is the Sherwood number, Re is the Reynolds number, Sc is the Schmidt number and Ga is the Galileo number. These dimensionless groups are defined as follows

$$Sh = \frac{k_L^o L}{D_{CO_2}} \quad (3.9)$$

$$Re = \frac{4 q}{\nu} \quad (3.10)$$

$$Sc = \frac{\nu}{D_{CO_2}} \quad (3.11)$$

$$Ga = \frac{g L^3}{\nu^2} \quad (3.12)$$

where  $D_{CO_2}$  is the diffusivity of  $CO_2$  in the solution,  $\nu$  is the kinematic viscosity of the solution,  $L$  is the effective contact length of the wetted wall column (6.7 cm) and  $q$  is the volumetric flow rate per unit length which in this case is the perimeter of the inner tube (3.01 cm). Density, viscosity and  $CO_2$  diffusivity for ethylene glycol solutions at 25°C were obtained from Hayduk and Malik (1971).



The area along the interfacial length was  $20.21\text{cm}^2$  and the surface area of the liquid pool was  $1.77\text{ cm}^2$ . The interfacial area of  $0.75\text{ cm}^2$  at the top of the inner tube was neglected. Equation 3.8 does not account for end effects. Hence it was necessary to perform a calibration of the apparatus. In the present work, the flow rate was kept fixed at about  $1.2\text{ cc/sec}$ . Only the solution viscosity was varied by changing the amounts of ethylene glycol. The desorption data are plotted as shown in Figure 3.3. The maximum Reynolds number obtained was close to 150 (which ensures laminar flow) and corresponded to the experiment with pure water. Addition of increasing amounts of ethylene glycol reduced the Reynolds number. Thus the low end corresponds to the experiment with pure ethylene glycol. The Reynolds number exponent and the constant in equation 3.8 are treated as the adjustable parameters. They correspond to the slope and intercept in Figure 3.3. The dimensionless correlation for the wetted wall column that accounts for the end effects too is

$$\text{Sh} = 0.795 \text{ Re}^{0.27} \text{ Sc}^{1/2} \text{ Ga}^{1/6} \quad (3.13)$$

Figure 3.4 compares this correlation to theory and relations obtained by Toman (1990)

$$\text{Sh} = 1.28 \text{ Re}^{0.23} \text{ Sc}^{1/2} \text{ Ga}^{1/6} \quad (3.14)$$

and Vivian and Peaceman (1956).

$$\text{Sh} = 0.433 \text{ Re}^{0.40} \text{ Sc}^{1/2} \text{ Ga}^{1/6} \quad (3.15)$$

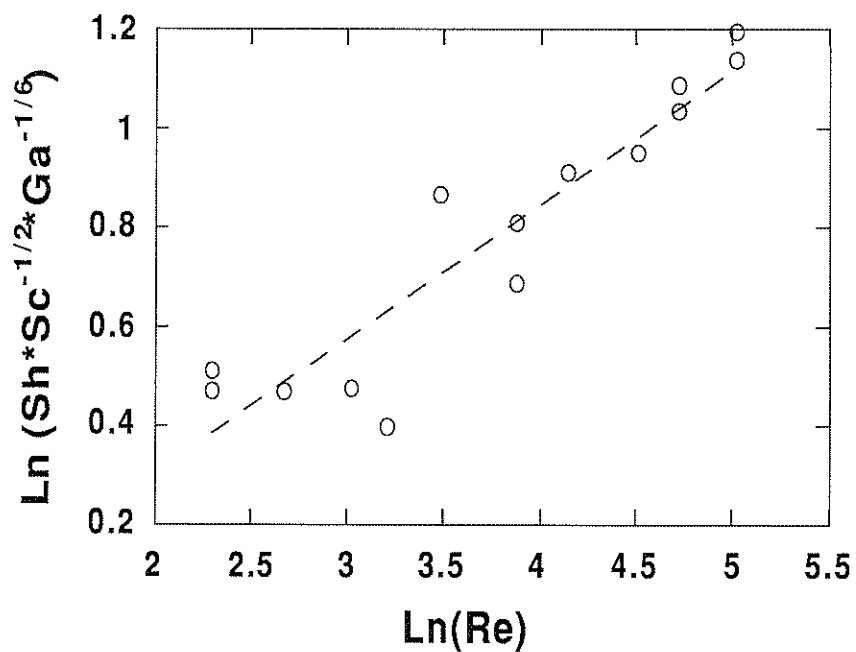


Figure 3.3 Dimensionless mass transfer correlation for the desorption of  $CO_2$  from aqueous ethylene glycol solutions of varying strengths in a wetted wall column. The line represents the equation  $y = -0.23 + 0.27x$ , and (o) refers to the experimental data points.

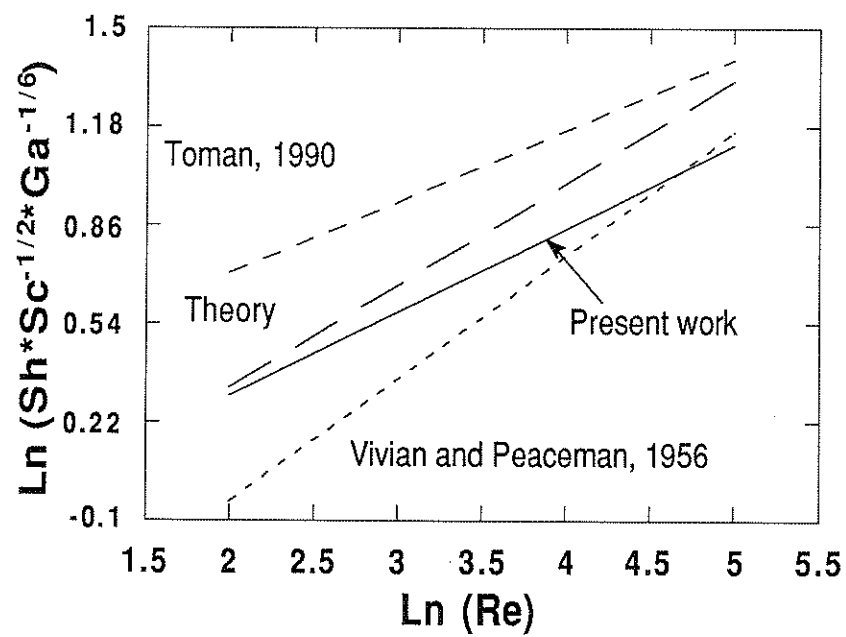


Figure 3.4 Comparison of different dimensionless mass transfer correlations for a wetted wall column.

### **3.3 Reactive absorption**

#### **3.3.1 General Methodology**

Absorption rates of CO<sub>2</sub> into 50 wt% alkanolamine solutions of MDEA and DEA were studied for a range of conditions as shown in Table 3.1. The blend composition is expressed on a mole basis. All compositions are on a CO<sub>2</sub> free basis.

**Table 3.1 Conditions for absorption of CO<sub>2</sub> into 50 wt% alkanolamine solutions.**

Amine	Temperature °C	Loading $\frac{\text{mol CO}_2}{\text{mol amine}}$	CO <sub>2</sub> partial pressure (atm)
Pure MDEA	25, 40	0 - 0.5	0.001 - 1.0
10% DEA - 90% MDEA	25, 40	0 - 0.6	0.001 - 1.0
50% DEA - 50% MDEA	25, 40	0 - 0.5	0.001 -- 1.0
Pure DEA	25, 40	0.2 - 0.6	0.001 - 1.0

*In the blended amines, the percentage is on a mole basis.*

The apparatus was set up as shown earlier in Figure 3.2. The flow controllers were set to attain the desired partial pressures of CO<sub>2</sub> as well as the requisite flow through the wetted wall column. Typically, the flow was about 40 cc/min but for DEA it was necessary to send about 150 cc/min because of its

fast reaction with CO<sub>2</sub>. The flow controllers used in this experimental work have been tabulated in Table 3.2. The allowable flow rates through those flow controllers are listed in Table 3.3. The micro pump was used at a setting of 40 where it provided a flow rate of about 1.2 cc/min for all solutions. The methodology was to run experiments for a particular amine at a given loading for a range of partial pressures (0.001-1.0 atm) at 25°C and 40°C and then change the loading with pure CO<sub>2</sub>. The large reservoir volume (600 mL) ensured that the CO<sub>2</sub> loading of the solution remained reasonably constant for the experiments over the range of partial pressures at two temperatures.

While making these measurements, the gas mixture was first sent through the bypass, diluted with nitrogen and then analyzed for carbon dioxide content using the CO<sub>2</sub> analyzer. The deflection was noted on a strip chart recorder. The gas mixture was then sent through the wetted wall column, with the liquid flowing down the outer walls of the inner tube. The process was continued till the deflection on the analyzer had become constant. This would be indicated by a flat curve on the strip chart recorder. This deflection was noted. The difference corresponded to the absorption rate of CO<sub>2</sub>. The partial pressure was then changed and the whole process repeated for a different partial pressure.

Usually the dilution rate and rate of N<sub>2</sub> used for mixing were kept fixed for experiments from 0.001 - 0.01 atm and 0.01 - 0.1 atm. Changes were

Table 3.2 Flow controllers for different amines and partial pressures of CO<sub>2</sub>

Amine	PCO <sub>2</sub>	analyzer	N <sub>2</sub> dil.	N <sub>2</sub> mix	CO <sub>2</sub>	N <sub>2</sub> /CO <sub>2</sub>
	(atm)	range				
MDEA	0.001-0.1	0-0.25%	9205HCO37101 <sup>b</sup>	405194 <sup>a</sup>	405196	9203HCO37102
MDEA	0.1-1.0	0-25%	9205HCO37101	405194	405188	9203HCO37102
				406558	405196	
DEA-MDEA	0.001-0.1	0-0.25%	9205HCO37101	9205HCO37103	405196	9203HCO37102
DEA-MDEA	0.001-0.1	0-25%	9205HCO37101	9205HCO37103	405196	9203HCO37102
DEA	0.001-0.01	0-0.25%	9205HCO37101	9205HCO37103	405196	405191
DEA	0.001-0.01	0-25%	9205HCO37101	9205HCO37103	405196	405191

\* DEA-MDEA refers to both blends.

\* 0-0.25% and 0-25% refer to the low and high range HORIBA PIR-2000 CO<sub>2</sub> analyzers.

<sup>a</sup> identifies the flow controller by the number on the University of Texas at Austin property trademark.

<sup>b</sup> identifies the flow controller by the serial number as provided by the manufacturer.

**Table 3.3 Ranges of flow controllers**

Flow controllers	Range <sup>a</sup> cc/min	Calibration gas
9205HCO37101	2000	N2
9203HCO37102	5000	N2
9205HCO37103	100	N2
406558	100	N2
405196	100	CO2
405188	500	CO2
405191	250	N2
405194	5000	air

<sup>a</sup> range refers to the upper limit on the flow rate. The lower limit is always 0 cc/min.

necessary while moving from one range to another. Experiments were performed at 25°C and 40°C.

As previously mentioned, in parallel with the measurement of absorption or desorption rates, calibration of the analyzer was performed. For most cases the 0-0.25 vol.% analyzer was used. The flux of CO<sub>2</sub> was measured from the difference of the inlet and outlet flow rates of CO<sub>2</sub> (with respect to the wetted wall column). Liquid phase analysis was used solely to measure the loading of the solution.

To change the loading, pure CO<sub>2</sub> was used to contact the liquid. The measurements at 1.0 atm were performed at this stage. The set up is identical to the one employed while performing the calibration experiments using the desorption technique (Section 3.2.2). While this uses the same equipment as

the other experiments at lower pressures, the configuration is different and hence could be thought of as a different experiment.

### **3.3.2 Equilibrium measurements**

In this work, at any given loading for a particular amine solution, both desorption and absorption rates were measured by variation of CO<sub>2</sub> partial pressure. This implied bracketing of equilibrium. This concept is illustrated by Figures 3.5 and 3.6. Figure 3.5 yields the equilibrium solubility of CO<sub>2</sub>. While inferring this value, only measurements close to equilibrium were considered. Also the partial pressure used was based on the outlet. A total pressure of 1 atm was assumed to which a correction for vapor pressure of water was applied. This was estimated from the data in Table 2.7.

Figure 3.6 also yields an equilibrium solubility. This value is based on log mean partial pressure and the entire range of measurements.

$$P_{\log \text{ mean}} = \frac{P_{\text{in}} - P_{\text{out}}}{\ln \frac{P_{\text{in}}}{P_{\text{out}}}} \quad (3.16)$$

The log mean basis is indicative of the plug flow assumption in a wetted wall column also used by Toman (1990). It is very essential that equilibrium be bracketed. Extrapolation as in Figure 3.7 does not yield good results. This is substantiated by comparison with the VLE model (Austgen, 1989) predictions in Figure 3.8.



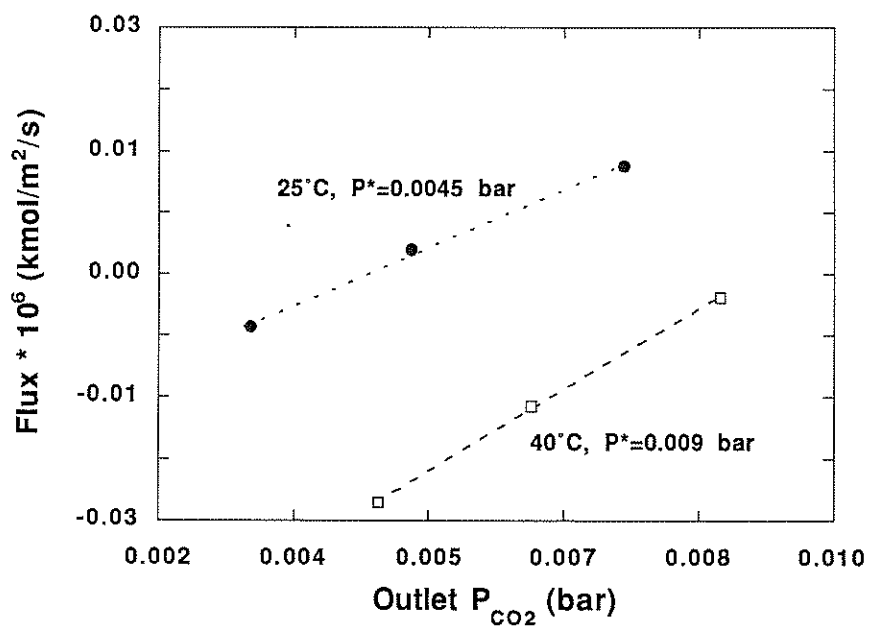


Figure 3.5 Extraction of CO<sub>2</sub> solubility based on the outlet partial pressure for 50 wt% aqueous solution of MDEA at a loading of 0.044.

---

---

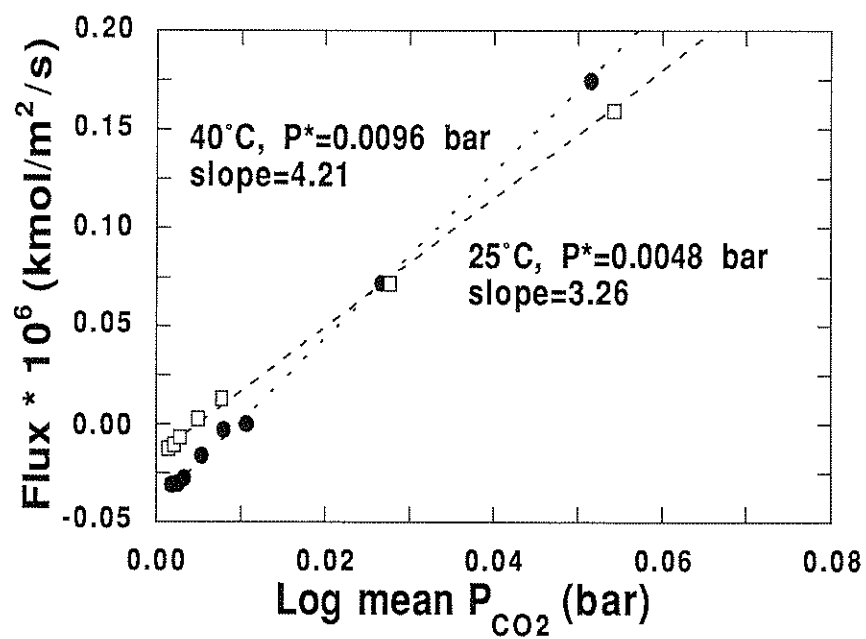


Figure 3.6 Extraction of CO<sub>2</sub> solubility based on the log mean partial pressure and normalized flux for 50 wt% aqueous solution of MDEA at a loading of 0.044.

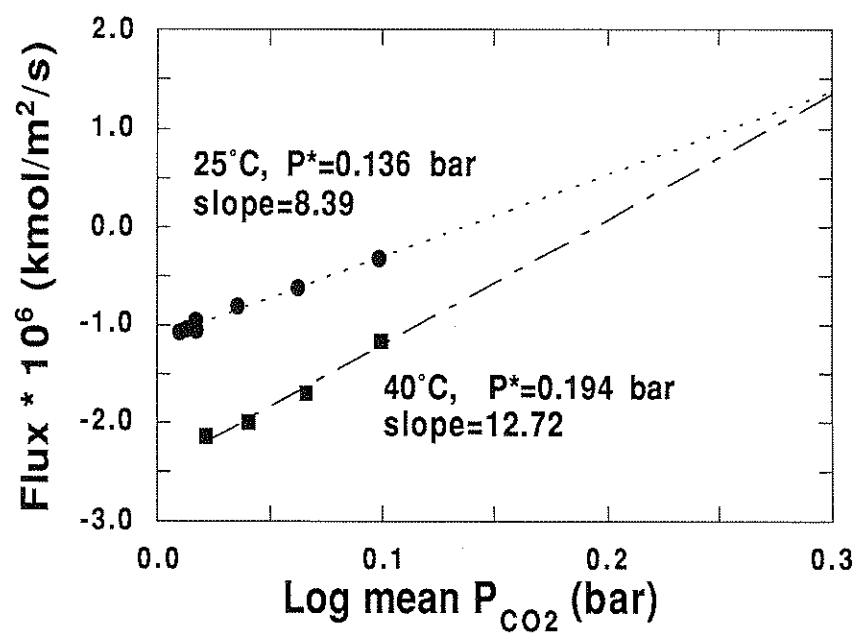


Figure 3.7 Extraction of CO<sub>2</sub> solubility based on the log mean partial pressure and normalized flux for 50 wt% aqueous solution of DEA at a loading of 0.613.

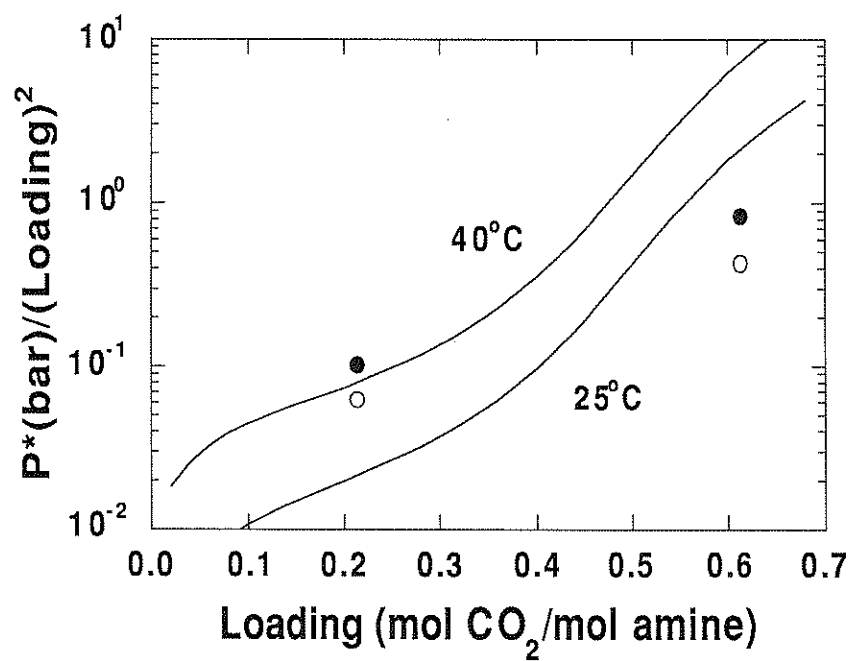


Figure 3.8 Normalized CO<sub>2</sub> solubility from interpolation of log mean  $P_{\text{CO}_2}$  in a 50 wt% aqueous solution of DEA.. Curves refer to the VLE model (Austgen, 1989) predictions. Points are the experimental data.

The equilibrium solubilities using both methods are tabulated in Table 3.4. They compare fairly well. Comparisons to model predictions and other experimental data are made with the equilibrium solubilities obtained from the analysis based on the log mean  $\text{CO}_2$  partial pressure. Subsequent work is based on the equilibrium  $\text{CO}_2$  solubility obtained by interpolation of the log mean partial pressure of  $\text{CO}_2$ .

The VLE model (Section 2.5.1) was developed by Austgen (1989) both on a stand-alone basis and in the framework of ASPEN PLUS. The latter was used in this work. This model used the Electrolyte-NRTL equation to estimate activity coefficients in the liquid phase and the Redlich-Kwong-Soave equation of state to calculate the fugacity coefficients in the gas phase. The parameters for these equations were obtained by regression of experimental data obtained from measurements of  $\text{CO}_2$  solubilities in aqueous mixtures of MDEA with MEA and DEA. They are tabulated in Tables 2.9 and 2.10.

The equilibrium  $\text{CO}_2$  solubilities obtained in (50 wt%) alkanolamine solutions of MDEA, 10% DEA - 90% MDEA, 50% DEA - 50% MDEA and DEA are compared to the VLE model predictions in Figures 3.8, 3.9, 3.10 and 3.11. The ordinate used is the equilibrium pressure normalized by the square of the loading. In general, the data at  $40^\circ\text{C}$  were better fit by the model as compared to the data at  $25^\circ\text{C}$ . This is primarily because Austgen (1989) performed regression of experimental data at  $25^\circ\text{C}$ ,  $40^\circ\text{C}$  and  $80^\circ\text{C}$ . As mentioned before the equilibrium data for DEA (Figure 3.11) do not compare

**Table 3.4 Experimental measurement of CO<sub>2</sub> solubility in solutions of DEA and MDEA at 25°C and 40°C.**

Amine	Loading mol CO <sub>2</sub> mol amine	CO <sub>2</sub> solubility (bar)					
		25°C			40°C		
		Outlet	Log mean	Model	Outlet	Log mean	Model
MDEA	4.40E-02	4.50E-03	4.80E-03	2.51E-03	9.10E-03	9.60E-03	6.67E-03
	9.03E-02	1.10E-02	1.09E-02	7.00E-03	2.50E-02	2.30E-02	1.88E-02
	1.95E-01	3.60E-02	3.70E-02	2.20E-02	9.60E-02	9.10E-02	6.20E-02
	3.10E-01	7.00E-02	8.70E-02	5.28E-02	1.70E-01	1.51E-01	1.52E-01
	4.68E-01	1.96E-01	1.89E-01	1.47E-01	4.30E-01	3.96E-01	4.45E-01
10% DEA - 90% MDEA	5.70E-02	2.50E-03	2.50E-03	2.11E-03	6.50E-03	6.00E-03	6.04E-03
	1.35E-01	1.05E-02	1.10E-02	8.62E-03	2.44E-02	2.40E-02	2.43E-02
	2.80E-01	5.70E-02	4.50E-02	3.56E-02	1.60E-01	1.45E-01	1.02E-01
	4.94E-01	2.08E-01	2.09E-01	1.66E-01	4.80E-01	4.43E-01	5.10E-01
	6.40E-01	5.30E-01	5.00E-01	4.55E-01	8.10E-01	8.04E-01	1.46E+0
50% DEA - 50% MDEA	1.36E-01	2.50E-03	3.00E-03	1.73E-03	6.80E-03	7.00E-03	5.76E-03
	2.36E-01	1.20E-02	1.10E-02	7.37E-03	2.80E-02	2.40E-02	2.33E-02
	4.35E-01	1.06E-01	9.40E-02	7.90E-02	2.07E-01	1.90E-01	2.45E-01
	5.42E-01	3.17E-01	3.00E-01	2.42E-01	6.52E-01	6.18E-01	7.72E-01
DEA	2.14E-01	2.85E-03	2.70E-03	9.63E-04	4.66E-03	4.30E-03	3.57E-03
	6.13E-01	1.61E-01	1.36E-01	7.94E-01	3.12E-01	1.94E-01	2.69E+0

1. outlet refers to the equilibrium CO<sub>2</sub> solubility based on gas phase partial pressure of CO<sub>2</sub> in the stream coming out of the wetted wall column.

2. log mean refers to the equilibrium CO<sub>2</sub> solubility based on the logarithmic mean of the inlet and outlet gas phase partial pressures of CO<sub>2</sub> with respect to the wetted wall column.

3. model refers to the equilibrium CO<sub>2</sub> solubility generated by the VLE model (Austgen, 1989).

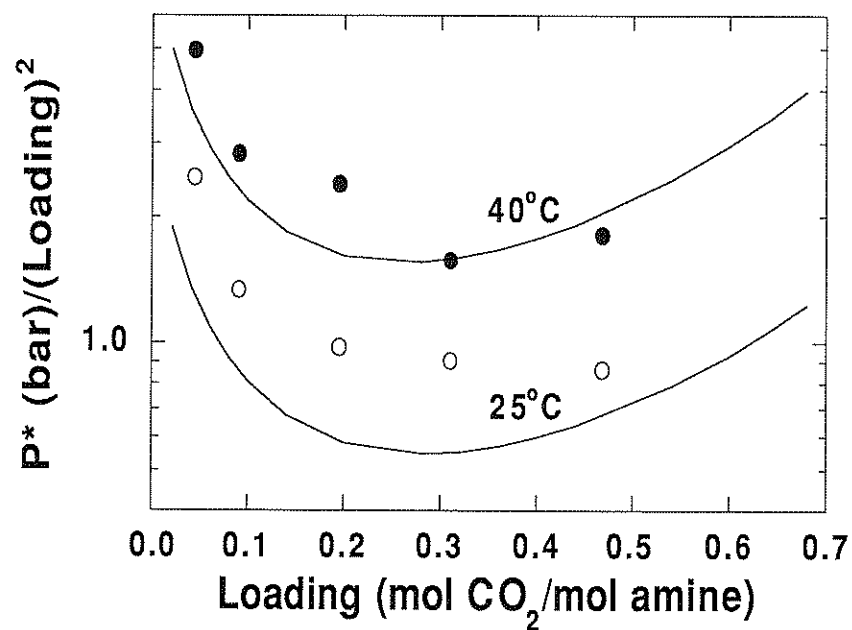


Figure 3.9 Normalized CO<sub>2</sub> solubility from interpolation of log mean  $P_{\text{CO}_2}$  in a 50 wt% aqueous solution of MDEA.. Curves refer to the VLE model (Austgen, 1989) predictions. Points are the experimental data.

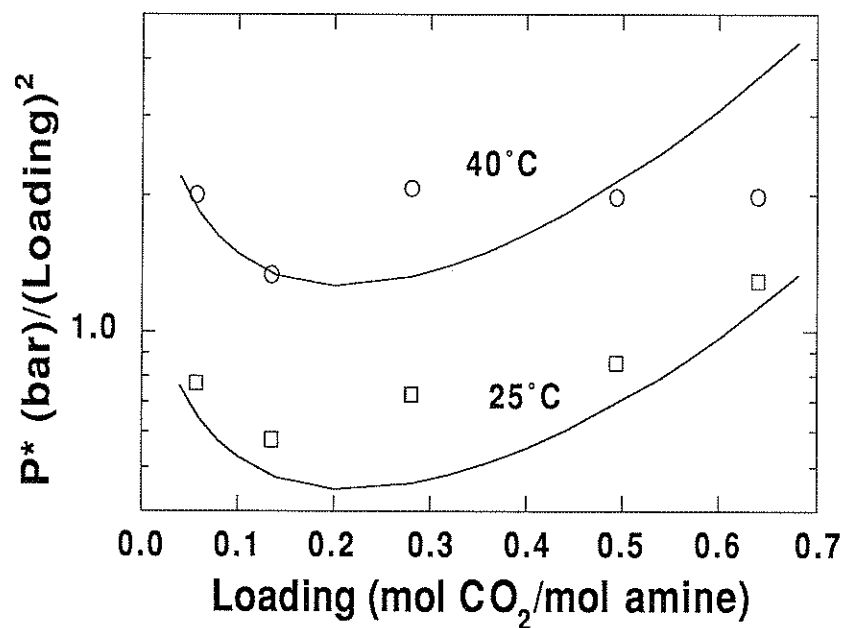


Figure 3.10 Normalized CO<sub>2</sub> solubility from interpolation of log mean  $P_{\text{CO}_2}$  in a 50 wt% aqueous amine solution with 10 mol% DEA and 90 mol% MDEA. Curves refer to the VLE model (Austgen, 1989) predictions. Points are the experimental data.



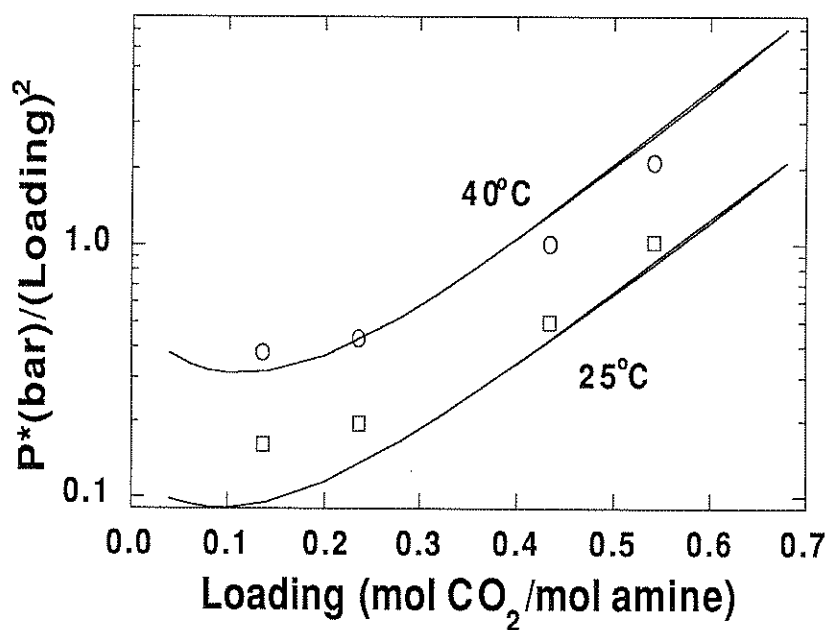


Figure 3.11 Normalized CO<sub>2</sub> solubility from interpolation of log mean  $P_{\text{CO}_2}$  in a 50 wt% aqueous amine solution with 50 mol% DEA and 50 mol% MDEA. Curves refer to the VLE model (Austgen, 1989) predictions. Points are the experimental data.

well primarily because equilibrium was not bracketed. It is also important to note that an error in measurement of loading rather than equilibrium CO<sub>2</sub> pressure is likely to cause deviations from the model predictions.

The equilibrium measurements in this work as well as those obtained by Austgen (1989) for 4.28M MDEA and 2M MDEA- 2M DEA at 40°C and Jou et al. (1982) for 4.28M MDEA at 25 and 40°C are compared to the model predictions in Figures 3.12 and 3.13. Austgen (1989) attributes the discrepancy at higher loadings to either a poor fit of the data or errors in experimental measurements.

The relative positions of the CO<sub>2</sub> solubility curves for the 4 amine solutions get inverted after a loading of approximately 0.54 mol/mol as shown in Figures 3.14 and 3.15. The experimental data for the blended amines conform to this trend. This crossover phenomenon was also observed (by means of the VLE model) and explained by Austgen (1989).

### **3.3.3 Rate Measurements**

The raw data obtained in this work are presented in Appendix A. The inlet and outlet CO<sub>2</sub> partial pressures are measured based on the N<sub>2</sub> and CO<sub>2</sub> flow rates. The log mean partial pressure is estimated from equation 3.16. The absorption rate is essentially the difference of the CO<sub>2</sub> flow rates in and out of the wetted wall column. The flow rates are measured with the CO<sub>2</sub> analyzer and converted to flux by dividing with the contact area of the wetted wall

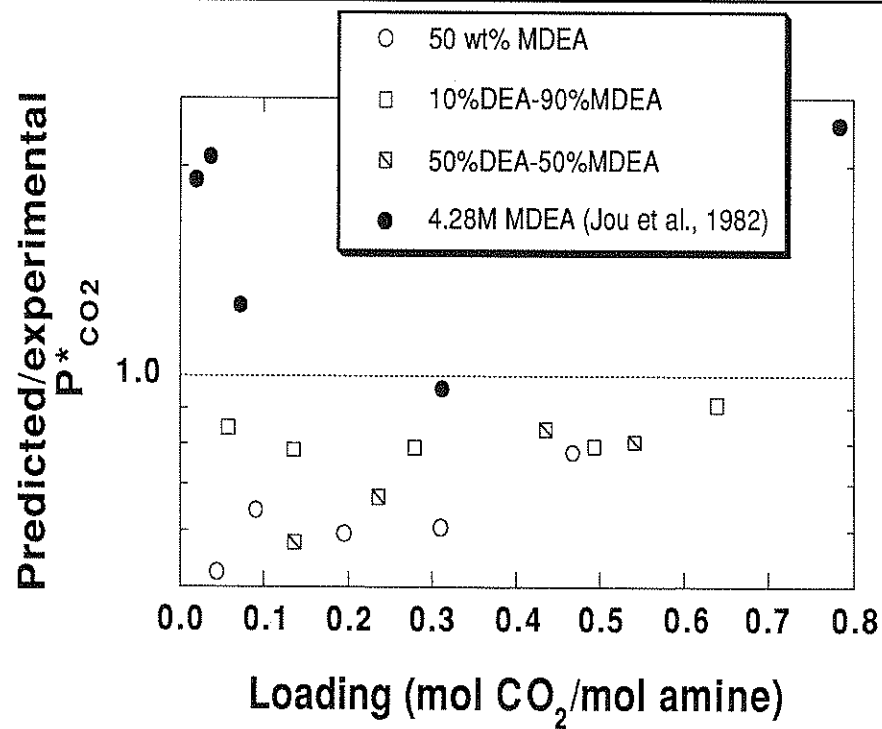


Figure 3.12 Comparison of experimental data on  $CO_2$  solubility from interpolation of log mean  $P_{CO_2}$  at  $25^\circ C$  to VLE model (Austgen, 1989) prediction.

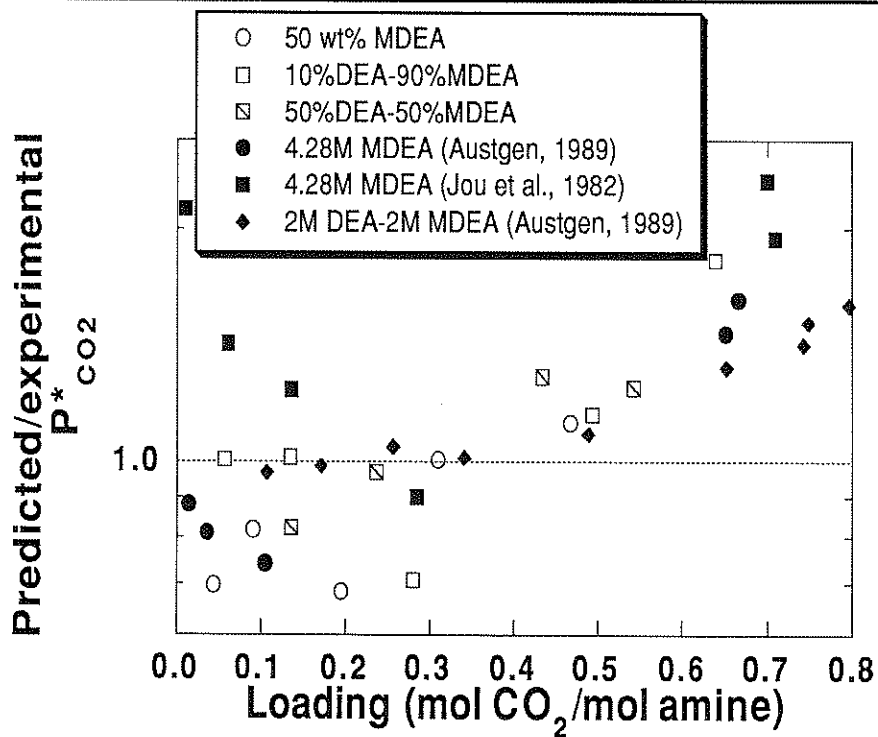


Figure 3.13 Comparison of experimental data on CO<sub>2</sub> solubility from interpolation of log mean  $P_{CO_2}$  at 40° C to VLE model (Austgen, 1989) prediction.

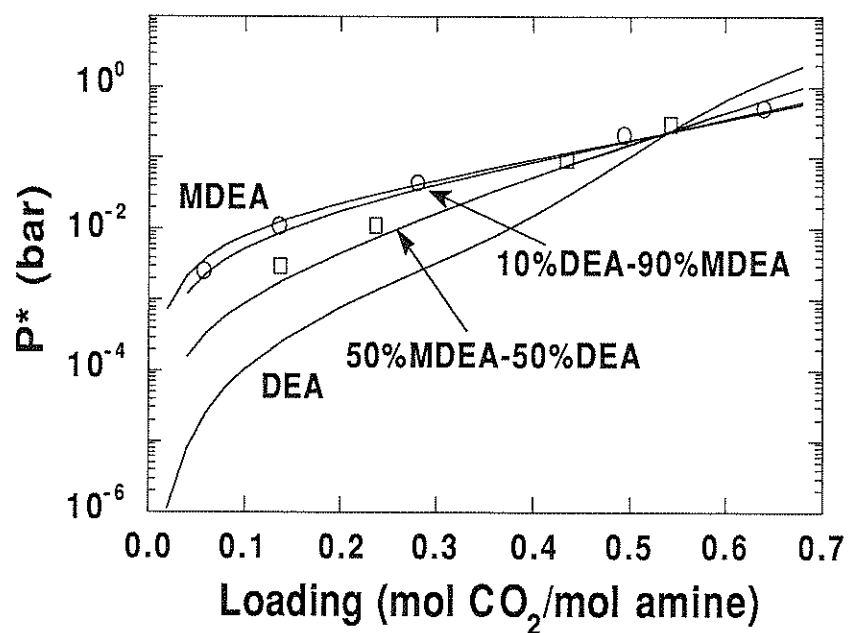


Figure 3.14 VLE model (Austgen, 1989) prediction versus experimental data for CO<sub>2</sub> solubility in 50 wt% blended amines with 10%DEA-90%MDEA and 50%DEA-50%MDEA (mole basis) at 25 °C. Points refer to experimental data and curves to model predictions.

---

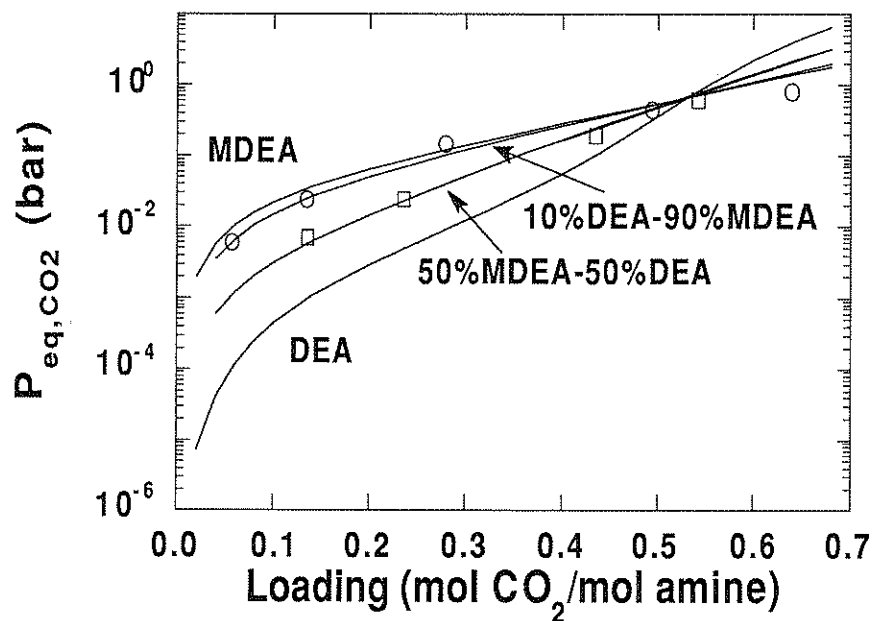


Figure 3.15 VLE model (Austgen, 1989) prediction versus experimental data for CO<sub>2</sub> solubility in 50 wt% blended amines with 10% DEA-90% MDEA and 50% DEA-50% MDEA (mole basis) at 40 °C. Points refer to experimental data and curves to model predictions.

column ( $21.98 \text{ cm}^2$ ). This contact area is the sum of the interfacial area along the contact length ( $20.21 \text{ cm}^2$ ) and the surface area of the liquid seal ( $1.77 \text{ cm}^2$ ). The area at the top of the inner tube ( $0.75 \text{ cm}^2$ ) was neglected. The loading was measured by solution analysis with the carbon analyzer. The procedure is described in Section 3.1.5. The mass transfer coefficient is estimated from equation 3.13. Temperature measurements were made in the jacketed reservoir and not the wetted wall column.

In this work, a simple analysis is used to validate the data obtained. Temperature deviations from  $25^\circ\text{C}$  and  $40^\circ\text{C}$  have been neglected for this purpose. The data for DEA were not used though each individual measurement could still be used when regressing each measurement of flux as a function of  $\text{CO}_2$  partial pressure independently.

Figure 3.6, shown earlier, represents the measured flux as a function of the log mean  $\text{CO}_2$  partial pressure for a typical solution composition. Expectedly the equilibrium pressure is lower at  $25^\circ\text{C}$  as absorption is an exothermic phenomenon. Also, away from equilibrium (on both sides) the kinetic effects dominate which yield higher absorption and desorption rates at  $40^\circ\text{C}$ .

The slope of the line in Figure 3.6 is the normalized flux:

$$\text{Normalized flux} = \frac{\text{Flux}}{P - P^*} \quad (3.17)$$

where  $P-P^*$  is the partial pressure driving force for  $\text{CO}_2$  absorption.  $P$  is the gas phase  $\text{CO}_2$  partial pressure and  $P^*$  is the equilibrium value in the bulk solution.

The normalized flux at  $25^\circ\text{C}$  and  $40^\circ\text{C}$  for the 4 amine solutions is plotted as a function of loading in Figures 3.16 and 3.17.

The enhancement factor can be calculated as follows

$$E = \frac{\text{Normalized flux}}{m_{\text{CO}_2} k_L^0} \quad (3.18)$$

where  $m_{\text{CO}_2}$  is the solubility constant of  $\text{CO}_2$  in the alkanolamine solution and has units of  $\text{kmol m}^{-3} \text{ bar}^{-1}$ .  $m_{\text{CO}_2}$  for pure MDEA was estimated as a function of amine composition at different temperatures by Toman (1990) who used the experimental data from his work, Al-Ghawas et al. (1989), Versteeg et al. (1988) and Haimor and Sandall (1984). Toman (1990) also estimated the effect of loading on the solubility of  $\text{CO}_2$  into 50 wt% MDEA. This parameter when used seemed to overcorrect for the effect of loading and so subsequent analysis did not take into account the effect of loading on  $\text{CO}_2$  solubility. Littell (1991) provides  $m_{\text{CO}_2}$  for pure DEA as a function of composition at different



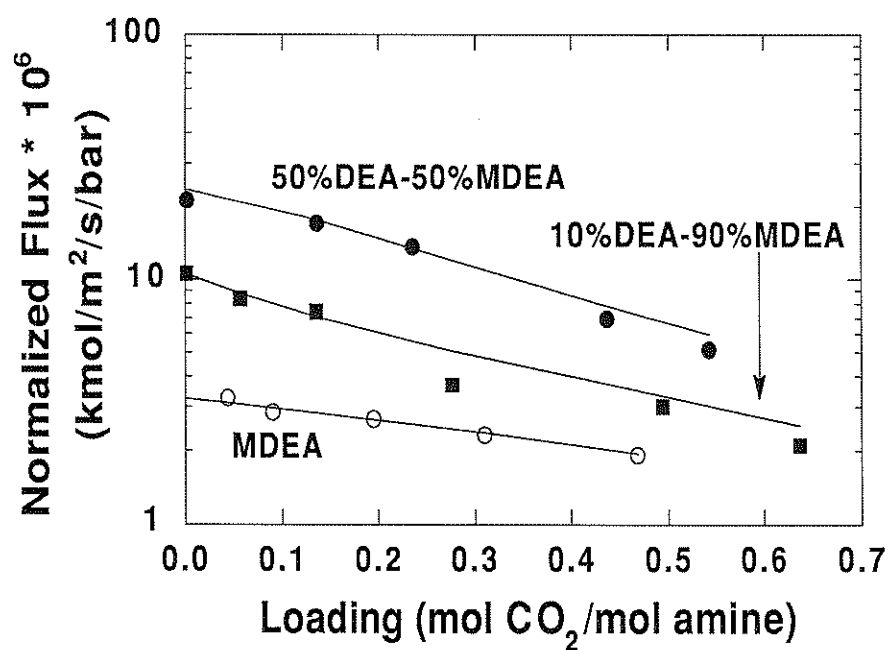


Figure 3.16 Normalized flux of CO<sub>2</sub> as a function of loading at 25 °C for 50 wt% amines. Points refer to the experimental data. Curves refer to the values predicted by the rate parameters in Table 3.10.

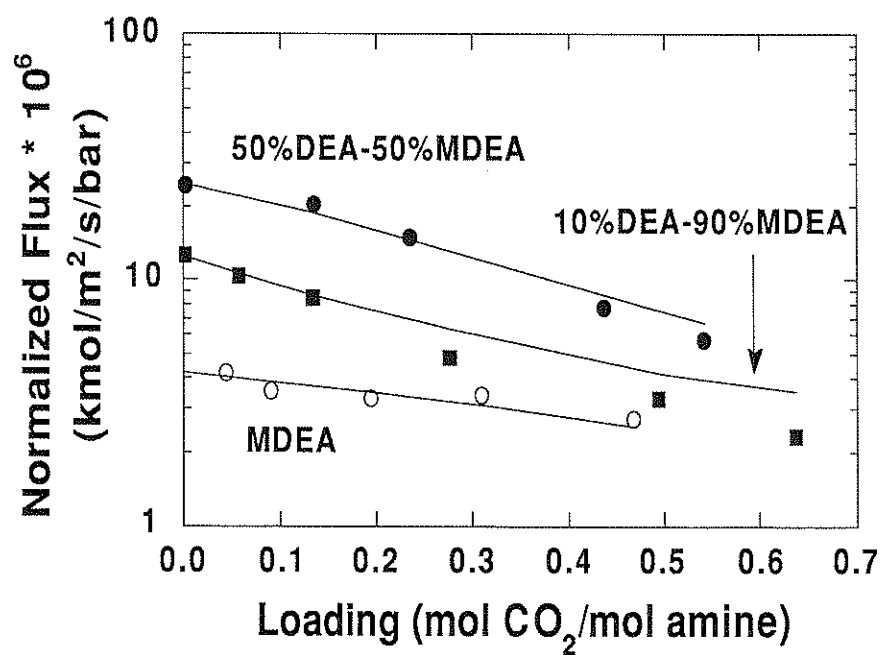


Figure 3.17 Normalized flux of CO<sub>2</sub> as a function of loading at 40 °C for 50 wt% amines. Points refer to the experimental data. Curves refer to the values predicted by the rate parameters in Table 3.10.

temperatures. For the blends,  $m_{CO_2}$  was estimated from a linear combination of  $m_{CO_2}$  for pure DEA and MDEA. For dilute solutions it reduces to the Henry's constant. Details about the calculation of this solubility parameter are presented in Appendix B.5.

The values obtained have been tabulated along with the pseudo first order rate constant in Tables 3.5 and 3.6. For pseudo first order conditions

$$E = \sqrt{1 + \frac{k_1 D_{CO_2}}{k_L^2}} \quad (3.19)$$

where  $k_1$  is the pseudo first order rate constant.

Details about estimation of the diffusion coefficient in unloaded and loaded amine solutions can be found in Appendix B.4.

The pseudo first order approximation implies that the conditions at the interface and bulk are identical. The analysis that was performed made this assumption. Hence it was necessary to check for depletion of DEA or hydroxide at the interface for the blended amine data.. The bulk was speciated using the VLE model (Austgen, 1989). From the flux, free DEA, carbamate and hydroxide ion concentrations were estimated at the interface with the assumption that all the flux arose from diffusion of carbamate or DEA. At low loadings (0.0015 for 10% DEA - 90% MDEA and 0.0023 for 50% DEA - 50% MDEA) there is depletion of hydroxide at the interface. At high loadings (0.49, 0.64 for 10% DEA - 90% MDEA and 0.54 for 50% DEA - 50% MDEA) there

Table 3.5 Summary of rate data at 25°C.

Amine	Range of PCO <sub>2</sub> (bar)		K <sub>L</sub> <sup>o</sup> x 10 <sup>5</sup> m/s	DCO <sub>2</sub> x 10 <sup>10</sup> m <sup>2</sup> /s	CO <sub>2</sub> solubility bar	Normalized flux kmol/m <sup>3</sup> /s/ bar	Deviation %	E	k <sub>1</sub>	
	Lowest	Highest							measured 1/s	calculated 1/s
MDEA	8.52E-04	4.88E-02	1.90E-03	3.04	4.79	2.76E-02	6.31	16	7.51	107
	1.37E-03	8.88E-02	4.40E-02	3.00	4.68	2.76E-02	3.26	4	3.94	27.8 b
	1.73E-03	9.82E-01	9.03E-02	2.95	4.56	2.76E-02	2.85	7.2	3.50	21.4 b
	1.28E-02	3.72E-01	1.95E-01	2.84	4.30	2.76E-02	2.67	23	3.41	19.9 b
	1.58E-02	5.69E-01	3.10E-01	2.72	4.03	2.76E-02	2.30	8.9	3.06	15.4 b
10% DEA - 90% MDEA	1.12E-01	5.76E-01	4.68E-01	2.57	3.69	2.76E-02	1.90	14.2	2.68	11.0 b
	2.04E-03	6.88E-02	1.50E-03	3.05	4.80	2.85E-02	10.60	6.2	12.2	286
	3.01E-03	7.46E-02	5.70E-02	2.99	4.65	2.85E-02	8.33	8	9.78	181 b
	4.37E-03	7.89E-02	1.35E-01	2.90	4.45	2.85E-02	7.39	5	8.93	148 b
	9.08E-02	9.87E-01	2.77E-01	2.75	4.11	2.85E-02	3.69	9.6	4.70	38.9
50% DEA - 50% MDEA	2.53E-02	9.81E-01	4.94E-01	2.55	3.64	2.85E-02	3.01	6.1	4.14	28.8
	3.24E-02	9.8E-01	6.37E-01	2.42	3.37	2.85E-02	2.09	14.6	3.02	14.2
	3.7E-03	5.02E-02	2.30E-03	3.08	4.87	3.01E-02	21.09	4	22.8	1004
	2.92E-03	5.79E-02	1.36E-01	2.93	4.51	3.01E-02	17.04	11.8	19.3	707
	5.17E-03	6.7E-02	2.36E-01	2.82	4.27	3.01E-02	13.72	8.5	16.1	484 b
DEA	1.34E-02	9.81E-01	4.36E-01	2.69	3.95	3.01E-02	6.91	18.4	8.53	131 b
	3.5E-02	9.84E-01	5.42E-01	2.60	3.76	3.01E-02	5.16	22	6.58	76.1
	3.01E-03	7.7E-02	2.14E-01	2.88	4.39	3.00E-02	33.71	50.4	38.8	4240
	1.72E-02	9.83E-02	6.13E-01	2.50	3.52	3.00E-02	8.39	5.5	11.2	692

% values refer to the maximum deviation of the experimentally measured fluxes from the flux calculated as the product of the normalized flux and the pressure driving force (Flux = [Normalized flux]x[P-P\*]).

a Calculated from parameters in Table 3.10. b Used in rate data regression

Table 3.6 Summary of rate data at 40°C

Amine	Range of PCO <sub>2</sub> (bar)		Loading	$K_L^o \times 10^5$ m/s	DCO <sub>2</sub> $\times 10^{10}$ m <sup>2</sup> /s	CO <sub>2</sub> solubility kmol/m <sup>3</sup> / bar	Normalized flux kmol/m <sup>2</sup> /s/ bar	Deviation %	E	k <sub>1</sub>	
	Lowest	Highest								measured 1/s	calculated 1/s
MDEA	8.63E-04	3.71E-02	1.90E-03	4.19	8.02	2.24E-02	8.04	19	8.56	157	41.5
	1.82E-03	8.38E-02	4.40E-02	4.12	7.8	2.24E-02	4.21	10.8	4.55	42.7 b	39.3
	2.67E-03	8.63E-02	9.03E-02	4.05	7.63	2.24E-02	3.54	6.9	3.89	30.4 b	36.8
	6.21E-03	3.59E-01	1.95E-01	3.90	7.20	2.24E-02	3.30	19.8	3.77	27.9 b	31.4
	2.14E-02	5.37E-01	3.10E-01	3.74	6.75	2.24E-02	3.40	9	4.05	31.9 b	26.1
10% DEA - 90% MDEA	1.23E-01	5.61E-01	4.68E-01	3.54	6.18	2.24E-02	2.73	3	3.44	21.9 b	18.8
	2.21E-03	6.33E-02	1.50E-03	4.19	8.03	2.28E-02	12.59	7	13.2	376	371
	3.55E-03	6.90E-02	5.70E-02	4.11	7.79	2.28E-02	10.30	9.7	11.0	259 b	274
	6.66E-03	7.73E-02	1.35E-01	3.99	7.45	2.28E-02	8.46	10.5	9.28	182 b	191
	2.26E-02	5.26E-01	2.77E-01	3.79	6.88	2.28E-02	4.84	10.8	5.60	63.3	110
50% DEA - 50% MDEA	3.69E-02	9.33E-01	4.94E-01	3.51	6.10	2.28E-02	3.27	6.6	4.09	31.6	52.9
	4.43E-02	9.47E-01	6.37E-01	3.33	5.65	2.28E-02	2.33	8	3.06	16.5	39.9
	2.17E-03	4.53E-02	2.30E-03	4.23	8.13	2.20E-02	24.28	2	26.1	1492	1538
	4.00E-03	5.38E-02	1.36E-01	4.03	7.54	2.20E-02	20.34	9	22.9	1129	955
	8.09E-03	6.80E-02	2.36E-01	3.88	7.13	2.20E-02	14.84	11.8	17.4	635 b	606
DEA	3.58E-02	5.06E-01	4.36E-01	3.69	6.60	2.20E-02	7.66	15.7	9.42	181 b	234
	1.50E-01	9.42E-01	5.42E-01	3.58	6.29	2.20E-02	5.70	13	7.23	104	144
	3.31E-03	7.22E-02	2.14E-01	3.95	7.31	2.04E-02	39.45	56.4	49.1	5133	1519
	9.96E-02	2.18E-02	6.13E-01	3.43	5.87	2.04E-02	12.72	4.2	12.7	658	221

% values refer to the maximum deviation of the experimentally measured fluxes from the flux calculated as the product of the normalized flux and the pressure driving force (Flux = [Normalized flux] $\times$ [P-P\*]).

a Calculated from parameters in Table 3.10. b Used in rate data regression.

was a significant depletion of free DEA and accumulation of carbamate at the interface. Hence these data were not used in the analysis. Depletion of DEA was estimated assuming that all the flux arises from the gradient in DEA in concentration. Depletion of hydroxide at the interface was calculated indirectly from the interfacial loading of CO<sub>2</sub>. Details are shown in the sample depletion calculations in Appendix D. Some of the results are shown in Tables 3.7 and 3.8.

**Table 3.7 Estimate of depletion of free DEA at the interface**

Amine	T	Flux x 10 <sup>6</sup>	PCO <sub>2</sub>	Loading	c <sub>DEA,b</sub>	c <sub>DEA,i</sub>	Depletion
	°C	$\frac{\text{kmol}}{\text{m}^2 \text{ s}}$	bar	$\frac{\text{mol CO}_2}{\text{mol amine}}$	$\frac{\text{kmol}}{\text{m}^3}$	$\frac{\text{kmol}}{\text{m}^3}$	%
10%DEA- 90%MDEA	25	0.25	0.65	0.637	0.032	0.017	47
10%DEA- 90%MDEA	25	0.75	0.48	0.494	0.053	0.013	78
10%DEA- 90%MDEA	25	1.2	0.38	0.277	0.114	0.047	59
50%DEA- 50%MDEA	25	2	0.8	0.542	0.25	0.07	28

**Table 3.8 Indirect estimate of depletion of hydroxide at the interface**

Amine	T	Flux $\times 10^6$	$P_{CO_2}$	Loading	$c_{CO_2,b}$	$c_{CO_2,i}$	Depletion
	$^{\circ}C$	$\frac{kmol}{m^2 s}$	bar	$\frac{mol CO_2}{mol amine}$	$\frac{kmol}{m^3}$	$\frac{kmol}{m^3}$	%
10%DEA- 90%MDEA	40	0.5	0.041	0.0015	0.007	0.029	75
10%DEA- 90%MDEA	25	0.5	0.047	0.0015	0.007	0.032	78
50%DEA- 50%MDEA	25	0.6	0.025	0.0023	0.01	0.04	75

Pseudo first order conditions are generally satisfied in a pure MDEA system. At low loadings the reaction of MDEA with  $CO_2$  catalyzed by hydroxide (reaction 2.12) contributes to an increased reaction rate. This contribution diminishes quickly as loading increases (Glasscock, 1990). The reaction rate with water is almost independent of loading. The higher rate at a low loading and slowly decreasing rate otherwise can be observed in Figures 3.16 and 3.17.

Some useful results can be inferred from Figure 3.17. At  $40^{\circ}C$ , DEA can increase the absorption rate of  $CO_2$  by a factor of 2 to 4 at 0.05 to 0.2 loading. With 10% DEA - 90% MDEA, the enhancement relative to pure MDEA vanishes at loading greater than 0.2. For 50% DEA - 50% MDEA the relative enhancement is still significant at a loading of 0.5.

The methodology adopted in this work was to fit the rate data that satisfied the pseudo first order conditions and extract the rate parameters for the reactions 2.11, 2.19 and 2.21 and also 2.20 if necessary. Concentrations were expressed in terms of mole fractions. The activities were based on mole fractions. The units of the regressed rate constants were in units of 1/s. Density of the solution could be used to express these constants in different units. Some of these details were described earlier in Section 2.3.5. Various approaches were considered. The parameter values along with the confidence intervals for some are shown in Table 3.9. The regression was performed with the multiple regression feature of Microsoft Excel which unfortunately did not allow for specification of constraints.

To simplify matters when using a concentration basis the low loading (0.0019) point for MDEA was not used. This obviated the consideration of reaction 2.12. However for activity based regressions the low loading point for MDEA was considered. Here, the pseudo first order rate constant for the CO<sub>2</sub>-MDEA reaction was expressed as (Glasscock, 1990).

$$k_{\text{MDEA}} = \frac{\gamma_{\text{CO}_2} \gamma_{\text{MDEA}}}{\gamma_{\text{HCO}_3^-}} \left[ k_{\text{OH}^-} \frac{\gamma_{\text{OH}^-} \gamma_{\text{CO}_2}}{\gamma_{\text{MDEA}}} + k_{\text{H}_2\text{O}} \frac{\gamma_{\text{H}_2\text{O}} \gamma_{\text{CO}_2}}{\gamma_{\text{MDEAH}^+}} \right] \quad (3.20)$$

Regression with reactions 2.11, 2.19, 2.20 and 2.21 resulted in a negative value with a large confidence interval for the rate constant of the CO<sub>2</sub>-DEA-DEA reaction and hence precluded it from consideration in further



Table 3.9 Comparison of parameter values from regressions on different basis

Method	Step	Step	Step	Step	1-stroke
Solubility	no loading	no loading	loading d	no loading	no loading
T °C	25	40	40	25	40
MDEA	204 ± 4%	317 ± 7.4%	449 ± 20%	204 ± 4.1%	472 ± 42%
DEA-MDEA	3.13 x 10 <sup>4</sup> ± 166%	8.25 x 10 <sup>4</sup> ± 125%	-1.08 x 10 <sup>5</sup> ± 50%	2.99 x 10 <sup>4</sup> ± 211%	-1.22 x 10 <sup>4</sup> ± 774%
DEA-H2O	1.73x 10 <sup>4</sup> ± 22%	2.22 x 10 <sup>4</sup> ± 33%	4.55 x 10 <sup>4</sup> ± 85%	1.81x 10 <sup>4</sup> ± 31%	2.89 x 10 <sup>4</sup> ± 23%
DEA-DEA				-1.64 x 10 <sup>4</sup> ± 445%	
R <sup>2</sup> a	0.92	0.53		0.92	
std error a	1.81	5.2	19.65	1.81	
R <sup>2</sup> b	0.99	0.98	0.997	0.98	0.984
std error b	32.64	69.52	36.32	39.48	52.1

Method	1-stroke	Step e	Step e	Step f	Step
Solubility	no loading	no loading	no loading	activity f	activity f
T °C	25	40	25	40	25
MDEA	211 ± 43%	317 ± 7.4%	204 ± 4.1%		
MDEA-H2O				80.9 ± 12.4%	36.1 ± 15.2%
MDEA-OH-				9.98 x 10 <sup>7</sup> ± 3.5%	9.95 x 10 <sup>7</sup> ± 3.4%
DEA-MDEA	3.01 x 10 <sup>4</sup> ± 122%	6.16 x 10 <sup>4</sup> ± 107%	3.67 x 10 <sup>4</sup> ± 155%	8.45 x 10 <sup>5</sup> ± 146%	1.18 x 10 <sup>7</sup> ± 34%
DEA-H2O	1.73 x 10 <sup>4</sup> ± 15%	2.07x 10 <sup>4</sup> ± 23%	1.77 x 10 <sup>4</sup> ± 23%	1.49 x 10 <sup>4</sup> ± 519%	-2.21 x 10 <sup>4</sup> ± 117%
DEA-DEA					
R <sup>2</sup> a		0.532	0.92	0.99	0.99
std error a		5.2	1.81	5.45	3.62
R <sup>2</sup> b	0.99	0.46	0.46	0.92	0.985
std error b	21.4	44.11	35.49	134.39	36.47

a refers to the fit and standard error in regressing the MDEA data alone.

b refers to the fit and standard error in 1-stroke regression or the regression of blended amine data in a 2-step regression

c concentration based regression which does not account for the effect of loading on solubility

d concentration based regression which does account for the effect of loading on solubility

e only 4 points were considered when regressing the blended amine data. Experiment corresponding to a loading of 0.136 with 50%MDEA-50%MDEA was not considered.

f activity based regression

analysis. This was a concentration based regression where the effect of loading on solubility was not accounted for.

The effect of performing the regression in one or two steps was also considered. When performed in two steps, the first step involved regressing the MDEA data alone to obtain the rate parameter for the CO<sub>2</sub>-MDEA reaction. The subsequent step involved regressing the blended amine data in conjunction with the rate constant for the CO<sub>2</sub>-MDEA reaction and obtaining the rate parameters for the CO<sub>2</sub>-DEA-H<sub>2</sub>O and CO<sub>2</sub>-DEA-MDEA reactions. Performing the regression in one stroke yielded a negative value with a large confidence interval for the CO<sub>2</sub>-DEA-MDEA reaction. Hence the two-step methodology was adopted. The reaction rate expression 2.14 for the CO<sub>2</sub>-MDEA reaction includes water. In the present work, water was not considered so as to facilitate direct comparison with the results of previous researchers. Including water accounted for a 10% increase in the estimated second order rate constant.

Three approaches were considered with respect to the solubility parameter  $m_{\text{CO}_2}$ . The reactions considered were 2.11, 2.19 and 2.21.

1. Using concentration (mole fraction) basis and accounting for the effect of loading on solubility.
2. Using concentration (mole fraction) basis and not accounting for the effect of loading on solubility.

3. Accounting for the effect of loading on solubility by basing the calculations on activities (mole fraction based).

The first approach was found unsuitable since it yielded a negative value for the rate constant of the CO<sub>2</sub>-DEA-MDEA reaction. The activity based regression was rejected because a negative rate constant with a large confidence interval (> 100 %) was obtained for the CO<sub>2</sub>-DEA-H<sub>2</sub>O reaction at 25°C.

The approach finally chosen involved using a concentration basis, not accounting for the effect of loading on solubility, not considering the CO<sub>2</sub>-DEA-DEA reaction and performing the regression in two steps. This method yielded values with reasonable confidence intervals for the CO<sub>2</sub>-MDEA and CO<sub>2</sub>-DEA-H<sub>2</sub>O reaction. However the rate parameter for the CO<sub>2</sub>-DEA-MDEA reaction had a confidence interval of at least 100%. These details are presented in Table 3.10.

The same approach was used with 1 fewer data point (corresponding to the experiment at 0.136 loading with 50% DEA - 50% MDEA). This reduced the confidence intervals (expectedly) but the confidence interval for the CO<sub>2</sub>-DEA-MDEA reaction still exceeded 100%. The rate parameters obtained by this regression were used to calculate pseudo first order rate constants and compare with the experimental results.

**Table 3.10 Parameters used in predictions to compare with experimental data**

<b>Parameter values</b>				
Basis	Mole fraction <sup>a</sup>		Concentration <sup>b</sup>	
T°C	25	40	25	40
MDEA	204±4.1%	317±7.4%	6.1	9.5
DEA-MDEA	3.67 x 10 <sup>4</sup> ± 155%	6.16 x 10 <sup>4</sup> ± 107%	32.7	54.9
DEA-H <sub>2</sub> O	1.77 x 10 <sup>4</sup> ± 23%	2.07 x 10 <sup>4</sup> ± 23%	15.8	18.4

**MDEA-DEA system:**

Concentration basis (kmol/m<sup>3</sup>)

25°C      $r = 6.1 [\text{CO}_2][\text{MDEA}] + 32.7 [\text{CO}_2][\text{DEA}][\text{MDEA}] + 15.8 [\text{CO}_2][\text{DEA}][\text{H}_2\text{O}]$

40°C      $r = 9.5 [\text{CO}_2][\text{MDEA}] + 54.9 [\text{CO}_2][\text{DEA}][\text{MDEA}] + 18.4 [\text{CO}_2][\text{DEA}][\text{H}_2\text{O}]$

Concentration basis (mole fraction)

25°C      $r = 204 x_{\text{MDEA}} x_{\text{CO}_2} + 3.67 \times 10^4 x_{\text{DEA}} x_{\text{MDEA}} x_{\text{CO}_2} + 1.77 \times 10^4 x_{\text{DEA}} x_{\text{H}_2\text{O}} x_{\text{CO}_2}$

40°C      $r = 317 x_{\text{MDEA}} x_{\text{CO}_2} + 6.16 \times 10^4 x_{\text{DEA}} x_{\text{MDEA}} x_{\text{CO}_2} + 2.07 \times 10^4 x_{\text{DEA}} x_{\text{H}_2\text{O}} x_{\text{CO}_2}$

1. The data used to regress for the mentioned rate parameters included experiments at 0.057 and 0.135 loading with 10%DEA-90%MDEA and 0.236 and 0.436 loading with 50%DEA-50%MDEA.

2. The regression was based on concentrations (mole fractions) and not activities. The effect of loading on CO<sub>2</sub> solubility was neglected.

3. The CO<sub>2</sub>-DEA-DEA reaction has not been considered.

a These values were directly obtained from the regression and have units of l/s.

b These rate parameters were derived from the mole fraction based rate parameters.

For the MDEA reaction, the units are  $\frac{\text{m}^3}{\text{kmol}\cdot\text{s}}$  and for the two DEA reactions the

units are  $\frac{\text{m}^6}{\text{kmol}^2\cdot\text{s}}$ . The conversion is achieved by dividing by the square and cube of the density of the solution which is typically 33.5 kmol/m<sup>3</sup>.

Figures 3.18 - 3.21 compare the predicted values of the apparent first order rate constants to the experimentally measured ones. The hydroxide depletion does not show a significant effect. This is primarily because the hydroxide contribution has not been accounted for in the reaction scheme. On the other hand, the depletion of free DEA at the interface at high loadings definitely has a very significant effect.

Table 3.11 compares the rate parameters obtained to those obtained by previous researchers. The second order rate constant for the MDEA system lies in the range of the values obtained by previous researchers. However, the activation energy is significantly lower. A possible reason could be that the temperature of the wetted wall column was lower than 40°C since it was not jacketed. A downward correction of 5°C yields an activation energy of 8080 kcal/kmol.

The rate constant for the DEA-H<sub>2</sub>O mechanism is significantly higher than the one calculated by Glasscock (1990). The (poorly predicted) rate constant for the CO<sub>2</sub>-DEA-MDEA reaction which has a confidence interval of 155% is much lower than Glasscock's prediction (1990).

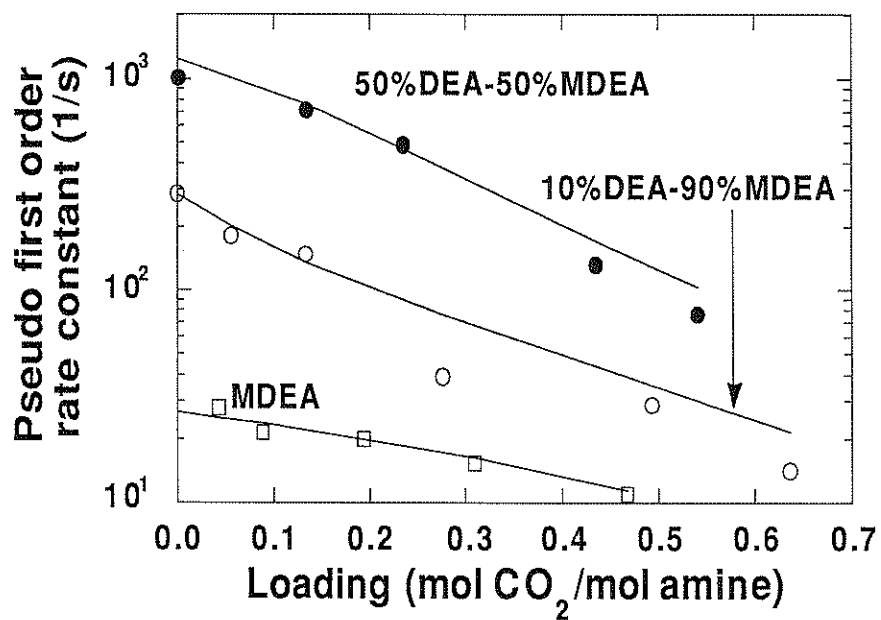


Figure 3.18 Predicted and experimental pseudo first order rate constants at 25 °C as a function of bulk loading. Points refer to the experimental data and the curves refer to values predicted by the rate parameters in Table 3.10.

---

---

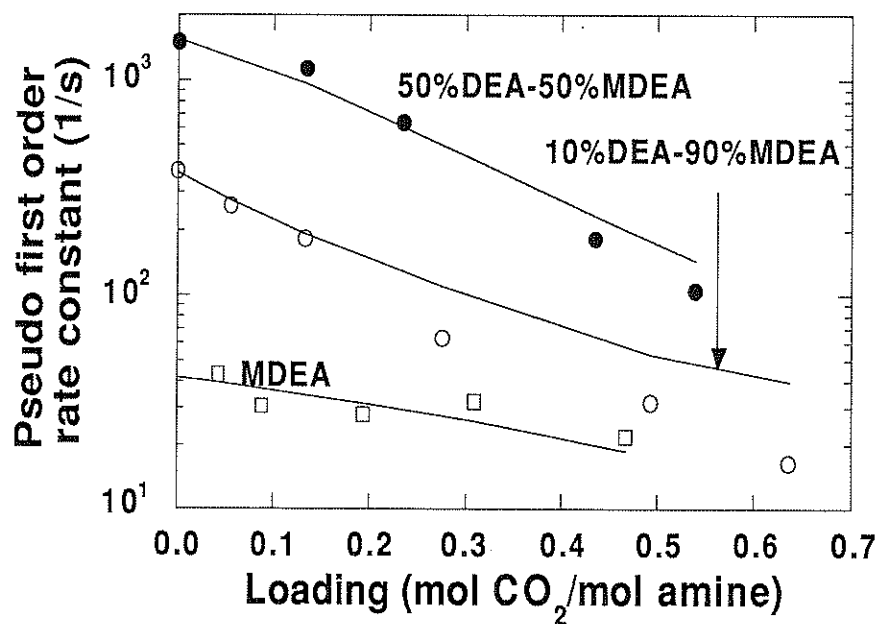


Figure 3.19 Predicted and experimental pseudo first order rate constants at 40 °C as a function of loading. Points refer to experimental data and curves refer to values predicted by the rate parameters in Table 3.10.

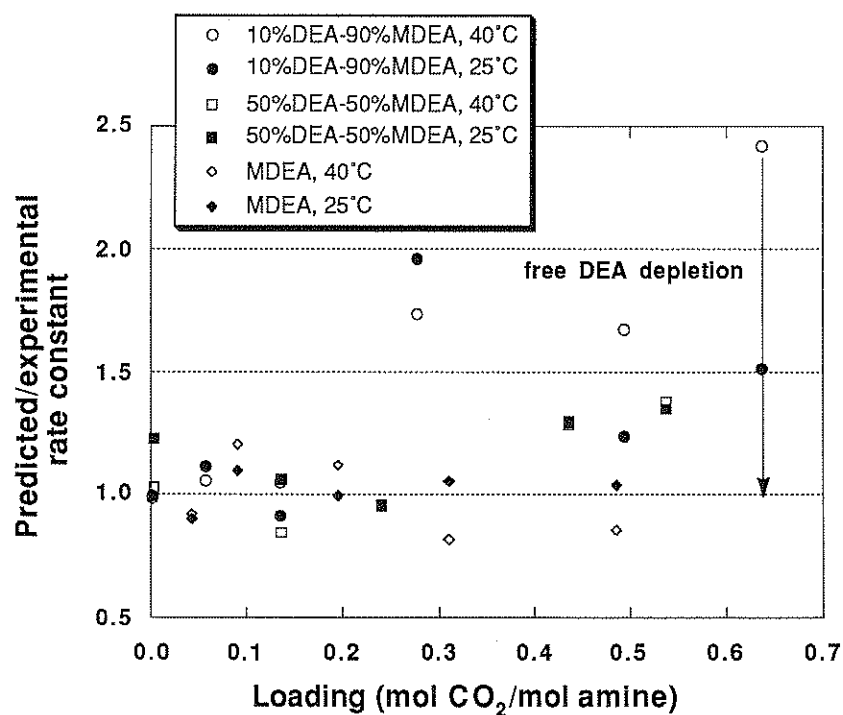


Figure 3.20 Comparison of predicted to experimental values of the rate constants as a function of loading.



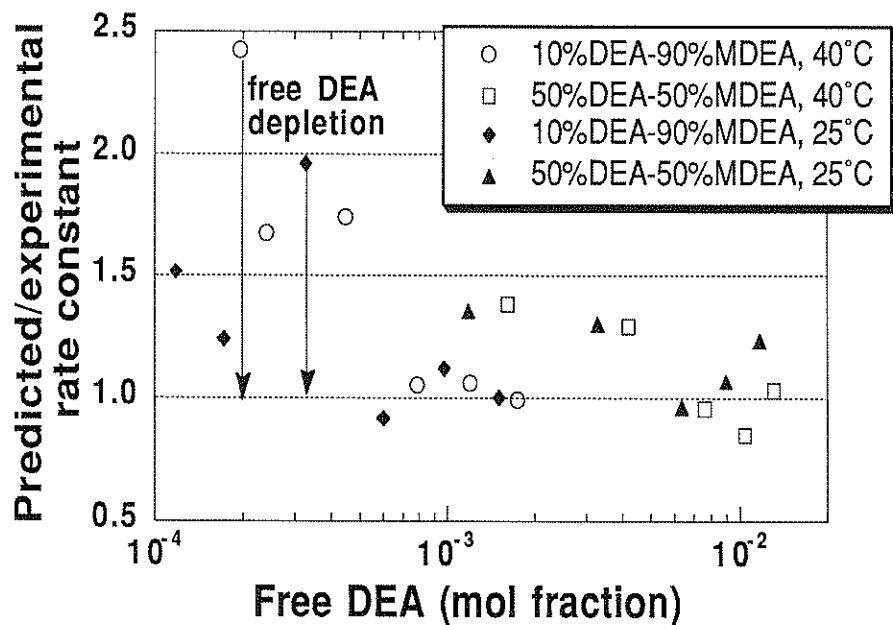


Figure 3.21 Comparison of predicted to experimental values of rate constants as a function of mole fraction of free DEA.

**Table 3.11 Comparison of Results with Literature Data**MDEA system:  $r = k_2[\text{CO}_2][\text{MDEA}]$ 

	$k_{298}$ $\frac{\text{m}^3}{\text{kmol}\cdot\text{s}}$	$E_a$ $\frac{\text{kcal}}{\text{kmol}}$
Critchfield (1988)	2.5	13700
Tomcej et al. (1986)	7.4	9400
Versteeg and Van Swaaij (1988c)	4.3	10100
Littel et al. (1990)	5.1	10700
Haimour et al. (1987)	2.5	17100
Toman and Rochelle (1989)	5.5	9968
Cordi and Bullin (1992)	2.0	15668
Present work	6.1	5474
Glasscock (1990)	1.5 - 30	6590-13600
Current work	6.1	5446

DEA system<sup>b</sup>:

$$r = [\text{CO}_2][\text{DEA}] \{k'_{\text{H}_2\text{O}}[\text{H}_2\text{O}] + k'_{\text{DEA}}[\text{DEA}] + k'_{\text{MDEA}}[\text{MDEA}]\}$$

Versteeg and van Swaaij (1988b)  $k'_{\text{H}_2\text{O}} = 5.3$   $k'_{\text{DEA}} = 228$ .Critchfield (1988)<sup>a</sup>  $100 < k'_{\text{MDEA}} < 400$ Glasscock (1990)  $k'_{\text{H}_2\text{O}} = 4.75$   $k'_{\text{DEA}} = 464$   $k'_{\text{MDEA}} = 468$ Present work  $k'_{\text{H}_2\text{O}} = 15.8 \pm 23\%$   $k'_{\text{MDEA}} = 32.7 \pm 155\%$ 

<sup>a</sup>Critchfield used a different expression for DEA. Shown is an approximate range of this interaction constant based upon conditions investigated by Glasscock (1990) from a linearized form of Critchfield's rate expression.

<sup>b</sup> All rate constants for the DEA system have units of  $\frac{\text{m}^6}{\text{kmol}^2\cdot\text{s}}$

A possible explanation could be put forward if one were to consider the two types of rate expressions used for a DEA/MDEA system. Critchfield (1988) employed the form proposed by Laddha and Danckwerts (1981). His rate expression was

$$r = \frac{[\text{CO}_2][\text{DEA}]}{\frac{1}{1410} + \frac{1}{1200[\text{DEA}] + 2326[\text{MDEA}]}} \quad (3.21)$$

The expression used by Glasscock (1990) at low loading was

$$r = [\text{CO}_2][\text{DEA}] (4.75[\text{H}_2\text{O}] + 464[\text{DEA}] + 468[\text{MDEA}]) \quad (3.22)$$

Glasscock noted that though expressions 3.21 and 3.22 predicted similar results in the conditions investigated in his work (about 20 wt% amine solutions), the predictions could diverge for high amine concentrations.

The experiments in this work involve 50 wt% amine solutions. Also a significant number of observations are at higher loadings. These could be possible reasons for the large discrepancy in the rate constant for the DEA-H<sub>2</sub>O and the DEA-MDEA mechanisms.

For high amine concentrations, equation 3.20 would predict a diminished contribution of the DEA-MDEA mechanism as compared to the DEA-H<sub>2</sub>O mechanism. Figures 3.22 and 3.23 which shows the relative contributions of the different mechanisms in the CO<sub>2</sub>-DEA-MDEA system seem to conform to this trend.

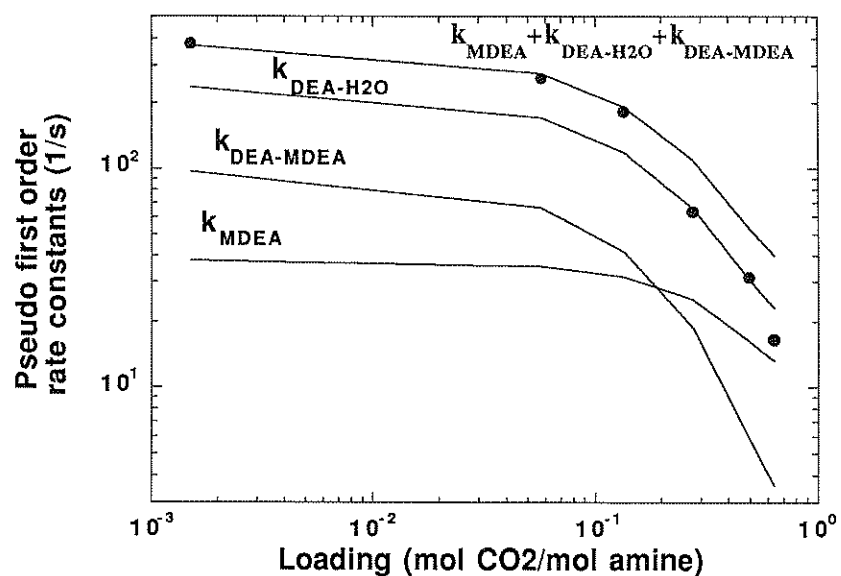


Figure 3.22 Contribution of different mechanisms to the pseudo first order rate constant for 10% DEA - 90% MDEA as a function of loading at 40 °C. Points refer to the experimental data and the curves refer to values predicted by the rate parameters in Table 3.10.

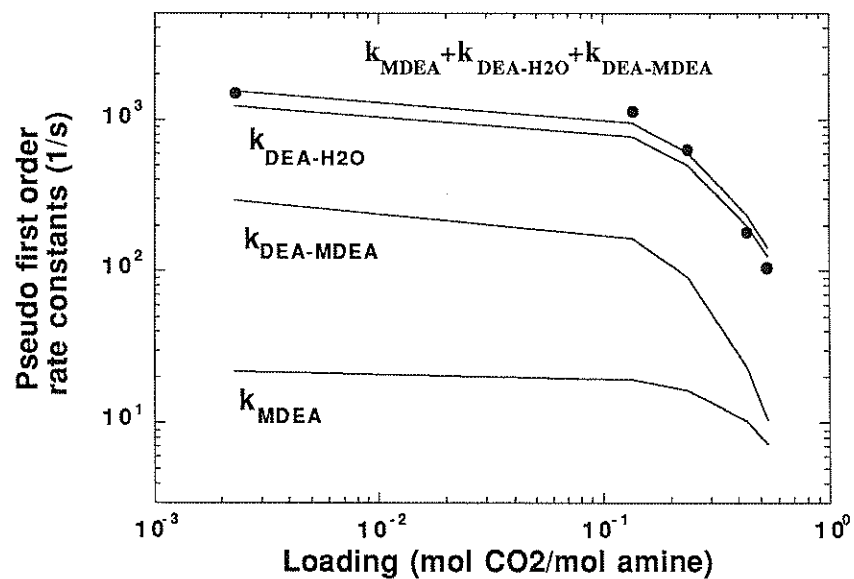


Figure 3.23 Contribution of different mechanisms to the pseudo first order rate constant for 50% DEA - 50% MDEA as a function of loading at 40 °C. Points refer to the experimental data and the curves refer to values predicted by the rate parameters in Table 3.10.

For the 10% DEA - 90% MDEA solution, the pseudo first order rate constants cross at a loading of about 0.2 while no crossing occurs for the 50% DEA - 50% MDEA solution in the range of conditions investigated.

Another reason for the discrepancy in the rate parameters for the CO<sub>2</sub>-DEA-H<sub>2</sub>O and CO<sub>2</sub>-DEA-MDEA reactions could be that the contribution from the CO<sub>2</sub>-DEA-DEA reaction, if any is absorbed to a greater extent by the CO<sub>2</sub>-DEA-H<sub>2</sub>O reaction.

## **CHAPTER FOUR**

### **CONCLUSIONS**

#### **4.1 Summary**

In this work, an attempt was made to model the problem of CO<sub>2</sub> absorption in alkanolamines in the framework of ASPEN PLUS by use of an approximate technique developed by Glasscock and Rochelle (1990). RATEFRAC, a rate-based model was used to tackle this problem. It was necessary to supply a reaction subroutine to account for the complex kinetics in the CO<sub>2</sub>-MDEA-DEA system. Outside of RATEFRAC, modeling of a single stage contactor was performed. Two approaches were applied in this case. One employed the activity coefficients from the equilibrated bulk solution while the other estimated activity coefficients at each step in the interfacial calculations as a function of composition. This essentially involved development of a routine that accounted for effects of chemical reaction on mass transfer through an enhancement factor.

The experimental work involved measuring absorption rates of CO<sub>2</sub> into pure MDEA and DEA as well as aqueous blends of MDEA and DEA. The contactor used was a wetted wall column. The experiments were performed with 50 wt% amines, at 25°C and 40°C over a range of loading from 0 to about 0.6. Partial pressures were varied from about 0.001 atm to 1.0 atm. Measurement of absorption and desorption rates yielded equilibrium data by interpolation.

#### **4.2 Results and Conclusions from the Modeling work**

The enhancement factor approach recommended by Carey (1990) could not be applied to RATEFRAC. So, the methodology adopted was to let RATEFRAC do the interfacial calculations while accounting only for the kinetics through a reaction rate subroutine. Only CO<sub>2</sub>-MDEA systems were handled. However severe convergence problems were encountered in both the initialization (equilibrium) and the actual rate-based calculations. Convergence was achieved only for a few cases where CO<sub>2</sub> was in stoichiometric excess as compared to MDEA. It was also necessary that the gas rate be much larger than the liquid rate for convergence in these cases.

The modeling of a single stage contactor through a routine that accounted for the effects of chemical reaction on mass transfer through an enhancement factor did yield results in all the cases studied. The approach that used activity coefficients from the bulk was compared to the results from



the rigorous analysis (Glasscock and Rochelle, 1990). It matched the predictions of the exact method only in some cases. The most likely reason for this discrepancy is the difference in activity coefficients predicted by the ASPEN model in this work and the rigorous model (Glasscock, 1990).

The approximate approach that let activity coefficients vary at the interface as a function of composition could not be compared to the rigorous or approximate results of Glasscock and Rochelle (1990) since they used bulk activity coefficients in the interfacial calculations. So the predictions of the 'rigorous approximate' approach were compared to the predictions of the approximate approach that used activity coefficients from the bulk. Surprising trends were observed in the predictions of the 'rigorous approximate' approach. For 30 wt% DEA - 20 wt% MDEA and 30 wt% DEA solutions the enhancement factor increased as the pressure was raised from 0.01 or 0.1 to 1.0 atm. For 5 wt% DEA - 45 wt% MDEA and 50 wt% MDEA solutions the enhancement factor decreased as the pressure was increased but it did so by a much smaller factor as compared to the approximate approach that uses bulk activity coefficients.

A correction was necessary to account for the wrong estimation of the concentration of  $\text{OH}^-$  and  $\text{H}_3\text{O}^+$  ions by the FLASH routine. The physical properties, viscosity, density and diffusivities, were estimated from empirical correlations.

Equilibrium  $\text{CO}_2$  activity in a blend of DEA and MDEA was redefined. Conversion of rate constants from concentration based activities to mole fraction based activities used density of the solution as opposed to the density of water at  $25^\circ\text{C}$  (Carey, 1990).

#### **4.3 Results and Conclusions from the Experimental work**

A dimensionless mass transfer correlation was developed to estimate the physical mass transfer coefficient of  $\text{CO}_2$ . The methodology adopted was desorption of  $\text{CO}_2$  from aqueous solutions of ethylene glycol.

Inferred values of  $\text{CO}_2$  solubilities were compared to the VLE model predictions (Austgen, 1989). Failure to bracket equilibrium did not yield good estimates of the solubility for DEA at a loading of 0.613. It was observed that the model fit equilibrium data at  $40^\circ\text{C}$  better. Model prediction of the crossover of equilibrium  $\text{CO}_2$  solubilities was confirmed. (Figures 3.14 and 3.15).

It is more likely that discrepancies arise due to errors in measurement of loading rather than the partial pressure of  $\text{CO}_2$ . Use of log mean pressure instead of outlet pressure did not affect the analysis significantly. The log mean pressure was used throughout this work.

Rate data was extracted from both desorption and absorption measurements. The measurement of flux as a function of  $\text{CO}_2$  partial pressure yielded a normalized flux. From the plot of normalized flux versus loading at  $40^\circ\text{C}$  (Figure, 3.17), one can conclude that the enhancement of 10% DEA -

90% MDEA relative to pure MDEA vanishes at loading greater than 0.2 while 50% DEA - 50% MDEA has a relatively significant enhancement at a loading of 0.5. Addition of DEA can increase the absorption rate by a factor of 2 to 4 at 0.05 to 0.2 loading.

An enhancement factor and a pseudo first order rate constant can be estimated from the normalized factor in conjunction with the physical mass transfer coefficient,  $\text{CO}_2$  diffusivity and solubility. The pseudo first order rate constants calculated from experimental measurements were regressed to yield the second or third order rate constants and the activation energies.

Various approaches were tried. The most favorable approach was the concentration (mole fraction) based regression which involved not accounting for the effect of loading on solubility, not considering the  $\text{CO}_2$ -DEA-DEA reaction and performing the regression in two steps. In the first step the MDEA data alone were regressed to yield the second order rate constant for the  $\text{CO}_2$ -MDEA reaction while in the second step the blended amine data were regressed in conjunction with the  $\text{CO}_2$ -MDEA reaction rate constant to yield parameters for the  $\text{CO}_2$ -DEA- $\text{H}_2\text{O}$  and  $\text{CO}_2$ -DEA-MDEA reactions.

The second order rate constant at  $25^\circ\text{C}$  for the  $\text{CO}_2$ -MDEA reaction lied in the range of those measured by previous researchers. However the activation energy was significantly lower leading one to believe that the wetted wall column was lower than  $40^\circ\text{C}$ . The third order rate constants at

25°C for the CO<sub>2</sub>-DEA-H<sub>2</sub>O and CO<sub>2</sub>-DEA-MDEA reactions had confidence intervals of 23% and 155%.

The rate constant for the CO<sub>2</sub>-DEA-H<sub>2</sub>O reaction was higher than Glasscock's prediction (1990) while the (poorly predicted) rate constant for the CO<sub>2</sub>-DEA-MDEA reaction was lower. The higher contribution of the CO<sub>2</sub>-DEA-H<sub>2</sub>O reaction as compared to the CO<sub>2</sub>-DEA-MDEA reaction could probably be reconciled by a reaction rate expression of the form proposed by Laddha and Danckwerts (1981) and used by Critchfield (1988)

$$r = \frac{[\text{CO}_2][\text{MDEA}]}{\frac{1}{1410} + \frac{1}{1200[\text{DEA}] + 2326[\text{MDEA}]}} \quad (3.21)$$

and not the form employed by Glasscock (1990)

$$r = [\text{CO}_2][\text{DEA}] (4.75[\text{H}_2\text{O}] + 464[\text{DEA}] + 468[\text{MDEA}]) \quad (3.22)$$

Another possibility is that the contribution of the CO<sub>2</sub>-DEA-DEA reaction if any is absorbed by the rate constant of the CO<sub>2</sub>-DEA-H<sub>2</sub>O reaction to a greater extent.

#### **4.4 Recommendations**

In this work, RATEFRAC was used to model only a single stage contactor. Convergence problems were encountered in most cases. Some of the problems like wrong temperature and composition estimates were tackled by use of bounds in the kinetic routine. Still convergence was elusive. If

convergence was attained then using RATEFRAC for system modeling would be an achievable extension. It is believed that the new version of RATEFRAC will be able to handle true components. This would definitely alleviate matters to a great extent.

The model of a single stage contactor outside of RATEFRAC yielded results that did not compare very favorably with the predictions of the rigorous model (Glasscock and Rochelle, 1990) even in cases where kinetic effects dominate. The rate parameters used were ones regressed using the rigorous technique (Glasscock et al., 1991). A possible course of future work could involve developing a method to directly regress the rate parameters using the approximate technique developed in this work. It would be preferable to use the approach that accounts for the effect of composition on activity coefficients for this purpose.

## APPENDIX A

### EXPERIMENTAL DATA

This section contains the raw data used for estimation of the dimensionless mass transfer coefficient correlation. The calibration experiments were conducted at 25°C and the viscosity, density and diffusivity data of aqueous ethylene glycol solutions were directly taken from Hayduk and Malik (1971) and linearly interpolated to give the tabulated values.

The rates of CO<sub>2</sub> absorption/desorption are also tabulated as a function of CO<sub>2</sub> partial pressure, loading and temperature for the 4 akanolamine solutions. Mass transfer coefficients can be estimated from the dimensionless correlation 3.13. The values used in the analysis are tabulated in Tables 3.5 and 3.6.

Loadings were typically measured after every 3 or 4 experiments. Reported are the averaged values. Also some observations do not have entries in the columns P<sub>CO2</sub> in and P<sub>CO2</sub> out. These correspond to 'load change' experiments that were performed by sending pure CO<sub>2</sub> through the wetted wall

column which corresponds to 1 atm. So the reported value (in the  $P_{CO_2}$  log mean ) column is 1 atm with the water vapor correction.

Legend associated with the experimental data

- \* measurement has been used to estimate equilibrium
- @ kinetic data has been extracted from the data point
- no disregard this measurement
- lo the measured value is significantly lower than the expected or predicted
- hi measured value is significantly higher than expected
- eq measurement is close to equilibrium, hence measurements could be in large errors

**ETHYLENE GLYCOL**

Wt%	Density	Viscosity	DCO <sub>2</sub>	Liquid flow rate	k <sub>L</sub> <sup>o</sup>
glycol	$\frac{g}{cc}$	cps	$\frac{cm^2}{sec}$	$\frac{cc}{min}$	$\frac{cm}{s}$
0	9.97E-01	8.94E-01	1.98E-05	1.03	8.16E-03
0	9.97E-01	8.94E-01	1.77E-05	1.03	7.70E-03
15	1.02E+00	1.29E+00	1.61E-05	1.08	7.34E-03
15	1.02E+00	1.29E+00	1.30E-05	1.08	6.97E-03
25	1.03E+00	1.68E+00	1.03E-05	1.12	6.36E-03
40	1.05E+00	2.45E+00	7.44E-06	1.11	5.82E-03
50	1.06E+00	3.26E+00	6.53E-06	1.13	4.91E-03
50	1.06E+00	3.26E+00	5.96E-06	1.13	4.35E-03
65	1.08E+00	4.93E+00	4.81E-06	1.13	4.72E-03
75	1.09E+00	6.82E+00	2.79E-06	1.17	2.91E-03
80	1.10E+00	8.03E+00	2.79E-06	1.14	3.09E-03
90	1.10E+00	1.15E+01	1.03E-05	1.15	2.93E-03
100	1.11E+00	1.70E+01	1.77E-05	1.15	2.38E-03
100	1.11E+00	1.70E+01	1.98E-05	1.15	2.48E-03



**50 WT% MDEA**

P <sub>CO2</sub> in	P <sub>CO2</sub> out	P <sub>CO2</sub> log mean	Loading	Temp	Flux		
(bar)	(bar)	(bar)	<u>mol CO<sub>2</sub></u> <u>mol amine</u>	K	kmol/m <sup>2</sup> /s		
9.66E-04	7.72E-04	8.52E-04	1.90E-03	298	3.03E-09	*	eq,@
1.77E-03	1.15E-03	1.42E-03	1.90E-03	298	9.42E-09	*	@
2.57E-03	1.65E-03	2.05E-03	1.90E-03	298	1.37E-08	*	@
5.00E-03	3.09E-03	3.91E-03	1.90E-03	298	2.85E-08	*	@
1.10E-02	6.77E-03	8.60E-03	1.90E-03	298	6.33E-08	*	@
2.11E-02	1.44E-02	1.72E-02	1.90E-03	298	1.02E-07	*	@
1.10E-02	9.26E-03	9.96E-03	1.90E-03	298	3.24E-08		no
3.04E-02	1.89E-02	2.38E-02	1.90E-03	298	1.63E-07	*	@
5.97E-02	4.06E-02	4.88E-02	1.90E-03	298	3.07E-07	*	@
9.86E-02	7.27E-02	8.37E-02	1.90E-03	298	4.13E-07		lo
		9.82E-01	7.80E-03	298	3.08E-06		lo
9.21E-04	8.74E-04	8.63E-04	1.90E-03	314	4.58E-10	*	eq,@
1.68E-03	1.27E-03	1.41E-03	1.90E-03	314	4.28E-09	*	eq,@
2.45E-03	1.52E-03	1.88E-03	1.90E-03	314	8.11E-09	*	eq,@
4.76E-03	2.39E-03	3.32E-03	1.90E-03	314	1.41E-08	*	@
1.05E-02	7.88E-03	8.80E-03	1.90E-03	314	5.06E-08		@
2.90E-02	1.87E-02	2.26E-02	1.90E-03	314	1.70E-07		@
5.69E-02	3.71E-02	4.46E-02	1.90E-03	314	3.51E-07		@
9.39E-02	6.54E-02	7.59E-02	1.90E-03	314	5.17E-07		lo
		9.40E-01	3.24E-02	313	3.88E-06		lo
9.64E-04	1.95E-03	1.37E-03	4.44E-02	299	-1.23E-08	*	eq,@
1.76E-03	2.52E-03	2.08E-03	4.44E-02	299	-1.05E-08	*	eq,@
2.57E-03	3.08E-03	2.77E-03	4.44E-02	299	-6.47E-09	*	eq,@
4.98E-03	4.99E-03	4.91E-03	4.44E-02	299.2	2.96E-09	*	eq,@
8.20E-03	7.51E-03	7.72E-03	4.44E-02	299.2	1.32E-08	*	lo,@
1.10E-02	1.09E-02	1.08E-02	4.44E-02	299.4	8.90E-09		no
3.04E-02	2.59E-02	2.76E-02	4.44E-02	299.4	7.18E-08	*	@
5.95E-02	5.08E-02	5.42E-02	4.44E-02	299	1.60E-07	*	@
9.84E-02	8.26E-02	8.88E-02	4.44E-02	299	2.76E-07	*	@
		9.82E-01	4.30E-02	298.5	2.91E-06		
		9.81E-01	5.30E-02	298.5	3.08E-06		

\* – used to extract equilibrium; @ – used to extract kinetics; no – disregard the experiment;  
lo – low measured value; hi – high measured value; eq – close to equilibrium

**50 WT% MDEA**

PCO <sub>2</sub> in	PCO <sub>2</sub> out	PCO <sub>2</sub> log mean	Loading	Temp	Flux		
(bar)	(bar)	(bar)	<u>mol CO<sub>2</sub></u> <u>mol amine</u>	K	kmol/m <sup>2</sup> /s		
9.21E-04	3.45E-03	1.82E-03	4.40E-02	314	-3.13E-08	*	@
1.68E-03	3.85E-03	2.50E-03	4.40E-02	314	-3.05E-08	*	@
2.45E-03	4.60E-03	3.27E-03	4.40E-02	313.9	-2.77E-08	*	@
4.77E-03	6.42E-03	5.33E-03	4.40E-02	313.5	-1.61E-08	*	@
7.86E-03	8.65E-03	7.93E-03	4.40E-02	313.5	-2.77E-09	*	eq, @
1.06E-02	1.15E-02	1.07E-02	4.40E-02	312.2	0.00E+00	*	eq, @
2.93E-02	2.59E-02	2.66E-02	4.40E-02	312.2	7.18E-08	*	@
5.71E-02	4.98E-02	5.15E-02	4.40E-02	312.9	1.75E-07	*	@
9.44E-02	7.99E-02	8.38E-02	4.40E-02	312.9	3.14E-07	*	@
		9.40E-01	4.30E-02	313	3.88E-06		
		9.40E-01	6.80E-02	313	3.38E-06		
9.78E-04	2.86E-03	1.73E-03	9.03E-02	296.2	-2.54E-08	*	@
1.79E-03	3.53E-03	2.52E-03	9.03E-02	296.2	-2.35E-08	*	@
2.59E-03	4.23E-03	3.29E-03	9.03E-02	296.2	-2.22E-08	*	@
5.01E-03	6.24E-03	5.52E-03	9.03E-02	296.2	-1.47E-08	*	@
8.23E-03	8.78E-03	8.38E-03	9.03E-02	296.2	-4.47E-09	*	eq, @
1.10E-02	1.19E-02	1.13E-02	9.03E-02	297.6	-6.73E-09	*	eq, @
3.02E-02	2.73E-02	2.83E-02	9.03E-02	297.4	4.83E-08	*	@
5.92E-02	5.20E-02	5.47E-02	9.03E-02	296	1.35E-07	*	@
9.74E-02	8.52E-02	8.99E-02	9.03E-02	296.8	2.21E-07	*	@
		9.82E-01	9.03E-02	298	2.90E-06	*	@
		9.82E-01	9.03E-02	297.7	2.63E-06	*	@
9.40E-04	6.21E-03	2.67E-03	9.03E-02	311.2	-7.20E-08		@
1.72E-03	6.81E-03	3.55E-03	9.03E-02	311.2	-6.91E-08		@
2.49E-03	7.38E-03	4.33E-03	9.03E-02	311.2	-6.60E-08		@
4.81E-03	9.16E-03	6.51E-03	9.03E-02	311.2	-5.53E-08		@
1.06E-02	1.44E-02	1.20E-02	9.03E-02	311.2	-4.08E-08	*	@
2.91E-02	2.99E-02	2.85E-02	9.03E-02	311.2	1.20E-08	*	eq, @
5.68E-02	5.40E-02	5.36E-02	9.03E-02	311.2	1.06E-07	*	@
9.37E-02	8.48E-02	8.63E-02	9.03E-02	311.2	2.26E-07	*	@

\* – used to extract equilibrium; @ – used to extract kinetics; no – disregard the experiment;  
 lo – low measured value; hi – high measured value; eq – close to equilibrium

**50 WT% MDEA**

PCO <sub>2</sub> in	PCO <sub>2</sub> out	PCO <sub>2</sub> log mean	Loading	Temp	Flux	
(bar)	(bar)	(bar)	<u>mol CO<sub>2</sub></u> <u>mol amine</u>	K	kmol/m <sup>2</sup> /s	
9.73E-04	7.97E-03	3.25E-03	1.95E-01	299	-9.56E-08	no
2.58E-03	1.31E-02	6.34E-03	1.95E-01	298.8	-1.48E-07	no
8.19E-03	3.31E-02	1.75E-02	1.95E-01	298.8	-3.47E-07	no
1.11E-02	1.53E-02	1.28E-02	1.95E-01	298	-5.22E-08	* hi,@
3.04E-02	3.16E-02	3.05E-02	1.95E-01	298.4	-8.90E-09	* eq,@
5.92E-02	5.77E-02	5.74E-02	1.95E-01	299.3	5.78E-08	* @
9.80E-02	9.19E-02	9.33E-02	1.95E-01	299	1.36E-07	* @
9.92E-02	9.77E-02	9.67E-02	1.95E-01	299.6	1.04E-07	no
1.97E-01	1.79E-01	1.85E-01	1.95E-01	299.8	3.73E-07	* @
2.96E-01	2.65E-01	2.76E-01	1.95E-01	299.5	6.42E-07	* @
3.94E-01	3.64E-01	3.72E-01	1.95E-01	299.7	9.07E-07	* @
		9.79E-01	1.95E-01	299.3	2.36E-06	
		9.79E-01	1.95E-01	299.2	2.19E-06	
9.35E-04	2.14E-02	6.21E-03	1.95E-01	312.5	-2.87E-07	no
2.48E-03	2.66E-02	9.68E-03	1.95E-01	312.5	-3.42E-07	no
1.06E-02	2.63E-02	1.66E-02	1.95E-01	312.5	-2.07E-07	* @
2.92E-02	4.45E-02	3.49E-02	1.95E-01	312.5	-1.99E-07	* @
5.69E-02	6.86E-02	6.03E-02	1.95E-01	312.5	-9.42E-08	* @
9.42E-02	1.00E-01	9.37E-02	1.95E-01	312.5	1.07E-08	* eq,@
9.54E-02	1.04E-01	9.60E-02	1.95E-01	312.6	9.45E-09	no
1.90E-01	1.87E-01	1.82E-01	1.95E-01	312.2	2.50E-07	* @
2.85E-01	2.71E-01	2.68E-01	1.95E-01	312	5.48E-07	* @
3.80E-01	3.62E-01	3.59E-01	1.95E-01	311.8	9.31E-07	* @
		9.37E-01	1.95E-01	313.6	2.78E-06	
1.10E-02	2.26E-02	1.58E-02	3.10E-01	299.6	-1.52E-07	* @
3.03E-02	4.02E-02	3.44E-02	3.10E-01	299.5	-1.36E-07	* @
5.93E-02	6.73E-02	6.21E-02	3.10E-01	299.4	-7.32E-08	* eq,@
9.80E-02	1.01E-01	9.78E-02	3.10E-01	299.2	0.00E+00	* eq,@
1.07E-01	1.07E-01	1.05E-01	3.10E-01	298	6.28E-08	* eq,@
2.99E-01	2.80E-01	2.85E-01	3.10E-01	298	4.91E-07	* @
5.89E-01	5.67E-01	5.69E-01	3.10E-01	298.2	1.09E-06	* @
		9.79E-01	3.10E-01	299.6	2.00E-06	hi
		9.84E-01	3.10E-01	296.9	2.39E-06	lo

\* – used to extract equilibrium; @ – used to extract kinetics; no – disregard the experiment;  
lo – low measured value; hi – high measured value; eq – close to equilibrium

**50 WT% MDEA**

PCO <sub>2</sub> in	PCO <sub>2</sub> out	PCO <sub>2</sub> log mean	Loading	Temp	Flux		
(bar)	(bar)	(bar)	<u>mol CO<sub>2</sub></u> <u>mol amine</u>	K	kmol/m <sup>2</sup> /s		
1.06E-02	4.09E-02	2.14E-02	3.10E-01	312.9	-4.15E-07	*	@
2.92E-02	5.91E-02	4.07E-02	3.10E-01	312.6	-4.12E-07	*	@
5.71E-02	8.23E-02	6.63E-02	3.10E-01	312.2	-2.93E-07	*	@
9.43E-02	1.13E-01	9.95E-02	3.10E-01	312.2	-1.75E-07	*	@
1.03E-01	1.18E-01	1.06E-01	3.10E-01	312.7	-1.02E-07	*	eq, @
2.86E-01	2.85E-01	2.75E-01	3.10E-01	313	4.04E-07	*	@
5.60E-01	5.59E-01	5.37E-01	3.10E-01	314.5	1.29E-06	*	@
		9.41E-01	3.10E-01	312.7	2.20E-06		hi
1.06E-01	1.22E-01	1.12E-01	4.68E-01	298.3	-1.66E-07	*	eq, @
2.99E-01	2.93E-01	2.91E-01	4.68E-01	298.3	2.28E-07	*	@
5.88E-01	5.83E-01	5.76E-01	4.68E-01	298.8	7.26E-07	*	@
		9.78E-01	4.68E-01	300	1.53E-06		
		9.80E-01	4.68E-01	299	1.27E-06		
1.02E-01	1.58E-01	1.23E-01	4.68E-01	311.4	-7.39E-07	*	@
2.88E-01	3.21E-01	2.94E-01	4.68E-01	311.2	-2.87E-07	*	@
5.68E-01	5.93E-01	5.61E-01	4.68E-01	311.2	4.51E-07	*	@
		9.44E-01	4.68E-01	311.8	1.34E-06		

\* – used to extract equilibrium; @ – used to extract kinetics; no – disregard the experiment;  
 lo – low measured value; hi – high measured value; eq – close to equilibrium

**10 MOL% DEA - 90 MOL% MDEA**

**(50 WT% AMINE)**

PCO <sub>2</sub> in	PCO <sub>2</sub> out	PCO <sub>2</sub> log mean	Loading	Temp	Flux		
(bar)	(bar)	(bar)	<u>mol CO<sub>2</sub></u> <u>mol amine</u>	K	kmol/m <sup>2</sup> /s		
3.10E-03	1.30E-03	2.04E-03	1.50E-03	296.9	2.57E-02	*	@
5.97E-03	2.67E-03	4.05E-03	1.50E-03	297.0	4.76E-02	*	@
9.80E-03	4.61E-03	6.79E-03	1.50E-03	297.1	7.55E-02	*	@
1.09E-02	7.67E-03	9.06E-03	1.50E-03	296.9	5.21E-02		no
3.00E-02	1.42E-02	2.09E-02	1.50E-03	297.1	2.23E-01	*	@
5.86E-02	2.82E-02	4.11E-02	1.50E-03	297.1	4.59E-01	*	@
9.69E-02	4.81E-02	6.88E-02	1.50E-03	297.1	7.25E-01	*	@
		9.84E-01	2.42E-02	297.0	7.42E+00		lo
2.96E-03	1.72E-03	2.21E-03	1.50E-03	312.5	2.01E-02	*	lo,@
5.72E-03	2.88E-03	4.01E-03	1.50E-03	312.4	4.51E-02	*	lo,@
9.39E-03	4.37E-03	6.36E-03	1.50E-03	312.4	7.93E-02	*	@
1.04E-02	7.27E-03	8.43E-03	1.50E-03	313.5	5.76E-02		no
2.87E-02	1.25E-02	1.89E-02	1.50E-03	313.1	2.46E-01	*	@
5.60E-02	2.49E-02	3.71E-02	1.50E-03	313.1	5.04E-01	*	@
9.26E-02	4.42E-02	6.33E-02	1.50E-03	313.1	7.78E-01	*	@
		9.40E-01	1.25E-02	313.1	8.02E+00		lo
3.09E-03	3.01E-03	3.01E-03	5.70E-02	297.2	2.34E-03	*	eq,@
5.97E-03	4.54E-03	5.15E-03	5.70E-02	297.0	2.22E-02	*	@
9.79E-03	6.54E-03	7.94E-03	5.70E-02	297.0	4.91E-02	*	@
1.09E-02	9.56E-03	1.01E-02	5.70E-02	297.0	2.62E-02		no
2.99E-02	1.87E-02	2.35E-02	5.70E-02	297.0	1.62E-01	*	@
5.83E-02	3.46E-02	4.48E-02	5.70E-02	297.0	3.69E-01	*	@
9.67E-02	5.79E-02	7.46E-02	5.70E-02	297.0	5.94E-01	*	@
		9.40E-01	6.10E-02	313.1	8.02E+00		lo

\* – used to extract equilibrium; @ – used to extract kinetics; no – disregard the experiment;  
lo – low measured value; hi – high measured value; eq – close to equilibrium

**10 MOL% DEA - 90 MOL% MDEA****(50 WT% AMINE)**

PCO <sub>2</sub> in	PCO <sub>2</sub> out	PCO <sub>2</sub> log mean	Loading	Temp	Flux		
(bar)	(bar)	(bar)	<u>mol CO<sub>2</sub></u> <u>mol amine</u>	K	kmol/m <sup>2</sup> /s		
2.95E-03	4.58E-03	3.55E-03	5.70E-02	313.5	-1.92E-02	*	lo,@
5.69E-03	6.12E-03	5.68E-03	5.70E-02	313.5	4.14E-04	*	eq,@
9.33E-03	8.50E-03	8.58E-03	5.70E-02	313.5	2.20E-02	*	eq,@
1.04E-02	1.05E-02	1.01E-02	5.70E-02	313.5	1.28E-02		no
2.85E-02	1.91E-02	2.26E-02	5.70E-02	313.5	1.56E-01	*	@
5.56E-02	3.35E-02	4.21E-02	5.70E-02	313.5	3.85E-01	*	@
9.22E-02	5.41E-02	6.90E-02	5.70E-02	313.5	6.46E-01	*	@
		9.84E-01	6.40E-02	297.0	6.64E+00		lo
3.10E-03	6.10E-03	4.37E-03	1.35E-01	295.1	-4.02E-02	*	@
5.99E-03	8.02E-03	6.86E-03	1.35E-01	295.1	-2.59E-02	*	@
9.80E-03	1.09E-02	1.02E-02	1.35E-01	295.4	-1.09E-02	*	eq,@
1.10E-02	1.27E-02	1.17E-02	1.35E-01	296.8	-1.59E-02	*	eq,@
3.01E-02	2.26E-02	2.58E-02	1.35E-01	296.8	1.08E-01	*	@
5.85E-02	4.06E-02	4.83E-02	1.35E-01	296.8	2.89E-01	*	@
9.69E-02	6.51E-02	7.89E-02	1.35E-01	296.8	4.94E-01	*	@
		9.84E-01	1.44E-01	297.0	5.21E+00		lo
		9.84E-01	1.30E-01	296.5	6.49E+00		lo
2.97E-03	1.35E-02	6.66E-03	1.35E-01	311.7	-1.43E-01	*	@
5.74E-03	1.46E-02	9.12E-03	1.35E-01	311.4	-1.17E-01	*	@
9.39E-03	1.71E-02	1.24E-02	1.35E-01	311.7	-9.79E-02	*	@
1.06E-02	1.77E-02	1.33E-02	1.35E-01	311.4	-8.52E-02	*	@
2.89E-02	2.81E-02	2.76E-02	1.35E-01	311.3	3.09E-02	*	@
5.62E-02	4.57E-02	4.91E-02	1.35E-01	311.7	2.18E-01	*	@
9.32E-02	6.79E-02	7.73E-02	1.35E-01	311.5	4.55E-01	*	@

\* – used to extract equilibrium; @ – used to extract kinetics; no – disregard the experiment;  
 lo – low measured value; hi – high measured value; eq – close to equilibrium

**10 MOL% DEA - 90 MOL% MDEA****(50 WT% AMINE)**

PCO <sub>2</sub> in	PCO <sub>2</sub> out	PCO <sub>2</sub> log mean	Loading	Temp	Flux		
(bar)	(bar)	(bar)	<u>mol CO<sub>2</sub></u> <u>mol amine</u>	K	kmol/m <sup>2</sup> /s		
9.64E-02	8.80E-02	9.08E-02	2.77E-01	296.8	1.66E-01	*	@
5.88E-02	6.05E-02	0.0	2.77E-01	296.2	0.00E+00	*	eq, @
2.98E-02	3.75E-02	3.30E-02	2.77E-01	296.0	-9.83E-02	*	eq, @
1.13E-02	2.33E-02	1.63E-02	2.77E-01	295.6	-1.65E-01	*	eq, @
1.06E-01	1.07E-01	1.05E-01	2.77E-01	296.1	3.23E-02		no
3.01E-01	2.64E-01	2.78E-01	2.77E-01	296.2	7.84E-01	*	@
5.90E-01	5.33E-01	5.53E-01	2.77E-01	296.1	1.85E+00	*	@
		9.87E-01	2.77E-01	295.0	3.51E+00	*	@
		9.87E-01	2.77E-01	295.0	3.87E+00		no
1.08E-02	4.38E-02	2.26E-02	2.77E-01	311.0	-4.63E-01		no
2.83E-02	6.41E-02	4.19E-02	2.77E-01	313.5	-4.88E-01	*	@
5.60E-02	8.38E-02	6.62E-02	2.77E-01	313.5	-3.44E-01	*	@
9.18E-02	1.09E-01	9.62E-02	2.77E-01	313.8	-1.45E-01	*	eq, @
1.01E-01	1.28E-01	1.10E-01	2.77E-01	313.6	-2.90E-01	*	eq, @
2.87E-01	2.77E-01	2.71E-01	2.77E-01	313.5	5.72E-01	*	@
5.62E-01	5.32E-01	5.26E-01	2.77E-01	313.5	1.87E+00	*	@
		9.87E-01	4.55E-01	295.0	2.51E+00		
1.09E-02	5.07E-02	2.53E-02	4.94E-01	298.3	-5.65E-01	*	@
2.99E-02	6.58E-02	4.47E-02	4.94E-01	298.3	-5.19E-01	*	@
5.85E-02	8.98E-02	7.18E-02	4.94E-01	298.4	-4.22E-01	*	@
9.65E-02	1.19E-01	1.06E-01	4.94E-01	299.1	-2.97E-01	*	@
1.07E-01	1.31E-01	1.17E-01	4.94E-01	298.1	-2.96E-01	*	@
3.00E-01	2.91E-01	2.91E-01	4.94E-01	298.5	3.00E-01	*	eq, @
5.88E-01	5.67E-01	5.68E-01	4.94E-01	298.5	1.11E+00	*	@
		9.87E-01	4.94E-01	295.0	2.31E+00	*	@
		9.81E-01	4.94E-01	298.4	2.33E+00	*	@

\* – used to extract equilibrium; @ – used to extract kinetics; no – disregard the experiment;  
 lo – low measured value; hi – high measured value; eq – close to equilibrium

**10 MOL% DEA - 90 MOL% MDEA****(50 WT% AMINE)**

PCO <sub>2</sub> in	PCO <sub>2</sub> out	PCO <sub>2</sub> log mean	Loading	Temp	Flux		
(bar)	(bar)	(bar)	<u>mol CO<sub>2</sub></u> mol amine	K	kmol/m <sup>2</sup> /s		
1.04E-02	9.73E-02	3.69E-02	4.94E-01	313.8	-1.30E+00	*	@
2.85E-02	1.14E-01	5.88E-02	4.94E-01	314.0	-1.29E+00	*	@
5.57E-02	1.34E-01	8.50E-02	4.94E-01	314.3	-1.12E+00	*	@
9.20E-02	1.53E-01	1.15E-01	4.94E-01	314.6	-8.43E-01		no
1.02E-01	1.78E-01	1.31E-01	4.94E-01	313.6	-1.08E+00	*	@
2.86E-01	3.35E-01	2.98E-01	4.94E-01	313.6	-5.03E-01	*	@
5.62E-01	5.93E-01	5.55E-01	4.94E-01	313.7	4.33E-01	*	eq,@
		9.38E-01	4.94E-01	313.5	3.09E+00		no
		9.33E-01	4.94E-01	314.6	1.58E+00	*	@
		9.80E-01	5.38E-01	298.8	1.82E+00		
1.08E-02	7.51E-02	3.24E-02	6.37E-01	298.8	-9.44E-01	*	@
2.98E-02	9.01E-02	5.34E-02	6.37E-01	298.8	-9.00E-01	*	@
5.81E-02	1.12E-01	8.06E-02	6.37E-01	298.6	-7.78E-01	*	@
9.60E-02	1.38E-01	1.14E-01	6.37E-01	298.7	-6.02E-01		no
1.08E-01	1.68E-01	1.33E-01	6.37E-01	298.4	-8.83E-01	*	@
3.00E-01	3.30E-01	3.10E-01	6.37E-01	297.6	-4.41E-01	*	@
5.91E-01	6.03E-01	5.88E-01	6.37E-01	296.4	1.69E-01	*	@
		9.80E-01	6.37E-01	298.8	1.04E+00	*	@
1.05E-02	1.26E-01	4.43E-02	6.37E-01	310.2	-1.79E+00	*	@
2.87E-02	1.37E-01	6.64E-02	6.37E-01	311.7	-1.69E+00	*	@
1.04E-01	1.96E-01	1.40E-01	6.37E-01	311.0	-1.57E+00	*	@
2.89E-01	3.63E-01	3.13E-01	6.37E-01	311.1	-1.24E+00	*	@
5.68E-01	6.13E-01	5.70E-01	6.37E-01	311.1	-3.54E-01	*	eq,@
		9.47E-01	6.37E-01	311.1	2.53E-01	*	eq,@

\* – used to extract equilibrium; @ – used to extract kinetics; no – disregard the experiment;  
 lo – low measured value; hi – high measured value; eq – close to equilibrium



**50 mol% DEA-50 mol% MDEA****50 WT% AMINE**

PCO <sub>2</sub> in	PCO <sub>2</sub> out	PCO <sub>2</sub> log mean	Loading	Temp	Flux		
(bar)	(bar)	(bar)	<u>mol CO<sub>2</sub></u> <u>mol amine</u>	K	kmol/m <sup>2</sup> /s		
5.93E-03	2.18E-03	3.70E-03	2.30E-03	298.5	5.42E-08	*	@
9.77E-03	2.92E-03	5.60E-03	2.30E-03	298.0	9.86E-08	*	@
1.13E-02	1.55E-02	1.31E-02	2.30E-03	298.5	-5.2E-08		no
2.78E-02	1.19E-02	1.85E-02	2.30E-03	298.6	2.32E-07		no
6.14E-02	1.50E-02	3.25E-02	2.30E-03	298.7	6.67E-07	*	@
9.51E-02	2.30E-02	5.02E-02	2.30E-03	298.8	1.03E-06	*	@
		9.87E-01	4.40E-03	294.8	2.55E-05		hi
2.94E-03	1.67E-03	2.17E-03	2.30E-03	314.7	2.1E-08	*	@
5.64E-03	2.19E-03	3.52E-03	2.30E-03	314.8	5.42E-08	*	@
9.28E-03	2.90E-03	5.31E-03	2.30E-03	314.8	9.89E-08	*	@
1.08E-02	1.55E-02	1.25E-02	2.30E-03	314.8	-5.2E-08		no
2.65E-02	1.21E-02	1.77E-02	2.30E-03	314.6	2.31E-07		no
5.84E-02	1.36E-02	2.98E-02	2.30E-03	315.0	6.86E-07	*	@
9.08E-02	1.99E-02	4.53E-02	2.30E-03	314.1	1.07E-06	*	@
3.10E-03	2.85E-03	2.92E-03	1.36E-01	299.8	4.96E-09	*	eq,@
5.94E-03	3.68E-03	4.64E-03	1.36E-01	299.6	3.45E-08	*	eq,@
9.78E-03	5.12E-03	7.09E-03	1.36E-01	299.6	6.97E-08	*	@
1.11E-02	8.24E-03	9.44E-03	1.36E-01	298.1	4.61E-08		no
2.99E-02	1.23E-02	1.95E-02	1.36E-01	298.7	2.51E-07		no
5.84E-02	2.01E-02	3.54E-02	1.36E-01	299.2	5.65E-07		@
9.64E-02	3.25E-02	5.79E-02	1.36E-01	299.1	9.36E-07		@
		9.81E-01	1.66E-01	298.6	2.76E-05		hi
		9.83E-01	1.00E-01	297.1	2.5E-05		hi

\* – used to extract equilibrium; @ – used to extract kinetics; no – disregard the experiment;  
 lo – low measured value; hi – high measured value; eq – close to equilibrium

**50 mol %DEA-50 mol % MDEA****50 WT% AMINE**

PCO <sub>2</sub> in	PCO <sub>2</sub> out	PCO <sub>2</sub> log mean	Loading	Temp	Flux		
(bar)	(bar)	(bar)	<u>mol CO<sub>2</sub></u> <u>mol amine</u>	K	kmol/m <sup>2</sup> /s		
2.96E-03	5.71E-03	4.00E-03	1.36E-01	314.4	-3.5E-08	*	eq,@
5.68E-03	6.43E-03	5.80E-03	1.36E-01	314.1	-3.9E-09	*	eq,@
9.33E-03	8.10E-03	8.37E-03	1.36E-01	314.1	2.79E-08	*	@
1.05E-02	1.00E-02	9.91E-03	1.36E-01	313.2	2.15E-08		no
2.86E-02	1.36E-02	1.95E-02	1.36E-01	313.9	2.32E-07	*	@
5.57E-02	2.07E-02	3.42E-02	1.36E-01	314.4	5.53E-07	*	@
9.20E-02	3.04E-02	5.38E-02	1.36E-01	314.1	9.62E-07	*	@
		9.34E-01	1.15E-01	314.5	2.61E-05		hi
3.10E-03	8.27E-03	5.17E-03	2.40E-01	299.6	-7.1E-08	*	eq,@
5.93E-03	9.37E-03	7.38E-03	2.40E-01	299.7	-4.5E-08	*	eq,@
9.73E-03	1.11E-02	1.02E-02	2.40E-01	299.7	-1.5E-08	*	eq,@
1.11E-02	1.26E-02	1.16E-02	2.40E-01	298.3	-1.2E-08	*	eq,@
2.99E-02	1.91E-02	2.37E-02	2.40E-01	299.0	1.58E-07	*	@
5.84E-02	2.98E-02	4.19E-02	2.40E-01	299.0	4.38E-07	*	@
9.65E-02	4.58E-02	6.70E-02	2.40E-01	299.0	7.61E-07	*	@
		9.77E-01	2.40E-01	300.5	1.61E-05		hi
		9.81E-01	2.40E-01	298.5	2.22E-05		hi
2.97E-03	1.86E-02	8.09E-03	2.40E-01	314.2	-2.1E-07	*	@
5.68E-03	1.97E-02	1.08E-02	2.40E-01	313.5	-1.9E-07	*	@
9.31E-03	2.18E-02	1.40E-02	2.40E-01	314.5	-1.6E-07	*	@
1.06E-02	2.08E-02	1.45E-02	2.40E-01	313.8	-1.1E-07	*	eq,@
2.85E-02	2.96E-02	2.79E-02	2.40E-01	314.2	1.05E-08	*	eq,@
5.58E-02	3.88E-02	4.51E-02	2.40E-01	314.0	3.15E-07	*	@
9.22E-02	5.25E-02	6.80E-02	2.40E-01	314.0	6.7E-07	*	@
		9.33E-01	2.40E-01	314.6	2.4E-05		hi
		9.83E-01	4.24E-01	297.5	1.09E-05		

\* – used to extract equilibrium; @ – used to extract kinetics; no – disregard the experiment;  
 lo – low measured value; hi – high measured value; eq – close to equilibrium

**50 mol % DEA-50 mol % MDEA****50 WT % AMINE**

PCO <sub>2</sub> in	PCO <sub>2</sub> out	PCO <sub>2</sub> log mean	Loading	Temp	Flux		
(bar)	(bar)	(bar)	$\frac{\text{mol CO}_2}{\text{mol amine}}$	K	kmol/m <sup>2</sup> /s		
3.14E-03	3.66E-02	1.34E-02	4.35E-01	296.7	-4.7E-07	*	@
5.98E-03	3.89E-02	1.72E-02	4.35E-01	296.6	-4.6E-07	*	@
9.83E-03	4.03E-02	2.12E-02	4.35E-01	296.6	-4.3E-07	*	@
1.12E-02	4.59E-02	2.41E-02	4.35E-01	296.8	-4.9E-07	*	@
3.00E-02	5.99E-02	4.25E-02	4.35E-01	297.0	-4.2E-07	*	@
5.86E-02	7.71E-02	6.64E-02	4.35E-01	296.8	-2.3E-07	*	@
9.69E-02	1.01E-01	9.76E-02	4.35E-01	297.0	-2.7E-08	*	eq,@
1.07E-01	1.09E-01	1.06E-01	4.35E-01	297.7	4.4E-08	*	eq,@
3.00E-01	2.38E-01	2.63E-01	4.35E-01	298.6	1.05E-06	*	@
5.88E-01	4.57E-01	5.11E-01	4.35E-01	298.9	2.96E-06	*	@
		9.81E-01	4.35E-01	298.2	7.01E-06	*	@
		9.84E-01	4.35E-01	297.0	7.57E-06		hi
1.07E-02	9.13E-02	3.58E-02	4.35E-01	312.2	-1.2E-06	*	@
2.88E-02	9.94E-02	5.46E-02	4.35E-01	312.0	-1.1E-06	*	@
5.61E-02	1.18E-01	7.99E-02	4.35E-01	312.5	-8.8E-07	*	@
9.30E-02	1.34E-01	1.08E-01	4.35E-01	312.0	-5.4E-07	*	@
1.03E-01	1.47E-01	1.19E-01	4.35E-01	312.2	-4.8E-07	*	@
2.89E-01	2.74E-01	2.72E-01	4.35E-01	311.9	5.02E-07	*	eq,@
5.66E-01	4.84E-01	5.06E-01	4.35E-01	311.9	2.47E-06	*	@
		9.39E-01	4.35E-01	313.3	6.65E-06		hi
1.11E-02	8.32E-02	3.50E-02	5.42E-01	297.2	-1.4E-06	*	@
2.99E-02	9.55E-02	5.55E-02	5.42E-01	297.1	-1.3E-06	*	@
5.84E-02	1.14E-01	8.18E-02	5.42E-01	297.1	-1.1E-06	*	@
9.64E-02	1.41E-01	1.15E-01	5.42E-01	297.6	-8.6E-07	*	@
1.07E-01	1.60E-01	1.29E-01	5.42E-01	298.4	-1E-06	*	@
3.00E-01	3.11E-01	3.00E-01	5.42E-01	299.0	-8.5E-08	*	eq,@
5.89E-01	5.59E-01	5.65E-01	5.42E-01	298.1	1.7E-06	*	hi
		9.84E-01	5.42E-01	296.6	3.7E-06	*	hi,@
		9.84E-01	5.42E-01	296.5	3.24E-06	*	hi,@
1.02E-01	2.28E-01	1.50E-01	5.42E-01	314.1	-2.6E-06	*	@
2.86E-01	3.75E-01	3.15E-01	5.42E-01	314.1	-1.8E-06	*	@
5.64E-01	6.15E-01	5.67E-01	5.42E-01	313.0	-2.5E-07	*	eq,@
		9.42E-01	5.42E-01	312.5	1.84E-06	*	hi,@

\* – used to extract equilibrium; @ – used to extract kinetics; no – disregard the experiment;  
 lo – low measured value; hi – high measured value; eq – close to equilibrium

**50 wt% DEA**

PCO <sub>2</sub> in	PCO <sub>2</sub> out	PCO <sub>2</sub> log mean	Loading	Temp	Flux		
(bar)	(bar)	(bar)	<u>mol CO<sub>2</sub></u> <u>mol amine</u>	K	kmol/m <sup>2</sup> /s		
3.11E-03	3.02E-03	3.01E-03	2.14E-01	298.4	1.25E-08	*	eq,@
5.97E-03	4.51E-03	5.13E-03	2.14E-01	298.0	1.10E-07	*	@
9.81E-03	6.48E-03	7.91E-03	2.14E-01	297.8	2.44E-07	*	@
3.01E-02	2.40E-02	2.65E-02	2.14E-01	297.5	5.05E-07	*	@
5.86E-02	3.96E-02	4.78E-02	2.14E-01	297.5	1.36E-06	*	@
9.67E-02	6.21E-02	7.70E-02	2.14E-01	297.6	2.60E-06	*	@
		9.81E-01	2.14E-01	298.6	4.42E-05		hi
		9.82E-01	2.14E-01	298.0	4.31E-05		hi
2.97E-03	3.98E-03	3.31E-03	2.14E-01	313.5	-5.17E-08	*	eq,@
5.70E-03	5.32E-03	5.30E-03	2.14E-01	313.4	5.63E-08	*	eq,@
9.35E-03	7.42E-03	8.04E-03	2.14E-01	313.7	1.80E-07	*	eq,@
2.87E-02	2.42E-02	2.55E-02	2.14E-01	313.4	4.89E-07	*	@
5.59E-02	3.86E-02	4.51E-02	2.14E-01	313.3	1.42E-06	*	@
9.23E-02	5.97E-02	7.22E-02	2.14E-01	313.5	2.76E-06	*	@
		9.38E-01	2.14E-01	313.5	5.06E-05		hi
9.79E-03	2.84E-02	1.72E-02	6.13E-01	297.5	-9.49E-07		@
5.95E-03	2.63E-02	1.34E-02	6.13E-01	298.2	-1.04E-06		@
3.12E-03	2.43E-02	1.01E-02	6.13E-01	298.1	-1.07E-06		@
9.67E-02	1.04E-01	9.88E-02	6.13E-01	297.8	-3.22E-07	*	@
5.85E-02	6.91E-02	6.27E-02	6.13E-01	298.0	-6.20E-07	*	@
3.01E-02	4.28E-02	3.55E-02	6.13E-01	298.2	-8.08E-07	*	@
1.11E-02	2.69E-02	1.75E-02	6.13E-01	299.2	-1.05E-06	*	@
		9.83E-01	6.13E-01	297.5	5.91E-06		
9.26E-02	1.16E-01	9.96E-02	6.13E-01	313.2	-1.16E-06	*	@
5.58E-02	8.41E-02	6.62E-02	6.13E-01	313.8	-1.70E-06	*	@
2.87E-02	5.95E-02	4.04E-02	6.13E-01	314.1	-1.99E-06	*	@
1.06E-02	4.22E-02	2.18E-02	6.13E-01	313.8	-2.14E-06	*	@
		9.35E-01	6.13E-01	314.1	4.58E-06		

\* – used to extract equilibrium; @ – used to extract kinetics; no – disregard the experiment;  
 lo – low measured value; hi – high measured value; eq – close to equilibrium

## APPENDIX B

### PHYSICAL PROPERTY CORRELATIONS

#### B.1 Viscosity of the Unloaded Solution

Based upon the data of Al-Ghawas et al. (1988), Critchfield (1988) and Sada et al. (1978), Glasscock (1990) developed the following correlation:

$$w_{am} = w_{mdea} + \mathbf{0.980}w_{dea} + \mathbf{0.876}w_{mea}$$

$$B_1 = -19.52 - 23.40*w_{am} - 31.24*w_{am}^2 + 36.17*w_{am}^3$$

$$B_2 = 3912 + \mathbf{4894}*w_{am} + 8477*w_{am}^2 - 8358*w_{am}^3$$

$$B_3 = 0.02112 + 0.03339*w_{am} + 0.02780*w_{am}^2 - \mathbf{0.04202}*w_{am}^3$$

$$\log_e \mu = B_1 + \frac{B_2}{T} + B_3T \quad (B.1)$$

$\mu$  is in cP and  $T$  is the temperature in degrees Kelvin.  $w_{mdea}$ ,  $w_{dea}$  and  $w_{mea}$  denote the weight fractions of MDEA, DEA, and MEA, respectively. The correlation is based upon the viscosity correlation for MDEA only by Al-Ghawas et al., with the parameters in bold adjusted to fit the experimental data

for all of the amines. This correlation is considered to be reasonable for 0 to 50 wt% total amine, and a temperature range of 290 to 320 K.

## **B.2 Viscosity of the Loaded Solution**

Toman (1989) determined the effect of CO<sub>2</sub> loading on the viscosity of 50 wt% MDEA at 298K. These data span the range of 0.001 to 0.76 moles of CO<sub>2</sub> per mole of amine, and Glasscock (1990) fit them by a second order equation:

$$r = 1.000 + 0.8031 \cdot \text{loading} + 0.35786 \cdot (\text{loading}^2) \quad (\text{B.2})$$

In order to estimate the viscosity of solutions other than 50 wt% MDEA, the corrected relative viscosity was estimated by Glasscock (1990) as follows:

$$\text{relative viscosity} = 1. + 2. \cdot (r-1) \cdot (\text{wt fraction amine}) \quad (\text{B.3})$$

For 50 wt% amine, this equation defaults to relative viscosity =  $r$ , whereas, for pure water (wt fraction amine = 0) this equation defaults yields 1 for the relative viscosity, despite the loading. This correlation makes obvious physical sense and is used for all amine solutions.

## **B.3 Density of the Solution**

The density correlation of Licht and Weiland (1989) was used for all amines. The correlation is of the following form:

$$\frac{1}{\rho} = u_w V_w^o e^{\{\beta_w (T - T_o)\}} + u_{A1} V_{A1}^o e^{\{\beta_{A1} (T - T_o)\}} + u_{A2} V_{A2}^o e^{\{\beta_{A2} (T - T_o)\}} + w_{CO_2} V_{CO_2}^o e^{\{\beta_{CO_2} (T - T_o)\}} \quad (B.4)$$

where  $T_o = 308K$

$T$  = temperature in degrees K

$u_w$  = weight fraction water

$u_{A1}$  = weight fraction amine 1

$u_{A2}$  = weight fraction amine 2 (if needed)

$w_{CO_2}$  = loaded basis weight fraction  $CO_2$

$V^o$  = specific volume, shown below

$\beta$  = bulk thermal expansivity

The density is in units of  $g/cm^3$ .

	<u>Water</u>	<u>MDEA</u>	<u>DEA</u>	<u>MEA</u>	<u>CO<sub>2</sub></u>
specific volume ( $cm^3/g$ )	1.01	0.918	0.894	0.964	0.0636
bulk expansivity ( $K^{-1}$ )	0.000344	0.000528	0.000487	0.00568	0.0036

## **B.4 Diffusion Coefficients**

### **B.4.1 Diffusion Coefficient of $CO_2$**

The diffusion coefficient of  $CO_2$  was estimated using the data and  $N_2O$  analogy of Versteeg and van Swaaij (1988). First, the diffusion coefficients of  $CO_2$  and  $N_2O$  in water are calculated:

$$D_{CO_2} = 2.35 \times 10^{-6} e^{\{-2119/T\}} \quad (B.5)$$

$$D_{N_2O} = 5.07 \times 10^{-6} e^{\{-2371/T\}} \quad (B.6)$$

T is in Kelvin, and D is in m<sup>2</sup>/s. The diffusion coefficient for N<sub>2</sub>O is then calculated according to the modified Stokes-Einstein relation:

$$(D_{N_2O} \mu^{0.80})_{\text{am soln}} = (D_{N_2O} \mu^{0.80})_{\text{water}} \quad (B.7)$$

The diffusion coefficient of CO<sub>2</sub> in the amine solution is then calculated using the N<sub>2</sub>O analogy:

$$\left(\frac{D_{N_2O}}{D_{CO_2}}\right)_{\text{am soln}} = \left(\frac{D_{N_2O}}{D_{CO_2}}\right)_{\text{water}} \quad (B.8)$$

Equation D.7 is used in the modeling aspects of the present work in order to emulate Glasscock's approach as closely as possible.

Toman (1990) found that an exponent of 0.6 instead of 0.8 led to a better estimate of diffusivity of CO<sub>2</sub> in unloaded solutions.

$$(D_{N_2O} \mu^{0.60})_{\text{am soln}} = (D_{N_2O} \mu^{0.60})_{\text{water}} \quad (B.9)$$

For loaded solutions, the following relation was used (Toman, 1990)

$$(D_{N_2O} \mu^{0.70})_{\text{unloaded am soln}} = (D_{N_2O} \mu^{0.70})_{\text{loaded am soln}} \quad (B.10)$$

#### B.4.2 Diffusion Coefficient of the Amines

The amine diffusion coefficients were calculated from the data of Versteeg and van Swaaij (1988) at 298K in water for DEA and MEA by



Glasscock (1990). The resulting diffusion coefficients in water at 298K are shown below:

$$D_{\text{MDEA}} = 8.02 \times 10^{-10} \text{ m}^2/\text{s}$$

$$D_{\text{DEA}} = 8.08 \times 10^{-10} \text{ m}^2/\text{s}$$

$$D_{\text{MEA}} = 11.72 \times 10^{-10} \text{ m}^2/\text{s}$$

The diffusion coefficients were corrected for viscosity and temperature using the modified Stokes-Einstein relationship:

$$D_{\text{am,soln}} = D_{\text{am,water}} \frac{T}{298} \left( \frac{\mu_{\text{H}_2\text{O}}}{\mu_{\text{soln}}} \right)^{0.6} \quad (\text{B.11})$$

### **B.5 Solubility of CO<sub>2</sub> in Amines**

To estimate the solubility of CO<sub>2</sub> in alkanolamine solutions the N<sub>2</sub>O-CO<sub>2</sub> analogy is used. For the modeling work, the analogy is definitely applicable but it was not used. The analogy is used only in analysis of the experimental data.

$$\frac{m_{\text{N}_2\text{O-H}_2\text{O}}}{m_{\text{CO}_2\text{-H}_2\text{O}}} = \frac{m_{\text{N}_2\text{O-am}}}{m_{\text{CO}_2\text{-am}}} \quad (\text{B.12})$$

where  $m$  is the solubility parameter. For water  $m$  reduces to the Henry's constant. The Henry's constant expressions for N<sub>2</sub>O and CO<sub>2</sub> were taken from Versteeg and Van Swaaij (1988).

$$H_{\text{N}_2\text{O}} = 11.7 \exp \left( \frac{2044}{T} \right) \frac{\text{kmol}}{\text{m}^3 \text{ bar}} \quad (\text{B.13})$$

$$H_{CO_2} = 35.4 \exp\left(\frac{2284}{T}\right) \frac{\text{kmol}}{\text{m}^3 \text{ bar}} \quad (\text{B.14})$$

For pure DEA, the N<sub>2</sub>O solubility data were taken from Littel (1991) and reduced to the following expression

$$m_{N_2O-DEA} = a_0 + a_1 c_{DEA} \quad (\text{B.15})$$

where  $m_{N_2O-DEA}$  has units of mol/mol and

$$a_0 = -162 + \frac{1.58 \times 10^5}{T} - \frac{5.12 \times 10^7}{T^2} + \frac{5.56 \times 10^9}{T^3} \quad (\text{B.16})$$

$$a_1 = -2.29 \times 10^{-4} + 6.87 \times 10^{-7} T \quad (\text{B.17})$$

Also in units of mol/mol,

$$H_{N_2O} = 8.99 \times 10^{-4} \exp\left(\frac{1943}{T}\right) \frac{\text{mol}}{\text{mol}} \quad (\text{B.18})$$

Combining equations B.12, B.14, B.15, B.16, B.17 and B.18 yields  $m_{CO_2-DEA}$ .

Toman (1990) estimated the solubility of N<sub>2</sub>O in MDEA at different temperatures and derived a relation for each temperature. In this work, these relations were combined to yield the following expression

$$\log\left(\frac{m_{N_2O-H_2O}}{m_{N_2O-MDEA}}\right) = 1.6 \exp\left(-592\left(\frac{1}{T} - \frac{1}{298}\right)\right) + 0.67 \times \exp\left(2729.27\left(\frac{1}{T} - \frac{1}{298}\right)\right) - 0.85 \times 2 \exp\left(1886.32\left(\frac{1}{T} - \frac{1}{298}\right)\right) - 5.111 + \frac{1040}{T} \quad (\text{B.19})$$

where

$$X = \frac{x_{\text{MDEA}} \text{MW}_{\text{MDEA}}^{0.4}}{x_{\text{MDEA}} \text{MW}_{\text{MDEA}}^{0.4} + x_{\text{H}_2\text{O}} \text{MW}_{\text{H}_2\text{O}}^{0.4}} \quad (\text{B.20})$$

$x$  is the mole fraction and  $\text{MW}$  is the molecular weight.

Combining B.12, B.14, B.19 and B.20 yield the solubility of  $\text{CO}_2$  in pure MDEA.

The solubility of  $\text{CO}_2$  in the blends was assumed to be the average of the solubilities of  $\text{CO}_2$  in MDEA and DEA weighted by their mole fractions. This was an arbitrary basis and is subject to verification. For the 10% DEA - 90% MDEA, DEA did not affect the solubility by a negligible amount and hence the solubility corresponded to the solubility of  $\text{CO}_2$  in MDEA. For 50% DEA -50% MDEA,

$$m_{\text{CO}_2\text{-blend}} = 0.5 m_{\text{CO}_2\text{-MDEA}} + 0.5 m_{\text{CO}_2\text{-DEA}} \quad (\text{B.21})$$

Toman (1990) also measured the effect of loading on solubility of  $\text{CO}_2$  in 50 wt% MDEA solutions and obtained the following relationship

$$\log \left( \frac{m_0}{m} \right) = 0.09 c_{\text{CO}_2} \quad (\text{B.22})$$

where  $m_0$  and  $m$  are the solubilities of  $\text{CO}_2$  in the unloaded and loaded solutions.

## APPENDIX C

### DETAILED SIMULATION RESULTS

This section compares the enhancement factors predicted by the model described in Section 2.7.1 to the enhancement factors predicted by the rigorous method as well as the approximate method that employs the Modified Combine Flux approximation (Glasscock and Rochelle, 1990). The values were taken from the spreadsheets that were used to prepare the plots in the mentioned paper.

Loading=0.01 mol CO<sub>2</sub>/mol amine, T=40°C,  $k_L^0=10^{-5}$ m/s

Wt% MDEA	Wt%DEA	PCO <sub>2</sub>	Enhancement factor		
		atm	Rigorous	Approximate	Present work
50	0	0.1	21.4	21.2	23.62
50	0	0.25	17.1	16.9	18.84
50	0	0.75	12.6	12.3	13.68
50	0	1.0	11.5	11.2	12.49
45	5	0.1	43.8	44.7	48.11
45	5	0.25	33.9	34.8	35.36
45	5	1.0	18.2	18.9	17.2
20	30	0.1	141	145	161.59
20	30	0.25	103	109	113
20	30	0.75	56.9	61.6	58.3
20	30	1.0	46.9	51.1	47.52

Loading=0.1 mol CO<sub>2</sub>/mol amine, T=40°C,  $k_L^0=10^{-5}$ m/s

Wt% MDEA	Wt%DEA	PCO <sub>2</sub>	Enhancement factor		
		atm	Rigorous	Approximate	Present work
50	0	0.1	14.8	14.7	18.73
50	0	0.25	13.9	13.8	17.41
50	0	0.75	12.1	11.9	14.77
50	0	1.0	11.5	11.2	17.41
45	5	0.1	43.9	48.5	53.25
45	5	0.25	33.9	34.8	36.33
45	5	1.0	18.4	20.8	23.07
20	30	0.1	155	166	199
20	30	0.25	111	121	126.1
20	30	1.0	48.1	54.2	89.73

Loading=0.01 mol CO<sub>2</sub>/mol amine, T=40°C,  $k_L^0=10^{-4}$ m/s

Wt% MDEA	Wt%DEA	PCO2	Enhancement factor		
			atm	Rigorous	Approximate
50	0	0.01	3.44	3.41	3.8
50	0	0.1	3.28	3.22	3.58
50	0	0.25	3.1	3.02	3.33
50	0	0.5	2.9	2.79	3.07
50	0	0.75	2.76	2.64	2.89
50	0	1.0	2.65	2.53	2.76
50	0	1.25	2.57	2.44	2.66
45	5	0.01	6.22	6.2	7.11
45	5	0.1	5.98	5.93	6.8
45	5	0.25	5.69	5.63	6.44
45	5	0.5	5.36	5.28	6.00
45	5	1.0	4.91	4.79	5.16
45	5	1.25	4.47	4.6	5.16
20	30	0.01	19.3	19.2	23.38
20	30	0.1	18.6	18.5	22.51
20	30	0.25	17.8	17.7	21.34
20	30	0.5	16.7	16.6	19.71
20	30	0.75	15.7	15.6	18.35
20	30	1.0	14.9	16.9	17.22
20	30	1.25	14.2	14.0	16.18
0	30	0.01	36.8	36.8	39.0
0	30	0.25	30.8	30.6	30.4
0	30	0.5	26.3	26.1	24.74
0	30	0.75	23.1	22.8	20.9
0	30	1.0	20.6	20.2	18.13
0	30	1.25	18.6	18.2	16.03

Loading=0.1 mol CO<sub>2</sub>/mol amine, T=40°C,  $k_L^0=10^{-4}$ m/s

Wt% MDEA	Wt%DEA	PCO <sub>2</sub> atm	Enhancement factor		
			Rigorous	Approximate	Present work
50	0	0.01	1.88	1.87	2.26
50	0	0.1	1.9	1.87	2.26
50	0	0.25	1.9	1.86	2.25
50	0	0.5	1.89	1.85	2.23
50	0	0.75	1.88	1.84	2.21
50	0	1.0	1.87	1.83	2.2
50	0	1.25	1.87	1.82	2.18
45	5	0.01	6.62	6.63	9.5
45	5	0.1	6.39	6.44	9.11
45	5	0.25	6.17	6.2	8.57
45	5	0.5	5.83	5.84	7.32
45	5	0.75	5.54	5.53	7.2
45	5	1.0	5.29	5.26	6.68
45	5	1.25	5.06	5.02	6.23
20	30	0.01	22.8	22.9	35.54
20	30	0.1	22.2	22.7	33.66
20	30	0.25	21.1	21.1	30.96
20	30	0.5	19.7	19.6	27.36
20	30	0.75	18.4	18.3	24.56
20	30	1.0	17.3	17.2	22.32
20	30	1.25	16.3	16.2	20.48
0	30	0.01	39.2	39.6	47.23
0	30	0.25	32.3	32.1	33.82
0	30	0.5	27.2	26.8	26.16
0	30	0.75	23.5	23.1	21.34
0	30	1.0	20.8	20.3	18.1
0	30	1.25	18.6	18.1	15.73



## APPENDIX D

### DEPLETION CALCULATIONS

The depletion calculations validate the applicability of the pseudo first order approximation. To this work, the estimation of depletion of free DEA at the interface is more significant than depletion of hydroxide since the effect of hydroxide has not been incorporated into the proposed rate expression. Depletion of free DEA typically occurs at high loadings while hydroxide gets depleted at low loadings. The depletion of free DEA could also be thought of as accumulation of carbamate.

An approximate method of estimating the depletion of free DEA is outlined. Assuming that MDEA concentration is the same in the bulk and at the interface, one could write the following expression

$$\text{Flux} = k_{L \text{ DEA}}^0 (c_{\text{DEA},b} - c_{\text{DEA},i}) \quad (\text{D.1})$$

where the mass transfer coefficient of DEA is estimated from the approximate film theory approximation (Chang and Rochelle, 1982) as follows:

$$k_{L \text{ DEA}}^0 = k_{L \text{ CO}_2}^0 \sqrt{\frac{D_{\text{DEA}}}{D_{\text{CO}_2}}} \quad (\text{D.2})$$

where  $k_{LCO_2}^o$  is estimated from the dimensionless mass transfer correlation (3.13). Using D.2, experimentally measured flux and free DEA in the bulk would yield the interfacial concentration of free DEA. The free DEA is calculated by the VLE model (Austgen, 1989). For an experiment at a given amine concentration and loading, the flux varies as a function of the CO<sub>2</sub> partial pressure. Typically the value of the chosen flux is between the middle and high end of the range of observed fluxes. For example, in the experiment corresponding to Figure 3.6 (shown earlier) the chosen flux would be close to  $0.1 \times 10^{-6}$  kmol/m<sup>2</sup>/s.

The depletion of free DEA is illustrated numerically by the following calculation which corresponds to the experiment with 50% DEA - 50% MDEA at a loading of 0.542 mol CO<sub>2</sub>/mol amine, CO<sub>2</sub> partial pressure of 0.8 bar and temperature of 25°C.

$$\text{Flux} = 3 \times 10^{-6} \frac{\text{kmol}}{\text{m}^2\text{s}}$$

Diffusion coefficients of CO<sub>2</sub> and DEA in the amine solution using the correlations in Appendix B.4.

$$D_{CO_2} = 3.8 \times 10^{-10} \frac{\text{m}^2}{\text{s}}$$

$$D_{DEA} = 1.64 \times 10^{-10} \frac{\text{m}^2}{\text{s}}$$

$$k_{LCO_2}^o = 2.6 \times 10^{-5} \frac{\text{m}}{\text{s}}$$

Using equation D.2,

$$k_{LDEA}^O = 1.7 \times 10^{-5} \frac{m}{s}$$

Speciation in the bulk yields

$$c_{DEA,b} = 0.25 \frac{kmol}{m^3}$$

Using the values of respective quantities in equations D.1 and D.2 yields,

$$c_{DEA,i} = 0.18 \frac{kmol}{m^3}$$

which implies 28% depletion of free DEA at the interface.

The depletion of hydroxide is estimated in an indirect manner as one cannot associate the hydroxide ion directly with a flux. It is calculated from the total CO<sub>2</sub> content. as follows

$$\frac{c_{CO_2,i}}{c_{CO_2,b}} = \frac{c_{OH,b}}{c_{OH,i}} \quad (D.3)$$

The method used to calculate the total CO<sub>2</sub> at the interface is analogous to the approach adopted for free DEA. The corresponding equation is

$$\text{Flux} = k_{LCO_2}^O (c_{CO_2,i} - c_{CO_2,b}) \quad (D.3)$$

The bulk concentrations are calculated by a speciation of the bulk using the VLE model (Austgen, 1989).

The example demonstrated corresponds to the experiment conducted with 10% DEA - 90% MDEA at a loading of 0.0015 mol CO<sub>2</sub>/mol amine, CO<sub>2</sub>, partial pressure of 0.04 bar and a temperature of 40°C.

$$D_{\text{CO}_2} = 8.04 \times 10^{-10} \frac{\text{m}^2}{\text{s}}$$

$$D_{\text{DEA}} = 4.39 \times 10^{-10} \frac{\text{m}^2}{\text{s}}$$

$$k_{\text{lCO}_2}^0 = 4.1 \times 10^{-5} \frac{\text{m}}{\text{s}}$$

Using equation D.2,

$$k_{\text{lDEA}}^0 = 3.03 \times 10^{-5} \frac{\text{m}}{\text{s}}$$

$$c_{\text{CO}_2, \text{b}} = 0.007 \frac{\text{kmol}}{\text{m}^3}$$

$$\text{Flux} = 0.5 \times 10^{-6} \frac{\text{kmol}}{\text{m}^2 \text{s}}$$

Using these values in equation D.3 yields,

$$c_{\text{CO}_2, \text{i}} = 0.029 \frac{\text{kmol}}{\text{m}^3}$$

Using the values of total CO<sub>2</sub> content in equation D.3 yields

$$\frac{c_{\text{OH}^- \text{b}}}{c_{\text{OH}^- \text{i}}} = 4.1$$

This corresponds to about 75% depletion of the hydroxide ions. Of course to the extent that hydroxide does not contribute significantly to the reaction, this depletion is not very important.

## APPENDIX E

### ERROR ANALYSIS

#### E.1 Introduction

This appendix has largely been taken from the dissertation of Glasscock (1990). Suppose we have a model of the form:

$$y = f(x_1, x_2, \dots, x_n) \quad (E.1)$$

If we wish to estimate the error in  $y$  due to the errors in  $x$ , we first assume that the model can be linearized about a point  $x$ :

$$y = f(x_1, \dots, x_n)_0 + \sum_{i=1}^n (\partial y, \partial x_i) (x_i - x_{i,0}) + (\text{Higher Order Terms}) \quad (E.2)$$

Once linearized, we can obtain the variance of  $y$  as a function of the independent variables (Draper and Smith, 1981):

$$\text{Var}(y) = \sum_{i=1}^n ((\partial y, \partial x_i))^2 \text{Var}(x_i) \quad (E.3)$$

We have neglected covariance between the independent variables in this formulation. Not only can we estimate the error in  $y$  from the error in the independent variables, we can also examine the relative contributions of the error, to see which variables contribute the most to uncertainty in experimental measurement.

## E.2 Gas Phase Error Analysis

The absorption rate of CO<sub>2</sub> can be determined by taking the difference between the inlet and outlet flowrates of CO<sub>2</sub> through the stirred tank reactor:

$$\frac{A}{\rho} R_{\text{abs}} = V_{\text{CO}_2, \text{in}} - V_{\text{CO}_2, \text{out}} \quad (\text{E.4})$$

The variable A is the interfacial area in cm<sup>2</sup>, and ρ is the density of the gas in moles/cc. V<sub>i</sub> designates the volumetric flowrate of the gas in standard cubic centimeters per minute. The Horiba Analyzers will measure the volumetric fraction of CO<sub>2</sub> in the gas phase, defined as r:

$$V_{\text{CO}_2, \text{out}} = r (V_{\text{H}_2\text{O}, \text{out}} + V_{\text{CO}_2, \text{out}} + V_{\text{N}_2}) \quad (\text{E.5})$$

Solving for the CO<sub>2</sub> flowrate:

$$V_{\text{CO}_2, \text{out}} = (V_{\text{H}_2\text{O}, \text{out}} + V_{\text{N}_2, \text{out}}) \frac{r}{1-r} \quad (\text{E.6})$$

Now, if the outlet gas is fully saturated with water, we can use the water vapor pressure to determine the partial water flowrate:

$$\begin{aligned} V_{\text{H}_2\text{O}, \text{out}} &= (V_{\text{H}_2\text{O}, \text{out}} + V_{\text{CO}_2, \text{out}} + V_{\text{N}_2, \text{out}}) P_{\text{H}_2\text{O}}^* \\ &= (V_{\text{CO}_2, \text{out}} + V_{\text{N}_2, \text{out}}) \frac{P_{\text{H}_2\text{O}}^*}{1 - P_{\text{H}_2\text{O}}^*} \end{aligned} \quad (\text{E.7})$$

Since we have provided a condenser out the outlet of the gas, we assume that the gas is no longer saturated with water, but is not completely dry either. The deviation from a perfectly dry gas is determined by a parameter ε, and we can determine the volumetric flowrate of the CO<sub>2</sub>:

$$\begin{aligned}
 V_{\text{CO}_2, \text{out}} &= r \left( V_{\text{N}_2, \text{out}} \left( 1 + \varepsilon \frac{P_{\text{H}_2\text{O}}^*}{1 - P_{\text{H}_2\text{O}}^*} \right) + V_{\text{CO}_2, \text{out}} \left( 1 + \varepsilon \frac{P_{\text{H}_2\text{O}}^*}{1 - P_{\text{H}_2\text{O}}^*} \right) \right) \\
 &= \frac{(V_{\text{N}_2, \text{out}} (r + \varepsilon r \frac{P_{\text{H}_2\text{O}}^*}{1 - P_{\text{H}_2\text{O}}^*}))}{1 - r - \varepsilon r \frac{P_{\text{H}_2\text{O}}^*}{1 - P_{\text{H}_2\text{O}}^*}} \quad (\text{E.8})
 \end{aligned}$$

The nitrogen absorption rate is negligible, so:

$$V_{\text{N}_2, \text{out}} = V_{\text{N}_2, \text{in}} \quad (\text{E.9})$$

Therefore, the net absorption rate of  $\text{CO}_2$  can be calculated as a function of the measured nitrogen and  $\text{CO}_2$  flowrates, the vapor pressure of  $\text{CO}_2$  at the reactor temperature, and the unknown but estimated value of  $\varepsilon$ , the deviation from perfect condensation:

$$R_v = \frac{A}{\rho} R_{\text{abs}} = V_{\text{CO}_2, \text{in}} \frac{(V_{\text{N}_2, \text{in}} (r + \varepsilon r \frac{P_{\text{H}_2\text{O}}^*}{1 - P_{\text{H}_2\text{O}}^*}))}{1 - r - \varepsilon r \frac{P_{\text{H}_2\text{O}}^*}{1 - P_{\text{H}_2\text{O}}^*}} \quad (\text{E.10})$$

Taking the appropriate partial derivatives:

$$\frac{\partial R_v}{\partial V_{CO2}} = 1 \quad (E.11)$$

$$\frac{\partial R_v}{\partial V_{N2}} = - \frac{(r + \epsilon r \frac{P_{H2O}^*}{1 - P_{H2O}^*})}{1 - r - \epsilon r \frac{P_{H2O}^*}{1 - P_{H2O}^*}} \quad (E.12)$$

$$\frac{\partial R_v}{\partial r} = - \frac{V_{N2}}{1 - r - \epsilon r \frac{P_{H2O}^*}{1 - P_{H2O}^*}} - \frac{(V_{N2,in} (r + \epsilon r \frac{P_{H2O}^*}{1 - P_{H2O}^*}))}{(1 - r - \epsilon r \frac{P_{H2O}^*}{1 - P_{H2O}^*})^2} \quad (E.13)$$

$$\frac{\partial R_v}{\partial \epsilon} = - \frac{V_{N2} r \frac{P_{H2O}^*}{1 - P_{H2O}^*}}{1 - r - \epsilon r \frac{P_{H2O}^*}{1 - P_{H2O}^*}} - \frac{(V_{N2,in} (r + \epsilon r \frac{P_{H2O}^*}{1 - P_{H2O}^*})) \frac{P_{H2O}^*}{1 - P_{H2O}^*}}{(1 - r - \epsilon r \frac{P_{H2O}^*}{1 - P_{H2O}^*})^2} \quad (E.14)$$

$$\begin{aligned} \text{Var}(R_v) = & \text{Var}(V_{CO2}) + \left(\frac{\partial R_v}{\partial V_{N2}}\right)^2 \text{Var}(V_{N2}) + \left(\frac{\partial R_v}{\partial r}\right)^2 \text{Var}(r) + \\ & \left(\frac{\partial R_v}{\partial \epsilon}\right)^2 \text{Var}(\epsilon) \end{aligned} \quad (E.15)$$

The following standard deviations are assumed based upon experience and manufacturers' literature:

$$\sigma_{VN2} = 0.005 * V_{N2}$$

$$\sigma_{VCO2} = 0.025 * V_{CO2}$$



$$\sigma_r = 0.00025$$

$$\varepsilon = 0.02, \sigma_\varepsilon = 0.01$$

We now take a typical case to determine the error (specific to the present work)

$$V_{N_2} = 500 \text{ sccm}$$

$$V_{CO_2} = 30 \text{ sccm}$$

$$r = 0.04$$

$$@40^\circ\text{C}, P^* = 0.072 \text{ atm}$$

Taking the partial derivatives:

$$\frac{\partial R_v}{\partial V_{N_2}} = 0.0417$$

$$\frac{\partial R_v}{\partial r} = -542$$

$$\frac{\partial R_v}{\partial \varepsilon} = -1.68$$

We now calculate the variance, as well as the actual molar absorption rate:

$$\text{Var}(R_v) = 0.59 + 0.0109 + 0.0184 + 2.82\text{e-}4$$

$$\sigma_{R_v} = 0.79$$

$$R_v = 9.13$$

We expect, therefore, about 10% error in the experimentally determined flux rates.

### E.3 CO<sub>2</sub> Partial Pressure Error Analysis

The equation for the partial pressure of CO<sub>2</sub> determined from the analyzer is shown in equation [B.16] (assuming complete water condensation):

$$r = y_{\text{CO}_2, \text{out}} = \frac{P_{\text{CO}_2}}{P_{\text{CO}_2} + P_{\text{N}_2}} \quad (\text{E.16})$$

Inside the reactor, the partial pressure of CO<sub>2</sub> is given by the following equation:

$$P_{\text{CO}_2} = P_{\text{TOT}} - P_{\text{N}_2} - P_{\text{H}_2\text{O}} \quad (\text{E.17})$$

We can use equation [B.16] to find the CO<sub>2</sub> partial pressure within the reactor as a function of the total pressure and the water vapor pressure:

$$(y_{\text{N}_2} + y_{\text{CO}_2}) = 1 - y_{\text{H}_2\text{O}}$$

$$y_{\text{CO}_2} \left( \frac{1-r}{r} + 1 \right) = 1 - y_{\text{H}_2\text{O}}$$

$$P_{\text{CO}_2} = r (P_{\text{TOT}} - P_{\text{H}_2\text{O}}) \quad (\text{E.18})$$

Once again, take the appropriate partial derivatives to find the variance:

$$\frac{\partial P_{\text{CO}_2}}{\partial r} = P_{\text{TOT}} - P_{\text{H}_2\text{O}}$$

$$\frac{\partial P_{\text{CO}_2}}{\partial P_{\text{TOT}}} = r$$

$$\frac{\partial P_{\text{CO}_2}}{\partial P_{\text{H}_2\text{O}}} = -r$$

Typical conditions and standard deviations are shown below:

$$P_{\text{TOT}} = 1, \sigma_{P_{\text{TOT}}} = 0.01$$

$$P_{\text{H}_2\text{O}}^* = 0.07, \sigma_{p^*} = 0.0007$$

$$r = 0.04, \sigma_r = 0.00025$$

We now estimate the standard deviation in the partial pressure of  $\text{CO}_2$ :

$$\text{Var}(P_{\text{CO}_2}) = 5.4\text{e-}8 + 1.6\text{e-}7 + 7.84\text{e-}10$$

$$\sigma_{P_{\text{CO}_2}} = 0.00046, \text{ or } 1.5\%$$

This value seems quite small, and in the calculations a standard deviation of 5% will be assumed.

#### **E.4 Error in Concentration Measurements**

The concentration of  $\text{CO}_2$  in a sample taken from the reactor by a syringe is given by equation [B.19]:

$$c = \frac{n}{V} \quad (\text{E.19})$$

$V$  is the volume of the syringe sample, and  $n$  is the total number of moles read by the analyzer. In order to estimate the error in  $V$ , we note that for a calibration, the concentration is constant, and we obtain a linear relationship between  $n$  and  $V$ . By regression analysis on a typical set of calibration data, we find that the standard deviation of the volume is  $0.086 \mu\text{L}$ . We can now estimate the error in concentration by equations [B.19] and [B.3]:

$$\sigma_c^2 = c^2 \frac{\sigma_v^2}{V^2} \quad (\text{E.20})$$

Note that no error in  $n$ , the number of moles, is assumed, since this is a direct function of a digital reading on the Oceanography analyzer. Taking a typical

case of  $V = 5 \mu\text{L}$ , we find the relative standard deviation of the concentration measurement:

$$\frac{\sigma_c}{c} = 1.7\% \quad (\text{E.21})$$

Once again, this value is quite small, and we will assume an actual relative standard deviation of 5% in the parameter estimation calculations.

## **APPENDIX F**

### **SPECIATION**

This section tabulates the speciations ( $x$ - mole fraction and  $\gamma$  - activity coefficient), as a function of loading for each of the amine solutions used in the experimental work. The speciation was performed with the VLE model (Austgen, 1989). Tables 2.9, 2.10 and 2.11 list the NRTL interaction parameters used in the model. In Table 2.11 there exist two alternatives. One set was regressed by Austgen (1989) and the other by Glasscock (1990). The present work uses the latter.

## 50 WT % MDEA

Loading													
mol CO <sub>2</sub>													
mol amine		0.0019	0.044	0.093	0.195	0.31	0.486						
		x	$\gamma$	x	$\gamma$	x	$\gamma$	x	$\gamma$	x	$\gamma$	x	$\gamma$
<b>T=313K</b>													
H <sub>2</sub> O		8.68E-01	1.00	8.63E-01	1.00	8.57E-01	1.01	8.43E-01	1.02	8.28E-01	1.02	8.05E-01	1.01
MDEA		1.31E-01	1.00	1.24E-01	1.00	1.16E-01	1.00	9.92E-02	1.02	8.23E-02	1.05	5.92E-02	1.11
CO <sub>2</sub>		1.13E-08	1.00	2.48E-06	1.05	6.69E-06	1.10	1.98E-05	1.23	4.42E-05	1.38	1.27E-04	1.61
H <sub>3</sub> O+		3.12E-13	1.26	6.39E-12	0.74	1.33E-11	0.62	2.98E-11	0.53	4.99E-11	0.51	8.87E-11	0.53
MDEAH+		3.99E-04	1.36	7.52E-03	0.83	1.53E-02	0.66	3.21E-02	0.53	4.91E-02	0.48	7.22E-02	0.48
OH-		1.59E-05	1.26	2.25E-06	0.74	1.54E-06	0.62	9.40E-07	0.52	5.90E-07	0.50	2.83E-07	0.53
HCO <sub>3</sub> -		1.16E-04	1.69	4.03E-03	0.93	8.44E-03	0.72	1.91E-02	0.55	3.23E-02	0.49	5.53E-02	0.48
CO <sub>3</sub> =		1.34E-04	3.52	1.74E-03	0.42	3.43E-03	0.20	6.54E-03	0.09	8.41E-03	0.07	8.46E-03	0.06
<b>T=298</b>													
H <sub>2</sub> O		8.68E-01	1.00	8.63E-01	1.01	8.57E-01	1.01	8.43E-01	1.02	8.28E-01	1.03	8.05E-01	1.02
MDEA		1.31E-01	1.00	1.23E-01	1.00	1.15E-01	1.00	9.73E-02	1.02	7.98E-02	1.05	5.64E-02	1.11
CO <sub>2</sub>		4.96E-09	1.01	1.10E-06	1.13	2.74E-06	1.28	6.95E-06	1.64	1.34E-05	2.08	3.20E-05	2.83
H <sub>3</sub> O+		1.63E-13	1.24	3.37E-12	0.72	6.99E-12	0.61	1.55E-11	0.52	2.56E-11	0.50	4.41E-11	0.52
MDEAH+		4.21E-04	1.31	8.10E-03	0.77	1.64E-02	0.62	3.40E-02	0.49	5.15E-02	0.44	7.49E-02	0.42
OH-		1.09E-05	1.24	1.54E-06	0.72	1.07E-06	0.60	6.52E-07	0.51	4.15E-07	0.50	2.06E-07	0.52
HCO <sub>3</sub> -		8.87E-05	1.66	3.46E-03	0.87	7.38E-03	0.66	1.72E-02	0.48	2.99E-02	0.42	5.27E-02	0.40
CO <sub>3</sub> =		1.61E-04	3.29	2.32E-03	0.39	4.50E-03	0.19	8.42E-03	0.09	1.08E-02	0.06	1.11E-02	0.06

*x=mole fraction  $\gamma$ =activity coefficient*

**10 MOL % DEA - 90 MOL % MDEA (50 WT % AMINE)**

Loading mol CO <sub>2</sub> mol amine	0.0015			0.057			0.135			0.277			0.494			0.637		
	x	γ	x	γ	x	γ	x	γ	x	γ	x	γ	x	γ	x	γ	x	γ
<b>T=313</b>																		
H <sub>2</sub> O	8.67E-01	1.00	8.62E-01	1.00	8.54E-01	1.01	8.37E-01	1.02	8.09E-01	1.01	7.97E-01	0.99						
MDEA	1.19E-01	1.00	1.12E-01	1.02	1.00E-01	1.04	7.93E-02	1.09	5.14E-02	1.16	4.14E-02	1.19						
DEA	1.32E-02	0.13	9.68E-03	0.12	6.66E-03	0.12	3.82E-03	0.12	1.84E-03	0.13	1.40E-03	0.14						
CO <sub>2</sub>	3.84E-09	1.00	2.19E-06	1.08	8.10E-06	1.19	2.92E-05	1.39	1.25E-04	1.69	2.17E-04	1.80						
H <sub>3</sub> O+	2.33E-13	1.19	7.90E-12	0.67	1.93E-11	0.55	4.31E-11	0.51	9.38E-11	0.54	1.24E-10	0.56						
MDEAH+	2.58E-04	1.37	7.92E-03	0.81	1.95E-02	0.61	4.02E-02	0.51	6.81E-02	0.50	7.80E-02	0.51						
DEAH+	6.00E-05	1.39	1.36E-03	0.80	2.44E-03	0.59	3.44E-03	0.50	4.42E-03	0.50	4.88E-03	0.52						
OH-	2.36E-05	1.19	2.22E-06	0.66	1.32E-06	0.55	6.80E-07	0.51	2.54E-07	0.54	1.67E-07	0.56						
DEACOO-	4.74E-05	2.40	2.24E-03	1.13	4.17E-03	0.80	6.02E-03	0.63	7.01E-03	0.64	6.99E-03	0.67						
HCO <sub>3</sub> -	5.68E-05	1.65	3.61E-03	0.84	9.73E-03	0.62	2.39E-02	0.51	5.13E-02	0.49	6.34E-02	0.50						
CO <sub>3</sub> =	9.49E-05	3.33	1.71E-03	0.31	4.01E-03	0.13	6.85E-03	0.07	7.12E-03	0.06	6.26E-03	0.06						
<b>T=298</b>																		
H <sub>2</sub> O	8.67E-01	1.00	8.62E-01	1.00	8.54E-01	1.013	8.37E-01	1.021	8.09E-01	1.01	7.90E-01	0.99						
MDEA	1.19E-01	1.00	1.11E-01	1.02	9.91E-02	1.038	7.76E-02	1.081	4.92E-02	1.16	3.30E-02	1.22						
DEA	1.32E-02	0.11	9.29E-03	0.10	6.17E-03	0.097	3.42E-03	0.096	1.59E-03	0.11	9.69E-04	0.12						
CO <sub>2</sub>	1.45E-09	1.01	8.82E-07	1.18	3.00E-06	1.459	9.16E-06	2.019	3.14E-05	2.99	7.04E-05	3.69						
H <sub>3</sub> O+	1.16E-13	1.17	4.04E-12	0.66	9.91E-12	0.547	2.20E-11	0.503	4.63E-11	0.53	7.34E-11	0.57						
MDEAH+	2.59E-04	1.31	8.21E-03	0.77	2.03E-02	0.575	4.19E-02	0.470	7.03E-02	0.44	8.64E-02	0.45						
DEAH+	6.82E-05	1.33	1.51E-03	0.76	2.63E-03	0.552	3.61E-03	0.451	4.59E-03	0.43	5.46E-03	0.45						
OH-	1.72E-05	1.17	1.56E-06	0.65	9.19E-07	0.541	4.76E-07	0.501	1.85E-07	0.53	9.20E-08	0.57						
DEACOO-	4.89E-05	2.36	2.47E-03	1.10	4.47E-03	0.771	6.25E-03	0.614	7.10E-03	0.62	6.85E-03	0.69						
HCO <sub>3</sub> -	3.97E-05	1.61	2.93E-03	0.79	8.39E-03	0.568	2.18E-02	0.442	4.91E-02	0.41	7.02E-02	0.43						
CO <sub>3</sub> =	1.10E-04	3.09	2.15E-03	0.29	5.06E-03	0.126	8.70E-03	0.072	9.34E-03	0.06	7.40E-03	0.06						

*x*-mole fraction; *γ*-activity coefficient

## 50 MOL% DEA - 50 MOL% MDEA (50 WT% AMINE)

Loading mol CO <sub>2</sub> mol amine	0.0023		0.136		0.24		0.436		0.537	
	x	γ	x	γ	x	γ	x	γ	x	γ
<b>T=313</b>										
H <sub>2</sub> O	8.61E-01	0.98	8.55E-01	0.99	8.49E-01	0.99	8.31E-01	0.97	8.18E-01	0.96
MDEA	6.91E-02	1.00	6.09E-02	1.15	5.22E-02	1.26	3.24E-02	1.40	2.29E-02	1.42
DEA	6.87E-02	0.19	4.37E-02	0.17	2.84E-02	0.17	1.16E-02	0.18	7.47E-03	0.18
CO <sub>2</sub>	9.60E-10	1.01	1.70E-06	1.33	6.18E-06	1.59	5.14E-05	2.01	1.43E-04	2.16
H <sub>3</sub> O+	2.31E-13	0.75	1.49E-11	0.46	2.88E-11	0.48	7.51E-11	0.57	1.22E-10	0.61
MDEAH+	1.41E-04	0.91	8.34E-03	0.63	1.70E-02	0.59	3.68E-02	0.59	4.64E-02	0.61
DEAH+	4.06E-04	0.98	1.35E-02	0.68	2.02E-02	0.60	2.76E-02	0.59	3.13E-02	0.61
OH-	5.78E-05	0.75	2.39E-06	0.45	1.11E-06	0.48	2.82E-07	0.57	1.39E-07	0.62
DEACOO-	1.17E-05	2.90	1.20E-02	0.95	2.06E-02	0.77	3.00E-02	0.74	3.05E-02	0.78
HCO <sub>3</sub> -	3.17E-05	1.14	3.77E-03	0.56	8.57E-03	0.53	2.63E-02	0.55	4.03E-02	0.57
CO <sub>3</sub> =	1.70E-04	1.12	3.04E-03	0.09	4.03E-03	0.07	4.04E-03	0.07	3.39E-03	0.08
<b>T=298</b>										
H <sub>2</sub> O	8.61E-01	0.98	8.55E-01	0.99	8.50E-01	0.99	8.32E-01	0.98	8.18E-01	0.96
MDEA	6.91E-02	0.99	6.12E-02	1.15	5.24E-02	1.27	3.19E-02	1.41	2.22E-02	1.44
DEA	6.87E-02	0.17	4.25E-02	0.15	2.68E-02	0.15	1.03E-02	0.15	6.42E-03	0.15
CO <sub>2</sub>	2.36E-10	1.01	5.13E-07	1.64	1.79E-06	2.24	1.31E-05	3.46	3.33E-05	4.05
H <sub>3</sub> O+	1.03E-13	0.69	7.08E-12	0.46	1.39E-11	0.48	3.67E-11	0.56	5.91E-11	0.61
MDEAH+	1.29E-04	0.81	8.06E-03	0.60	1.69E-02	0.57	3.73E-02	0.56	4.70E-02	0.56
DEAH+	4.45E-04	0.85	1.44E-02	0.64	2.11E-02	0.57	2.80E-02	0.54	3.16E-02	0.54
OH-	5.26E-05	0.69	1.80E-06	0.45	7.98E-07	0.48	2.01E-07	0.57	1.02E-07	0.62
DEACOO-	9.76E-05	0.80	1.23E-02	0.93	2.14E-02	0.76	3.09E-02	0.72	3.12E-02	0.77
HCO <sub>3</sub> -	1.80E-05	1.05	2.89E-03	0.51	7.12E-03	0.47	2.45E-02	0.46	3.88E-02	0.47
CO <sub>3</sub> =	2.03E-04	0.93	3.63E-03	0.09	4.74E-03	0.07	4.98E-03	0.07	4.32E-03	0.08

x- mole fraction; γ- activity coefficient



## APPENDIX G

### SRP REPORT

#### ABSORPTION OF CARBON DIOXIDE IN AQUEOUS BLENDS OF DIETHANOLAMINE AND METHYLDIETHANOLAMINE

This effort has focused on two areas:

1. Measuring the absorption rates of CO<sub>2</sub> into concentrated blends (50 wt%) of MDEA and DEA.
2. Modeling the absorption of CO<sub>2</sub> into blends of DEA and MDEA using ASPEN PLUS, a commercial simulator.

The objective of the experimental work was to obtain the absorption/desorption rates of CO<sub>2</sub> into 50 wt% solutions of pure MDEA and DEA, and blends of 10 mol% DEA-90 mol% MDEA and 50 mol% DEA-50 mol% MDEA over a range of partial pressures from 0.001 - 1.0 atm at temperatures of 25°C and 40°C. Loading was varied from 0 to 0.6. The contactor used was a wetted wall column.

Measuring absorption and desorption rates facilitated estimation of equilibrium by interpolation. The equilibrium CO<sub>2</sub> solubilities at 25°C and

40°C obtained by this method are compared to the predictions of the VLE model (Austgen, 1989) in Figures G.1 and G.2. Also shown are some of the data of Austgen (1989) and Jou et al. (1982). The model fit the data at 40°C and tended to underestimate the equilibrium solubilities at 25°C. The crossing of CO<sub>2</sub> solubilities in different amine solutions was verified experimentally as in Figure G.3.

The experiments measured the CO<sub>2</sub> flux as a function of CO<sub>2</sub> partial pressure for a given amine solution of a certain loading at 25°C and 40°C. Typically the flux-PCO<sub>2</sub> relationship showed a linear behavior as in Figure G.4. The intercept is related to the equilibrium solubility while the slope yields the normalized flux. The normalized flux for all amine solutions as a function of loading at 40°C is shown in Figure G.5 which indicates that the enhancement of 10% DEA - 90% MDEA relative to pure MDEA vanishes at loading greater than 0.2 while 50% DEA - 50% MDEA has a relatively significant enhancement at a loading of 0.5. Addition of DEA can increase the absorption rate by a factor of 2 to 4 at 0.05 to 0.2 loading.

Pseudo first order rate constants were calculated from the normalized fluxes. Before regressing these data to extract rate parameters, care was taken to not include points that correspond to depletion of free DEA or hydroxide i.e. places where pseudo first order conditions were not satisfied. For pure MDEA pseudo first order conditions were satisfied. However for the blends of 10% DEA - 90% MDEA and 50% DEA - 50% MDEA there was significant depletion of free DEA at loadings greater than 0.4 and depletion of

hydroxide at loadings less than 0.01. The comparison of predicted to experimental values is shown as a function of loading and free DEA in Figures G.6 and G.7 respectively.

At high loadings or low free DEA content, the depletion of free DEA causes the predicted value to be higher than the experimental value of pseudo first order constant. The hydroxide effect is not as apparent since it was not accounted for in the reaction scheme. Table G.1 compares the estimated rate constants to those obtained by previous researchers. The lower activation energy for the CO<sub>2</sub>-MDEA reaction could probably be explained on the basis that the actual temperature of the wetted wall column was less than 40°C. This is because the wetted wall column was not jacketed.

The relative contributions of the different reactions for a blend of 10% DEA - 40% MDEA at 40°C are shown in Figure G.8. For the reactions of CO<sub>2</sub> with DEA, the rate constant for the CO<sub>2</sub>-DEA-H<sub>2</sub>O reaction is higher than that obtained by Glasscock (1990) and the CO<sub>2</sub>-DEA-MDEA rate constant (with a large confidence interval) is significantly lower. This observation can be reconciled if one were to consider a form of expression proposed by Laddha and Danckwerts (1981). Glasscock (1990) observed that the predictions of this rate expression diverge from the predictions of the form he employed. Another reason could be that the contribution of the CO<sub>2</sub>-DEA-DEA reaction if any is absorbed by the rate constant of the CO<sub>2</sub>-DEA-H<sub>2</sub>O reaction.

Absorption of CO<sub>2</sub> into an aqueous alkanolamine solution is a problem of gas liquid mass transfer with chemical reaction at the interface. Often approximate techniques are used to solve this problem since a rigorous approach would involve solution of a system of differential and algebraic equations. The approximations help reduce it to a set of algebraic equations.

The modeling effort is to a large extent based on the work of Glasscock (1990), Glasscock and Rochelle (1990) and Carey (1990). Glasscock and Rochelle (1990) took into account all possible reactions in a CO<sub>2</sub>-DEA-MDEA system but developed approximations for the prediction of absorption rates. The main goal of this work was to develop the approximate approach in the framework of ASPEN PLUS. This involved modeling of a single stage contactor to handle bench scale experimental data. An attempt was also made to use RATEFRAC, a rate-based model to handle this problem so that the approximate approach could be scaled up to do system modeling.

The enhancement factor approach recommended by Carey (1990) could not be applied to RATEFRAC. So, the methodology adopted was to let RATEFRAC do the interfacial calculations while accounting only for the kinetics through a reaction rate subroutine. Only CO<sub>2</sub>-MDEA systems were handled. However severe convergence problems were encountered in both the initialization (equilibrium) and the actual rate-based calculations. Convergence was achieved only for a few cases where CO<sub>2</sub> was in stoichiometric excess as compared to MDEA. It was also necessary that the gas rate be much larger than the liquid rate for convergence in these cases.

A single stage contactor was modeled through a routine that accounted for the effects of chemical reaction on mass transfer through an enhancement factor. Two methods were inspected - one that used activity coefficients from the equilibrated bulk solution for the interfacial calculations and another that calculated activity coefficients at the interface as a function of the changing composition. The approach that used activity coefficients from the bulk was compared to the results from the rigorous analysis (Glasscock and Rochelle (1990) who also used bulk activity coefficients in the interfacial calculations) as in Figure G.9. Even at low  $P_{CO_2}$  where kinetic effects dominate, there exist significant differences in the predictions of the rigorous and approximate techniques. The most likely reason for this discrepancy is the difference in activity coefficients predicted by the ASPEN model in this work and the rigorous model (Glasscock, 1990).

Another 'rigorous approximate' approach was employed that accounted for the effect of changing interfacial composition on the activity coefficients. However this could not be compared to the rigorous results of Glasscock (1990) as he also used activity coefficients from the equilibrated bulk. Instead the enhancement factors predicted by this approximate technique were compared to the predictions of the approximate technique that used bulk or equilibrated activity coefficients (Table G.2).

A surprising prediction from the approximate approach that calculates activity coefficients at the interface is that for 30 wt% DEA - 20 wt% MDEA and 30 wt% DEA solutions, at loadings of 0.01 and 0.01 mol  $CO_2$ /mol amine

and mass transfer coefficients of  $10^{-4}$  and  $10^{-5}$  m/s, the enhancement factor increases as partial pressure of CO<sub>2</sub> increases from 0.01 to 1 atm. Also for 5 wt% DEA - 45 wt% MDEA and 50 wt% MDEA, the enhancement factor decreases by a much smaller factor when P<sub>CO<sub>2</sub></sub> increases from 0.1 to 1 atm as compared to the approximate approach that uses bulk activity coefficients.

### References Cited

- Austgen, D.M., *A Model of Vapor-Liquid Equilibria for Acid Gas-Alkanolamine-Water Systems*, Ph.D. dissertation, The University of Texas at Austin, 1989.
- Carey, T.R., *Rate-Based Modeling of Acid Gas Absorption and Stripping using Aqueous Alkanolamine Solutions*, M.S. Thesis, The University of Texas at Austin, Austin, TX, 1990.
- Glasscock, D.A., *Modelling and Experimental Study of Carbon Dioxide Absorption into Aqueous Alkanolamines*, Ph.D. Dissertation, The University of Texas at Austin, Austin, TX, 1990.
- Glasscock, D.A., and G.T. Rochelle, "Approximate Simulation of CO<sub>2</sub> and H<sub>2</sub>S Absorption into Aqueous Alkanolamines," Submitted to *AIChE J.*, September, 1990.

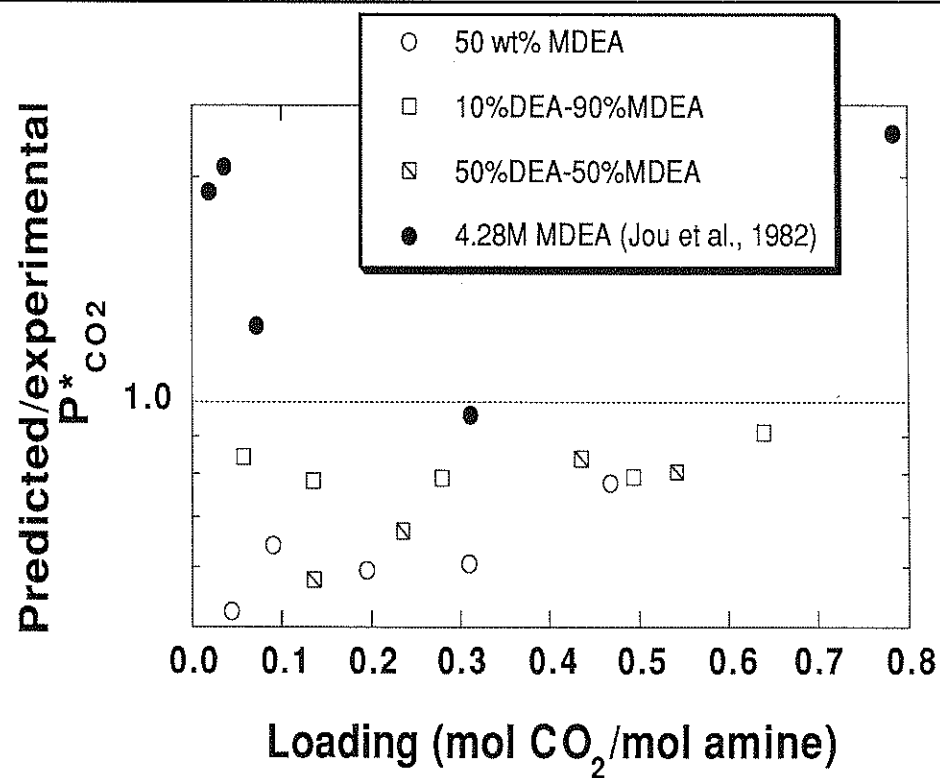


Figure G.1 Comparison of experimental data on  $CO_2$  solubility at 25 °C to VLE model (Austgen, 1989) prediction.

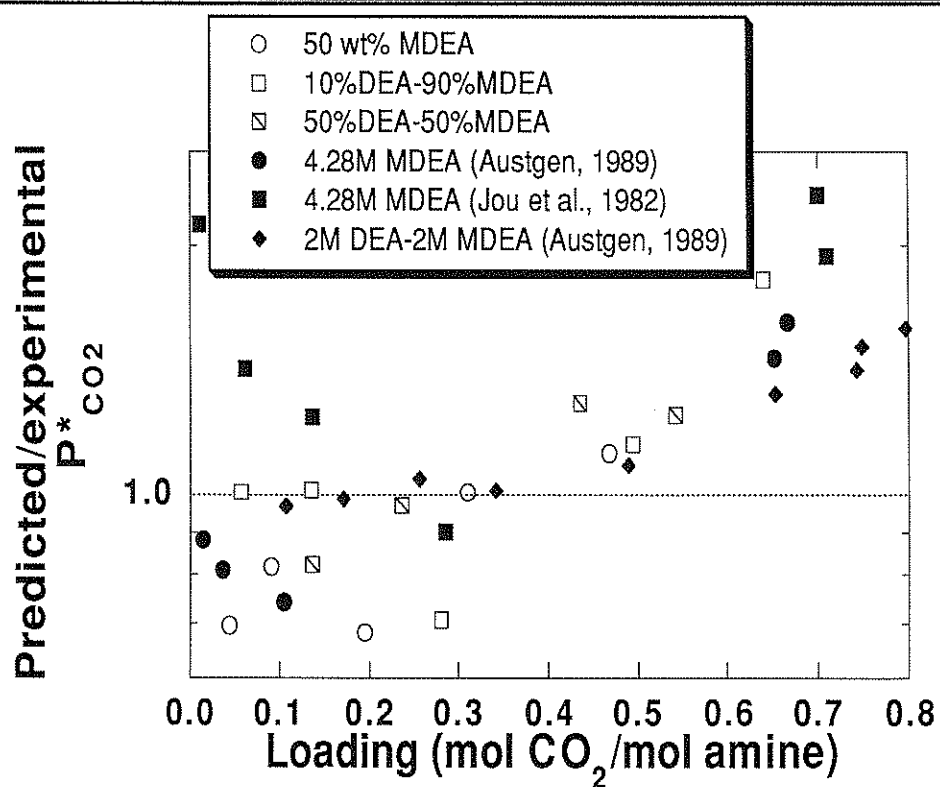


Figure G.2 Comparison of experimental data on  $CO_2$  solubility at  $40^\circ C$  to VLE model (Austgen, 1989) prediction.



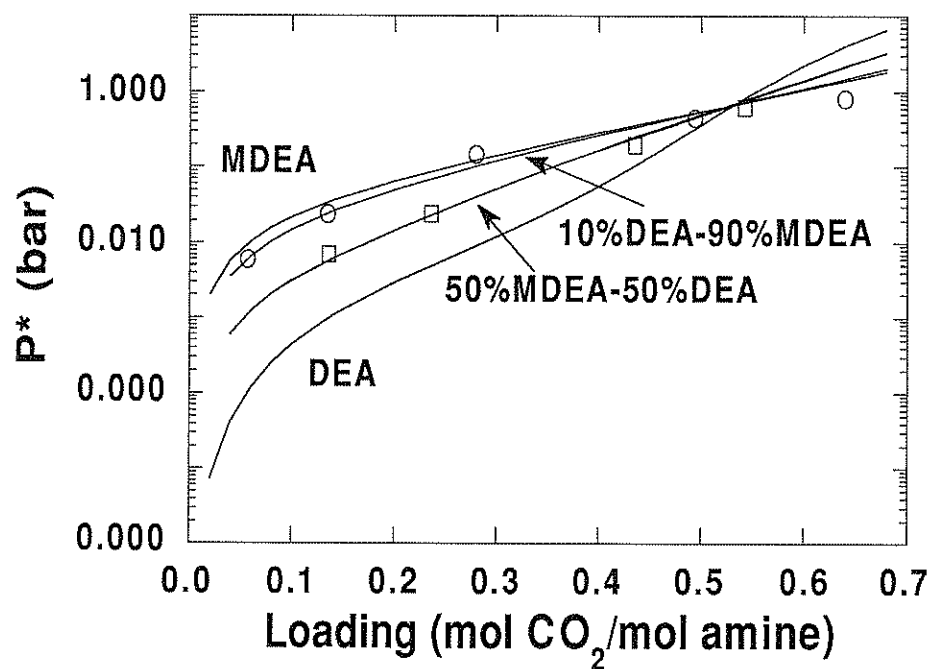


Figure G.3 VLE model (Austgen, 1989) prediction versus experimental data for CO<sub>2</sub> solubility in 50 wt% blended amines with 10%DEA-90%MDEA and 50%DEA-50%MDEA (mole basis) at 40 °C. Points refer to experimental data and curves to model predictions.

---

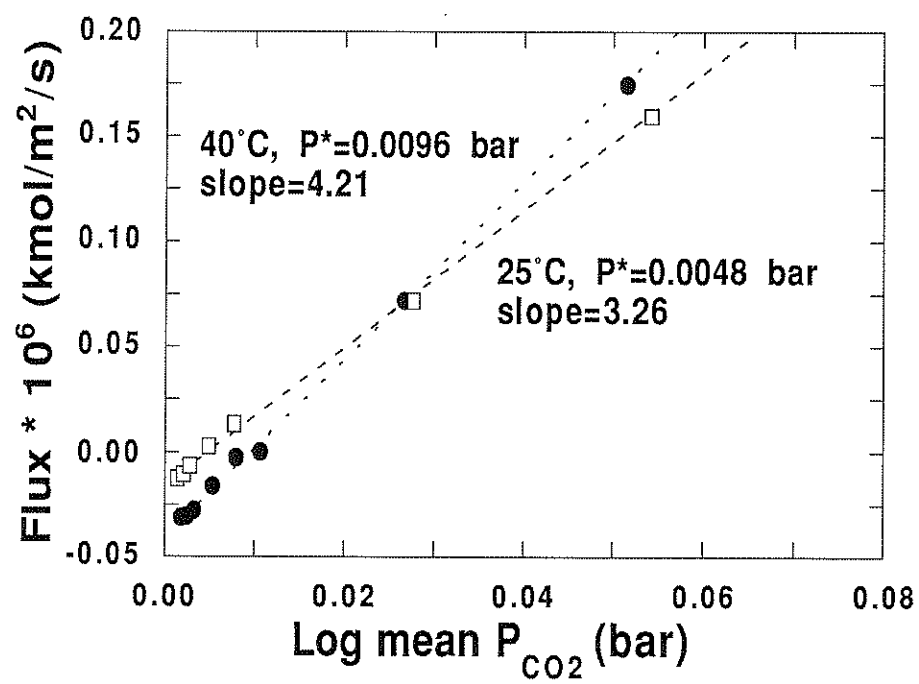


Figure G.4 Extraction of CO<sub>2</sub> solubility based on the log mean partial pressure and normalized flux for 50 wt% aqueous solution of MDEA at a loading of 0.044.

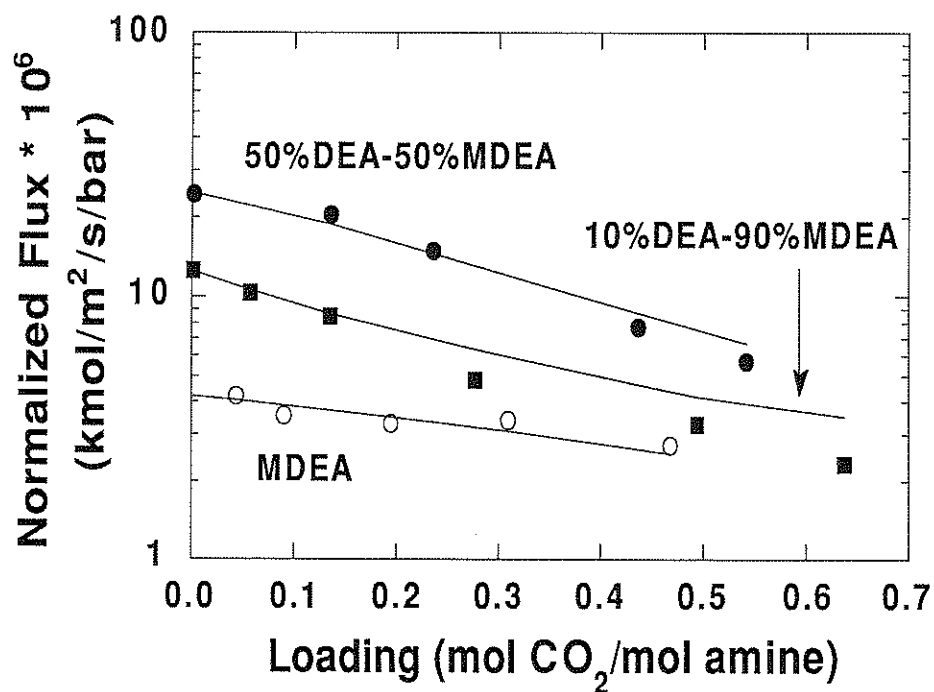
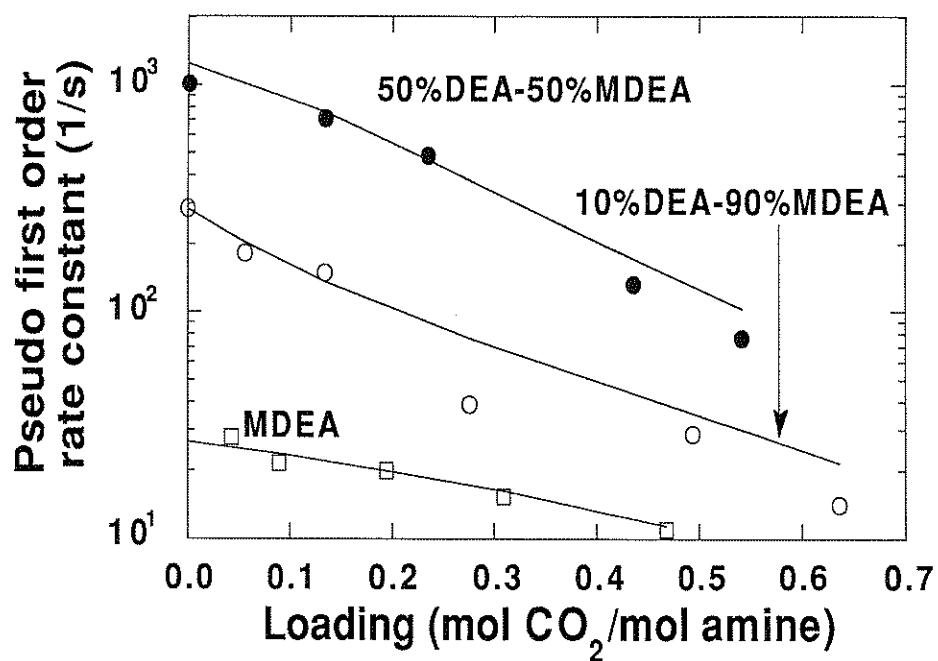


Figure G.5 Normalized flux of CO<sub>2</sub> as a function of loading at 40 °C for 50 wt% amines. Points refer to the experimental data and the curves refer to the values calculated using the parameters obtained in the present work and tabulated in Table G.2.

---

---



---

Figure G.6 Predicted and experimental pseudo first order rate constants at 25 °C as a function of bulk loading. Points refer to the experimental data and the curves refer to the values calculated using the parameters obtained in the present work and tabulated in Table G.2.

---

---

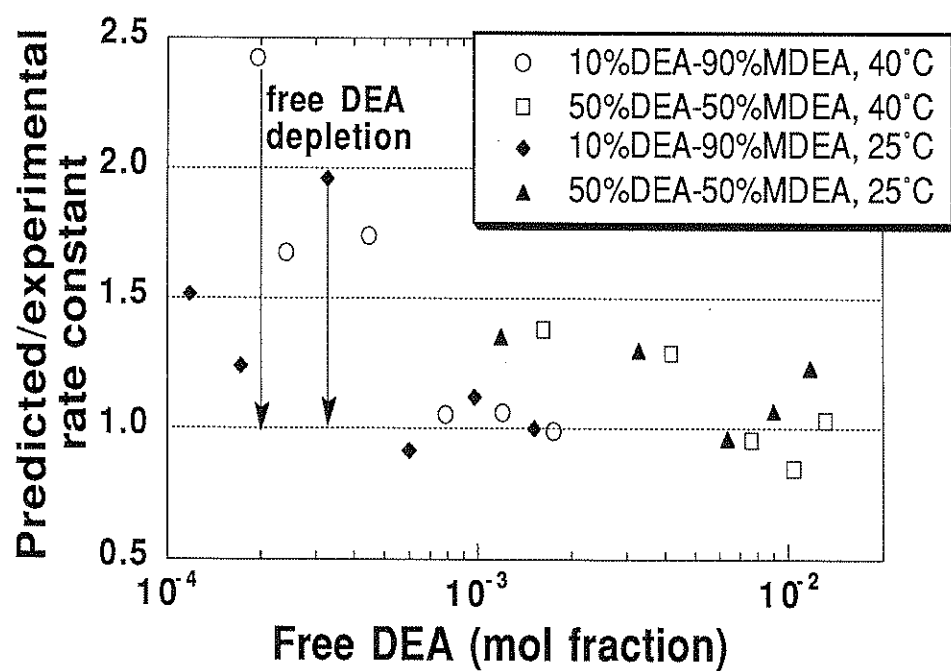


Figure G.7 Comparison of predicted to experimental values of rate constants as a function of mole fraction of free DEA.

---

---

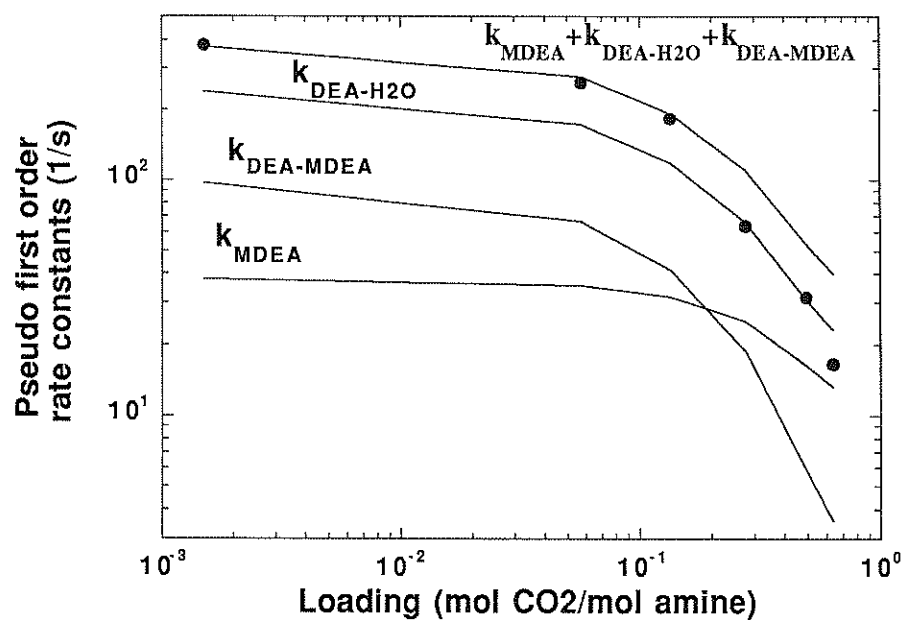


Figure G.8 Contribution of different mechanisms to the pseudo first order rate constant for 10% DEA - 90% MDEA as a function of loading at 40 °C. Points refer to the experimental data and the curves refer to model predictions.

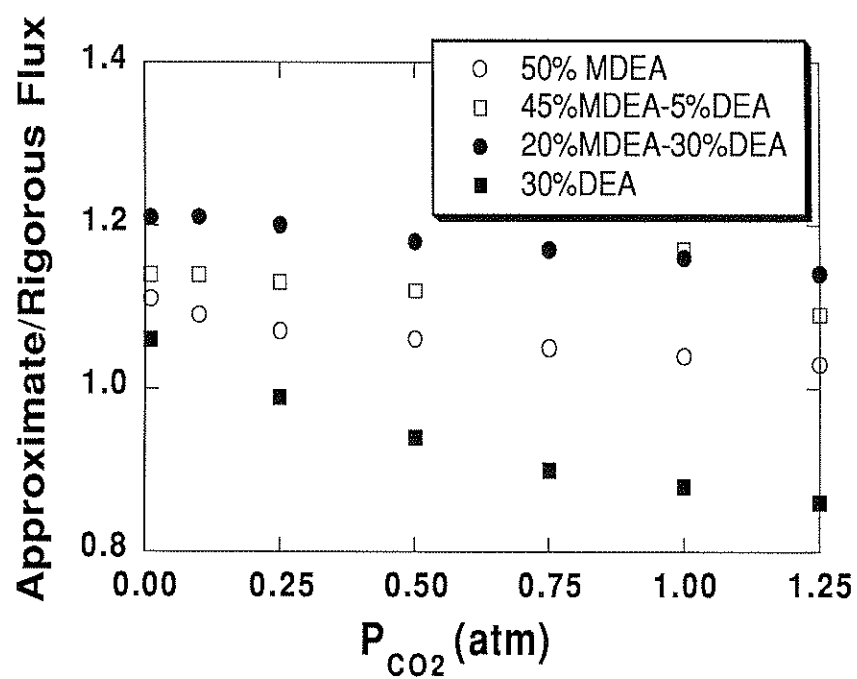


Figure G.9 Comparison of approximate to rigorous flux as a function of  $CO_2$  partial pressure for loading = 0.01 mol  $CO_2$ /mol amine,  $k_L = 10^{-4}$  m/s,  $T = 40^\circ C$ .

**Table G.1 Comparison of Results with Literature Data**MDEA system:  $r = k_2[\text{CO}_2][\text{MDEA}]$ 

	$k_{298}$ $\frac{\text{m}^3}{\text{kmol}\cdot\text{s}}$	$E_a$ $\frac{\text{kcal}}{\text{kmol}}$
Critchfield (1988)	2.5	13700
Tomcej et al. (1986)	7.4	9400
Versteeg and Van Swaaij (1988c)	4.3	10100
Littel et al. (1990)	5.1	10700
Haimour et al. (1987)	2.5	17100
Toman and Rochelle (1989)	5.5	9968
Cordi and Bullin (1992)	2.0	15668
Present work	6.1	5474
Glasscock (1990)	1.5 - 30	6590-13600
Current work	6.1	5446

DEA system<sup>b</sup>:

$$r = [\text{CO}_2][\text{DEA}] \{k'_{\text{H}_2\text{O}}[\text{H}_2\text{O}] + k'_{\text{DEA}}[\text{DEA}] + k'_{\text{MDEA}}[\text{MDEA}]\}$$

Versteeg and van Swaaij (1988b)  $k'_{\text{H}_2\text{O}} = 5.3$   $k'_{\text{DEA}} = 228$ .Critchfield (1988)<sup>a</sup>  $100 < k'_{\text{MDEA}} < 400$ Glasscock (1990)  $k'_{\text{H}_2\text{O}} = 4.75$   $k'_{\text{DEA}} = 464$   $k'_{\text{MDEA}} = 468$ Present work  $k'_{\text{H}_2\text{O}} = 15.8 \pm 23\%$   $k'_{\text{MDEA}} = 32.7 \pm 155\%$ 

<sup>a</sup>Critchfield used a different expression for DEA. Shown is an approximate range of this interaction constant based upon conditions investigated by Glasscock (1990) from a linearized form of Critchfield's rate expression.

<sup>b</sup> All rate constants for the DEA system have units of  $\frac{\text{m}^6}{\text{kmol}^2\cdot\text{s}}$



**Table G.2 Comparison of enhancement factors predicted by approximate methods developed in ASPEN PLUS**

Wt % MDEA	Wt% DEA	$k_L^o$ $\frac{m}{s}$	$P_{CO_2}$ atm	loading $\frac{mol\ CO_2}{mol\ amine}$	$E_{int}^a$	$E_{bulk}^b$
50	0	1.00E-04	0.1	0.01	3.65	3.58
50	0	1.00E-04	1	0.01	3.03	2.76
50	0	1.00E-05	0.1	0.01	27.58	23.62
50	0	1.00E-05	1	0.01	19.15	12.49
50	0	1.00E-04	0.1	0.1	2.34	2.26
50	0	1.00E-04	1	0.1	2.17	2.195
50	0	1.00E-05	0.1	0.1	21.40	18.73
50	0	1.00E-05	1	0.1	16.62	13.91
5	45	1.00E-04	0.1	0.01	7.12	6.8
5	45	1.00E-04	1	0.01	7.03	5.74
5	45	1.00E-05	0.1	0.01	69.15	48.1
5	45	1.00E-05	1	0.01	60.42	17.2
5	45	1.00E-04	0.1	0.1	9.37	9.1
5	45	1.00E-04	1	0.1	9.15	6.68
5	45	1.00E-05	1	0.1	86.74	53.3
5	45	1.00E-05	0.1	0.1	51.20	23.1
20	30	1.00E-04	0.1	0.01	21.58	22.5
20	30	1.00E-04	1	0.01	23.10	17.2
20	30	1.00E-05	0.1	0.01	232.4	162
20	30	1.00E-05	1	0.01	264.7	47.5
20	30	1.00E-04	0.1	0.1	35.90	33.7
20	30	1.00E-04	1	0.1	38.84	22.3
20	30	1.00E-05	0.1	0.1	383.5	199
20	30	1.00E-05	1	0.1	225.4	89.7
0	30	1.00E-04	0.01	0.01	38.80	39
0	30	1.00E-04	1	0.01	42.00	18.1
0	30	1.00E-04	0.01	0.1	48.00	47.2
0	30	1.00E-04	1	0.1	50.31	18.1

<sup>a</sup>  $E_{int}$  refers to the enhancement factor calculated from the approximate method that lets activity coefficients vary at the interface as a function of composition (Section 2.7.1).

<sup>b</sup>  $E_{bulk}$  refers to the enhancement factor calculated from the approximate method that lets activity coefficients vary at the interface as a function of composition (Section 2.7.2).

## NOMENCLATURE

a	contact area, $m^2$
a	activity
c	concentration, $kmol/m^3$
D	diffusion coefficient, $m^2/s$
E	enhancement factor
$E_a$	activation energy, $kcal/kmol$
$f_{carb}$	fraction of $CO_2$ that exists as carbamate
g	acceleration due to gravity, $m^2/s$
G	gas flow rate, $m^3/s$
k	rate constant, $m^6/kmol^2/s$
$k_1$	pseudo first order rate constant, $kmol/m^3/s$ in Ch.2, $1/s$ in Ch.3
$k'$	modified rate constant, $m^6/kmol^2/s$
K	equilibrium constant based on mole fraction activities
$k_g$	gas phase mass transfer coefficient (typically of $CO_2$ )
$k_L^0$	physical mass transfer coefficient (typically of $CO_2$ ), $m/s$
L	characteristic length of the wetted wall column, m
$m_{CO_2}$	solubility of $CO_2$ in the aqueous alkanolamine solution, $kmol/m^3/bar$
P	pressure, bar
$P_{CO_2}$	partial pressure of $CO_2$ , bar
$P^*$	equilibrium $CO_2$ partial pressure in bulk solution, bar
q	volumetric flow rate, $m^3/s$
R	reaction rate, $kmol/m^3/s$
	universal gas constant
t	time, s
T	temperature, K
$V_L$	liquid volume, $m^3$
X	reading on the analyzer

**Greek symbols**

$\rho$	density, kmol/m <sup>3</sup>
$\gamma$	activity coefficient
$\nu$	kinematic viscosity, m <sup>2</sup> /s
$\beta$	factor that accounts for the effect of changing ionic strength
$\Delta c$	concentration gradient, kmol/m <sup>3</sup>
$\nu$	viscosity, kg/m/s

**Dimensionless groups**

Ga	Galileo number, defined by equation 3.9
Re	Reynolds number, defined by equation 3.10
Sc	Schmidt number, defined by equation 3.11
Sh	Sherwood number, defined by equation 3.12

**Subscripts**

am	DEA (secondary amine)
b	bulk
g	gas phase
go	gas phase at t=0
i	interface
in	gas stream entering the wetted wall column
out	gas stream leaving the wetted wall column
tam	MDEA (tertiary amine)
w	water

## **BIBLIOGRAPHY**

- Al-Ghawas, H.A., G. Ruiz-Ibanez, and O.C. Sandall, "Absorption of Carbonyl Sulfide in Aqueous Methyldiethanolamine," *Chem. Eng. Sci.*, **44**(3), 631, 1989.
- Aspen Technology, Inc., *ASPEN PLUS™ Electrolytes Manual*, Second Edition, Aspen Technology, Inc., Cambridge, MA, 1988.
- Aspen Technology, Inc., *ASPEN PLUS™ Notes on Interfaces and User Models*, Second Edition, Aspen Technology, Inc., Cambridge, MA, 1988.
- Aspen Technology, Inc., *ASPEN PLUS™ RATEFRAC User Manual*, Aspen Technology, Inc., Cambridge, MA, 1990.
- Aspen Technology, Inc., *ASPEN PLUS™ System Maintenance Guide: VAX/VMS Version*, Aspen Technology, Inc., Cambridge, MA, 1988.
- Aspen Technology, Inc., *ASPEN PLUS™ User Guide*, Aspen Technology, Inc., Cambridge, MA, 1988.
- Aspen Technology, Inc., *ASPEN PLUS™ Data Regression Manual*, Cambridge, MA, 1988.
- Astarita, G., D.W. Savage, and A. Bisio, *Gas Treating with Chemical Solvents*, John Wiley & Sons, New York, 1983.
- Austgen, D.M., *A Model of Vapor-Liquid Equilibria for Acid Gas-Alkanolamine-Water Systems*, Ph.D. dissertation, The University of Texas at Austin, 1989.

- Bates, R.G., and G.D. Pinching, "Acidic Dissociation Constant and Related Thermodynamic Quantities for Monoethanolammonium Ion in Water from 0° to 50°C," *J. Res. Nat. Bur. Stand.*, **46**(5), 349, 1951.
- Blauwhoff, P.M.M., B. Kamphuis, W.P.M. van Swaaij, and K.R. Westerterp, "Absorber Design in Sour Natural Gas Treatment Plants: Impact of Process Variables on Operation and Economics," *Chem. Eng. Process.*, **19**, 1, 1985.
- Bottoms, R.R., U.S. Patent 1,783,901, 1930.
- Bower, V.E., R.A. Robinson, and R.G. Bates, "Acidic Dissociation Constant and Related Thermodynamic Quantities for Diethanolammonium Ion in Water from 0° to 50°C," *J. Res. Nat. Stands. - A. Physics and Chemistry*, **66A**(1), 71, 1962.
- Brian, P.L.T., and M.C. Beaverstock, "Gas Absorption Accompanied by a Two-Step Chemical Reaction," *Chem. Eng. Sci.*, **20**, 47, 1965.
- Brian, P.L.T., "Gas Absorption Accompanied by an Irreversible Reaction of General Order," *AIChE J.*, **10**(1), 5, 1964.
- Brian, P.L.T., J.F. Hurley, and E.H. Hasseltine, "Penetration Theory for Gas Absorption Accompanied by a Second Order Chemical Reaction," *AIChE J.*, **7**(2), 226, 1961.
- Byrne, G.D., and P.R. Ponzi, "Differential-Algebraic Systems, Their Applications and Solutions," *Comput. Chem. Engng.*, **12**(5), 377, 1988.
- Campbell, S.W., and R.H. Weiland, "Modelling CO<sub>2</sub> Removal by Amine Blends," Presented at the AIChE Spring National Meeting, Houston, TX, 1989.
- Carey, T.R., Rate-Based Modeling of Acid Gas Absorption and Stripping using Aqueous Alkanolamine Solutions, M.S. Thesis, The University of Texas at Austin, Austin, TX, 1990.
- Carta, G., and R.L. Pigford, "Absorption of Nitric Oxide in Nitric Acid and Water," *Ind. Eng. Chem. Fundam.*, **22**, 329, 1983.

- Chang, C.-S., and G.T. Rochelle, "Mass Transfer Enhanced by Equilibrium Reactions," *Ind. Eng. Chem. Fundam.*, **21**, 379, 1982.
- Chen, C.C., H.I. Britt, J.F. Boston, and L.B. Evans, "Extension and Application of the Pitzer Equation for Vapor-Liquid Equilibrium of Aqueous Electrolyte Systems with Molecular Solutes," *AIChE J.*, **25**(5), 820, 1979.
- Conte, S.D., and C.D. Boor, *Elementary Numerical Analysis*, McGraw-Hill, 1972.
- Cordi, E.M., and J.A. Bullin, "Kinetics of Carbon Dioxide and Methyldiethanolamine with Phosphoric Acid," *AIChE J.*, **38**(3), 455, 1992.
- Cornelisse, R., A.A.C.M. Beenackers, F.P.H. Van Beckum, and W.P.M. Van Swaaij, "Numerical Calculation of Simultaneous Mass Transfer of Two Gases Accompanied by Complex Reversible Reactions," *Chem. Eng. Sci.*, **35**, 1245, 1980.
- Critchfield, J.E., *CO<sub>2</sub> Absorption/Desorption in Methyldiethanolamine Solutions Promoted with Monoethanolamine and Diethanolamine: Mass Transfer and Reaction Kinetics*, PhD. dissertation, The University of Texas at Austin, 1988.
- Danckwerts, P.V., "Absorption by Simultaneous Diffusion and Chemical Reaction into Particles of Various Shapes and into Falling Drops," *Trans. Faraday Soc.*, **47**, 1014, 1951.
- Danckwerts, P.V., *Gas-Liquid Reactions*, McGraw-Hill, New York, 1970.
- Daubert, T.E., and R.P. Danner, *Data Compilation Tables of Properties of Pure Compounds*, Design Institute for Physical Property Data - Americal Institute of Chemical Engineers, New York, NY, 1985.
- Dingman, J.C., J.L. Jackson, T.F. Moore, and J.A. Branson, "Equilibrium Data for the H<sub>2</sub>S - CO<sub>2</sub> - Diglycolamine Agent - Water System," Presented at the 62<sup>nd</sup> Annual Gas Processors Association Convention, San Francisco, CA, 1983.
- Dow Chemical Co. *Gas Treating Handbook*, Gas/Spec Technology Group, Dow Chemical Co., Houston, TX, 1987.

- Draper, N.R., and H. Smith, *Applied Regression Analysis*, 2nd Ed., John Wiley & Sons, New York, 1981.
- Edwards, T.J., G. Maurer, J. Newman, and J.M. Prausnitz, "Vapor-Liquid Equilibria in Multicomponent Aqueous Solutions of Volatile Weak Electrolytes," *AIChE J.*, **24**(6), 966, 1978.
- Glasscock, D.A., *Modelling and Experimental Study of Carbon Dioxide Absorption into Aqueous Alkanolamines*, Ph.D. Dissertation, The University of Texas at Austin, Austin, TX, 1990.
- Glasscock, D.A., J.E. Critchfield and G.T. Rochelle, "CO<sub>2</sub> Absorption/Desorption in Mixtures of Methyldiethanolamine or Diethanolamine," *Chem. Eng. Sci.*, **46**(11), 2829, 1991.
- Glasscock, D.A., and G.T. Rochelle, "Approximate Simulation of CO<sub>2</sub> and H<sub>2</sub>S Absorption into Aqueous Alkanolamines," Submitted to *AIChE J.*, September, 1990.
- Glasscock, D.A., and G.T. Rochelle, "Comparison of Steady- and Unsteady-State Theories for Multicomponent Diffusion/Reaction in Gas Absorption Processes," *AIChE J.*, **35**(8), 1271, 1989.
- Haimour, N., A. Bidarian, and O.C. Sandall, "Kinetics of the Reaction Between Carbon Dioxide and Methyldiethanolamine," *Chem. Eng. Sci.*, **42**(6), 1393, 1987.
- Haimour, N., and O.C. Sandall, "Absorption of Carbon Dioxide into Aqueous Methyldiethanolamine," *Chem. Eng. Sci.*, **39**(12), 1791, 1984.
- Hayduk, W., and V.K. Malik, "Density, Viscosity, and Carbon Dioxide Solubility and Diffusivity in Aqueous Ethylene Glycol Solutions," *J. Chem. Eng. Data*, **16**(2), 143, 1971.
- Higbie, R., "The Rate of Absorption of a Pure Gas into a Still Liquid During Short Periods of Exposure," *Trans. Am. Inst. Chem. Eng.*, **31**, 365, 1935.
- Huang, D.T.-J., J.J. Carberry, and A. Varma, "Gas Absorption with Consecutive Second-Order Reactions," *AIChE J.*, **26**(5), 832, 1980.

- Ikada, E., Y. Hida, H. Okamoto, and N. Koizumi, "Dielectric Properties of Ethanolamines," *Bull. Inst. Chem. Res., Kyoto Univ.*, **46**(5), 239, 1968.
- Jou, F.Y., A.E. Mather, and F.D. Otto, "Solubility of H<sub>2</sub>S and CO<sub>2</sub> in Aqueous Methyldiethanolamine Solutions," *Ind. Eng. Chem. Process Des. Dev.*, **21**, 539, 1982.
- Katti, S.S., and R.A. Wolcott, "Fundamental Aspects of Gas Treating with Formulated Amine Mixtures," Presented at AIChE National Meeting, Minneapolis, MN, August, 1987.
- King, C. J., "Turbulent Liquid Phase Mass Transfer at a Free Gas-Liquid Interface," *Ind. Eng. Chem. Fund.*, **5**(1), 1, 1966.
- Kohl, A.L., and F.C. Riesenfeld, *Gas Purification*, 4th ed., Gulf Publishing Co., Houston, 1985.
- Laddha, S.S., and P.V. Danckwerts, "Reaction of CO<sub>2</sub> with Ethanolamines: Kinetics from Gas Absorption," *Chem. Eng. Sci.*, **36**, 479, 1981.
- Laddha, S.S., J.M. Diav, and P.V. Danckwerts, "The N<sub>2</sub>O Analogy: the Solubilities of CO<sub>2</sub> and N<sub>2</sub>O in Aqueous Solutions of Organic Compounds," *Chem. Eng. Sci.*, **36**, 228, 1981.
- Lewis, W.K., and W.G. Whitman, "Principles of Gas Absorption," *Ind. Eng. Chem.*, **16**(12), 1215, 1924.
- Licht, S.E., and R.H. Weiland, "Density and Physical Solubility of CO<sub>2</sub> in Partially Loaded Solutions of MEA, DEA and MDEA," Presented at AIChE 1989 Spring National Meeting, Paper No. 57f, Houston, TX (April 2-6, 1989)
- Littel, R.J., *Selective Carbonyl Sulfide Removal in Acid Gas Treating Processes*, dissertation, University of Twente, The Netherlands, 1991.
- Littel, R.J., W.P.M. van Swaaij, and G.F. Versteeg, "Kinetics of Carbon Dioxide with Tertiary Amines in Aqueous Solution," *AIChE J.*, **36**(11), 1633, 1990.



- Matheron, E.R., and O.C. Sandall, "Gas Absorption Accompanied by a Second-Order Chemical Reaction Modeled According to the Danckwerts Surface Renewal Theory," *AIChE J.*, **24**(3), 552, 1978.
- Mshewa, M.M., Private communication, 1991.
- Onda, K., E. Sada, T. Kobayashi, and M. Fujine, "Gas Absorption Accompanied by Complex Chemical Reactions - I. Reversible Chemical Reactions," *Chem. Eng. Sci.*, **25**, 753, 1970a.
- Onda, K., E. Sada, T. Kobayashi, and M. Fujine, "Gas Absorption Accompanied by Complex Chemical Reactions - II. Consecutive Chemical Reactions," *Chem. Eng. Sci.*, **25**, 761, 1970b.
- Ozturk, S.S., and Y.T. Shah, "Gas Absorption with Chemical Reaction Involving a Volatile Liquid Reactant: Penetration Theory Solution," *Chem. Eng. Commun.*, **46**, 65, 1986.
- Pearson, J.R.A., "Diffusion of One Substance into a Semi-Infinite Medium Containing Another with Second-Order Reaction," *Appl. Sci. Res.*, **11**(A), 321, 1963.
- Peng, X., SINOPEC Beijing Design Institute, Private communication with Dave Austgen at Aspen Technology, Inc., 1988.
- Perry, R.H., and R.L. Pigford, "Kinetics of Gas-Liquid Reactions," *Ind. Eng. Chem.*, **45**(6), 1247, 1953.
- Petzold, L.R. "A Description of DASSL: A Differential/Algebraic System Solver," Scientific Computing, IMACS/North-Holland Publishing Co., R. Stepleman et al. (eds.), 65, 1983.
- Polasek, J.C., S.T. Donnelly, and J.A. Bullin, "The Use of MDEA and Mixtures of Amines for Bulk CO<sub>2</sub> Removal," Presented at the AIChE National Spring Meeting, Orlando, FL, 1990.
- Rochelle, G.T., H.T. Chang and S. Chakravarti, "Research Needs for Acid Gas Kinetics and Equilibria in Alkanolamine Systems," GRI Report No.92/0069, 1992.

- Sada, E., H. Kumazawa, and M.A. Butt, "Solubility and Diffusivity of Gases in Aqueous Solutions of Amines," *J. Chem. Eng. Data*, **23**(2), 161, 1978.
- Secor, R.M., and J.A. Beutler, "Penetration Theory for Diffusion Accompanied by a Reversible Chemical Reaction with Generalized Kinetics," *AIChE J.*, **13**(2), 365, 1967.
- Schwabe, K., W. Graichen, and D. Spiethoff, "Physikalisch-chemische Untersuchungen an Alkanolaminen," *Z. Phys. Chem. Neue Folge*, **20**, 68, 1959.
- Sheu, Y.E., Texaco Chemical Co., Austin, TX, Private communication with Dave Austgen, 1989.
- Texaco Chemical Co., *Diglycolamine Agent*, Technical Publication, Austin, TX, undated.
- Toman, J.J., Ph.D. dissertation draft, The University of Texas at Austin, Austin, TX, 1990.
- Toman, J.J., Private Communication, 1992.
- Toman, J.J., and G.T. Rochelle, "Carbon Dioxide Absorption Rates and Physical Solubility in 50% Aqueous Methyldiethanolamine Partially Neutralized with Sulfuric Acid," Presented at the AIChE Spring National Meeting, Paper No. 56c, Houston, TX, 1989.
- Tomcej, R.A., D. Lal, H.A. Rangwala, and F.D. Otto, "Absorption of Carbon Dioxide into Aqueous Solutions of Methyldiethanolamine," Presented at the AIChE Annual Meeting, Miami Beach, Florida, Nov., 1986.
- Versteeg, G.F., *Mass Transfer and Chemical Reaction Kinetics in Acid Gas Treating Processes*, dissertation, University of Twente, The Netherlands, 1986.
- Versteeg, G.F., and W.P.M. van Swaaij, "Solubility and Diffusivity of Acid Gases (CO<sub>2</sub>, N<sub>2</sub>O) in Aqueous Alkanolamine Solutions," *J. Chem. Eng. Data*, **33**, 29, 1988a.
- Versteeg, G.F., and W.P.M. van Swaaij, "On the Kinetics Between CO<sub>2</sub> and Alkanolamines both in Aqueous and Non-aqueous Solutions. Part I: -Primary and Secondary Amines," *Chem. Eng. Sci.*, **43**(3), 573, 1988b.

- Versteeg, G.F., and W.P.M. van Swaaij, "On the Kinetics Between CO<sub>2</sub> and Alkanolamines both in Aqueous and Non-aqueous Solutions. Part II: -Tertiary Amines," *Chem. Eng. Sci.*, **43**(3), 587, 1988c.
- Vivian, J.E., and D.W. Peaceman, "Liquid-Side Resistance in Gas Absorption," *AIChE J.*, **2**(4), 437, 1956.

## VITA

Shrikar Chakravarti was born in Madras, India on April 26, 1969 the son of Chakravarti and Rama Anantanarayanan. He did his schooling at Our Lady of Perpetual Succour High School, Bombay, India. In 1986, he entered the Indian Institute of Technology, Bombay. He graduated in May 1990, and then joined the Graduate School of the University of Texas at Austin in August 1990.

Permanent address: 12 Kambhoji, Uttam Society,  
St. Anthony's Road, Chembur,  
Bombay, 400071  
India

This thesis was typed by Shrikar Chakravarti and partly formatted by Missa Trueper.